Seed Coat Permeability of Active Ingredients

Permeabilität von Samenschalen für Aktivsubstanzen

Doctoral thesis for a doctoral degree
at the Graduate School of Life Sciences,
Julius-Maximilians-Universität Würzburg,
Section Integrative Biology

submitted by

Sylvia Niemann

from

Stadthagen

Würzburg 2013

Seed Coat Permeability of Active Ingredients

Permeabilität von Samenschalen für Aktivsubstanzen

Doctoral thesis for a doctoral degree
at the Graduate School of Life Sciences,
Julius-Maximilians-Universität Würzburg,
Section Integrative Biology

submitted by

Sylvia Niemann

from

Stadthagen

Würzburg 2013

Submitted on: ……..……..

Members of the *Promotionskomitee*:

Chairperson: Prof. Dr. Jörg Schultz

Primary Supervisor: Prof. Dr. Markus Riederer

Supervisor (Second): Prof. Dr. Wolfgang Dröge-Laser

Supervisor (Third): Dr. Christian Popp

Date of Public Defence: ……..……

Date of Receipt of Certificates: ……

Table of contents

Summary

The seed coat is the barrier controlling exchange of solutes between the plant embryo and its environment. This exchange is of importance for example in the uptake of germination inhibitors or in the uptake of agrochemicals applied as seed treatment. A thorough understanding of the basic mechanisms underlying solute permeation across the seed coat would help to improve the effectiveness of seed treatment formulations. In seed treatment formulations, additives can be used to enhance or decrease mobility or uptake of the active ingredient (AI). In the present study the seed coat barrier properties and the seed coat permeation process was examined with the model species *Pisum sativum* and with a set of model solutes.

The lipophilic fraction of the seed coat was analysed by gas chromatography and mass spectrometry and it was found that the total lipophilic compartment of the seed coat represents 0.61 % of the weight of a swollen seed coat. The seed is covered by a lipophilic cuticle. The seed coat coverage with cuticular waxes is ten to 18-fold lower than wax coverage of pea leaves, though. In order to examine sorption of solutes in the small lipophilic compartment of the seed coat, seed coat/water partition coefficients were determined. These cover a much smaller range than the corresponding *n*-octanol/water partition coefficients. The lipophilic sorption compartment as calculated from the seed coat/water partition coefficient data is smaller than the analysed total lipophilic compartment of the seed coat since not all of the lipid components can act as sorption compartment.

During seed swelling, the pea seed nearly doubles its weight. The uptake of water is driven by the very low water potential of the dry seed and controlled by the seed coat hydraulic conductivity both of which increase during seed swelling. Depending on the available form of water, water uptake can take place by diffusion from air humidity or by mass flow from liquid water. Water uptake by a seed in moist sand takes place by a combination of both uptake mechanisms.

The basic transport mechanism underlying solute permeation of seed coats was analysed by steady-state experiments with a newly devised experimental setup. The permeance P for permeation of the set of model compounds across isolated seed coat halves ranged from 3.34 x 10^{-8} m s^{-1} for abamectin to 18.9 x 10^{-8} m s^{-1} for

caffeine. It was found that solute permeation across the seed coat takes aqueous pathways. This was concluded from the facts that molar volume instead of lipophilicity of the solutes determine permeation and that the temperature effect on permeation is very small. This is in contrast to typical leaf and fruit cuticular uptake where lipophilic pathways dominate. Solute uptake across the seed coat can take place by two different mechanisms both of which take aqueous pathways. Uptake can be by diffusion and in the presence of a bulk flow of water driven by a water potential difference also by solvent drag. The presence of the solvent drag uptake mechanism shows that the aqueous pathways form an aqueous continuum across the seed coat. These findings indicate that the seed coat covering cuticle does not form a continuous barrier enclosing the seed.

In order to examine solute uptake across the seed coat under conditions close to a situation taking place in the field, the process of uptake of a seed treatment AI in the field was simulated. In the situation of a treated seed in the field, the seed treatment residue dissolves and then the AI can move either into the surrounding soil or across the seed coat into the seed. Uptake across the seed coat can take place either by diffusion or during seed swelling by the solvent drag mechanism. Since the seed treatment residue depletes over time, non-steady-state uptake takes place. To simulate these processes, laboratory scale seed treatment methods were established to produce treated seeds and isolated treated seed coat halves. Experimental setups for non-steady-state uptake experiments were established with whole treated seeds and with isolated treated seed coat halves as simplified screening tool. By modelling of the AI uptake as a first-order process the rate constant k and the final relative uptake amount $M_{t\rightarrow\infty}\ M_0^{-1}$ were obtained. With k and $M_{t\rightarrow\infty}\ M_0^{-1}$ a quantification and comparison of the uptake curves was possible.

Both in the experiments with whole treated seeds and with isolated treated seed coats, uptake of metalaxyl-M was much faster than uptake of sedaxane. In the uptake of a seed treatment AI, not only the solute's molar volume but also its water solubility determine uptake. The solute's water solubility is important for dissolution of the AI from the seed treatment residue and thus determines availability of the AI for uptake. Water solubility also controls the possible concentration in solution and thus the driving force for diffusive uptake. Furthermore, the AI amount taken up by solvent

drag is determined by concentration in the inflowing water and thus by water solubility.

In the experiments with whole treated seeds the additive effects on uptake were smaller than in the experiments with isolated treated seed coats or not significant. Adigor functions as an emulsifier and can lead to a slight increase of AI mobilisation from the seed treatment residue. NeoCryl A-2099 can cause a slowed down release of the AI from the seed treatment residue. The effects of both additives were smaller than the effect caused by different AI physico-chemical properties. Therefore, the most important factor determining uptake of a seed treatment AI are the AI's physico-chemical properties, especially its water solubility.

Zusammenfassung

Die Samenschale fungiert als Barriere, welche den Stoffaustausch zwischen dem pflanzlichen Embryo und seiner Umgebung kontrolliert. Dieser Stoffaustausch ist beispielsweise bei der Aufnahme von keimungshemmenden Substanzen oder aufgebeizten Pestiziden von Bedeutung. Ein besseres Verständnis des zugrundeliegenden Mechanismus bei der Permeation über die Samenschale wäre hilfreich für die Optimierung von Beizmittelformulierungen. Bei der Formulierung von Beizprodukten kann die Mobilität oder Aufnahme der Wirkstoffe je nach Bedarf durch Zugabe von Additiven beschleunigt oder verlangsamt werden. In der vorliegenden Arbeit wurden daher die Barriereeigenschaften der Samenschale und der Permeationsprozess über die Samenschale anhand der Modellpflanze *Pisum sativum* und mit einem Set von Modellsubstanzen untersucht.

Die lipophile Fraktion der Samenschale wurde mittels Gaschromatographie und Massenspektrometrie analysiert. Hierdurch konnte ermittelt werden, dass das komplette lipophile Kompartiment der Samenschale 0.61 % des Gewichtes ausmacht. Die Samenschale wird, wie es auch bei Blättern der Fall ist, von einer lipophilen Kutikula bedeckt. Die Bedeckung mit kutikulären Wachsen ist bei Erbsensamen allerdings zehn- bis 18-fach geringer als bei Blättern von Erbsenpflanzen. Um die Sorption von Substanzen in dem kleinen lipophilen Kompartiment der Samenschale zu untersuchen, wurden Samenschale/Wasser Verteilungskoeffizienten bestimmt. Diese erfassen einen sehr viel kleineren Größenbereich als die entsprechenden *n*-Oktanol/Wasser Verteilungskoeffizienten. Das lipophile Sorptionskompartiment, welches mittels der Samenschale/Wasser Verteilungskoeffizienten berechnet wurde, ist kleiner als das analysierte lipophile Kompartiment, da nicht alle analysierten lipophilen Samenschalenbestandteile als Sorptionskompartiment fungieren können.

Bei der Quellung von Erbsensamen kommt es nahezu zu einer Verdoppelung des Gewichtes. Die Wasseraufnahme wird durch das sehr niedrige Wasserpotential des trockenen Samens angetrieben und über die hydraulische Leitfähigkeit der Samenschale kontrolliert, wobei beide während der Quellung ansteigen. Je nachdem in welcher Form das verfügbare Wasser vorliegt kann die Wasseraufnahme durch Diffusion aus Luftfeuchte oder über einen Massenfluss aus flüssigem Wasser

erfolgen. Ein Same in feuchtem Sand nimmt Wasser mittels einer Kombination beider Mechanismen auf.

Der zugrunde liegende Transportmechanismus in der Substanzpermeation über Samenschalen wurde mit einem neu entwickelten Versuchsaufbau in Steady-State Versuchen analysiert. Der Leitwert P für die Permeation der Modellsubstanzen lag hierbei zwischen 3.34 x 10^{-8} m s^{-1} für Abamectin und 18.9 x 10^{-8} m s^{-1} für Koffein. Die Substanzpermeation über die Samenschale verläuft über wässrige Permeationswege. Dies wurde daraus geschlossen, dass das molare Volumen anstelle der Substanzlipophilie den Leitwert bestimmt und dass der Temperatureffekt auf die Permeation klein ist. Dies ist im Gegensatz zur typischen Permeation über die Kutikeln von Blättern und Früchten, welche meist über lipophile Wege verläuft. Substanzaufnahme kann durch zwei verschiedene Mechanismen über die wässrigen Wege durch die Samenschale stattfinden. Aufnahme kann sowohl durch Diffusion stattfinden oder, in Gegenwart eines Volumenflusses von Wasser welcher durch eine Wasserpotentialdifferenz angetrieben wird, auch durch den *solvent drag* Mechanismus. Das Vorhandensein des *solvent drag* Aufnahmemechanismus beweist, dass die wässrigen Wege in der Samenschale ein wässriges Kontinuum durch die Samenschale bilden. Diese Ergebnisse zeigen, dass die Kutikula, welche der Samenschale aufliegt, keine kontinuierliche Barriere um den Samen bildet.

Um den Aufnahmeprozess von Substanzen unter anwendungsnahen Bedingungen zu untersuchen, wurde die Aufnahme eines aufgebeizten Pflanzenschutzmittelwirkstoffes im Feld in Versuchen simuliert. In der Situation eines gebeizten Samens im Feld löst sich der Beizrückstand an und der Wirkstoff kann sich entweder in Richtung umgebender Erde oder über die Samenschale in das Sameninnere bewegen. Die Aufnahme über die Samenschale kann mittels Diffusion oder durch den *solvent drag* Mechanismus erfolgen. Da der Beizmittelrückstand auf der Samenoberfläche mit der Zeit verarmt, liegt eine *non-steady-state* Aufnahmesituation vor. Um diese Prozesse zu simulieren, wurden zuerst Beizmethoden im Labormaßstab etabliert um ganze gebeizte Samen sowie isolierte gebeizte Samenschalen zu produzieren. Dann wurden Versuchsaufbaue für *non-steady-state* Versuche mit ganzen gebeizten Samen sowie als vereinfachtes Modell mit isolierten gebeizten Samenschalen etabliert. Indem die gemessene

Wirkstoffaufnahme als Prozess erster Ordnung modelliert wurde, konnten die Geschwindigkeitskonstante k sowie die finale relative Aufnahmemenge $M_{t\rightarrow\infty}$ M_0^{-1} berechnet werden. Mit k und $M_{t\rightarrow\infty}$ M_0^{-1} konnten dann die Aufnahmekurven quantifiziert und verglichen werden.

Sowohl in den Versuchen mit ganzen gebeizten Samen als auch in den Versuchen mit isolierten gebeizten Samenschalen war die Aufnahme von Metalaxyl-M um ein Vielfaches schneller als die Aufnahme von Sedaxane. Bei der Aufnahme von einem Beizmittelwirkstoff über die Samenschale spielt nicht nur das molare Volumen des Wirkstoffes eine Rolle, sondern auch seine Wasserlöslichkeit. Die Wasserlöslichkeit ist wichtig für die Lösung des Wirkstoffes aus dem Beizmittelrückstand und bestimmt dadurch die Verfügbarkeit für die Aufnahme. Die Wasserlöslichkeit der Substanz bestimmt auch die mögliche Konzentration des Wirkstoffes in der Lösung und dadurch die treibende Kraft für diffusive Aufnahme über die Schale. Außerdem wird die Wirkstoffmenge, welche mittels des *solvent drag* Mechanismus über die Samenschale gezogen wird, durch die Konzentration in Lösung und daher ebenfalls durch die Wasserlöslichkeit bestimmt.

In den Versuchen mit ganzen gebeizten Erbsen war der Effekt der Additive kleiner als in den Versuchen mit isolierten gebeizten Schalen oder nicht signifikant. Adigor wirkt als Emulgator und kann die Mobilisierung des Wirkstoffes vom Beizmittelrückstand erhöhen. NeoCryl A-2099 kann eine verzögerte Mobilisierung des Wirkstoffes vom Beizmittelrückstand bewirken. In beiden Fällen war der Additiv-Effekt kleiner als der Effekt, der durch die Unterschiede in den Substanzeigenschaften hervorgerufen wurde. Daher sind die physikalisch-chemischen Eigenschaften des Wirkstoffes, insbesondere seine Wasserlöslichkeit, die wichtigsten Faktoren welche die Aufnahme in den gebeizten Samen bestimmen.

Acknowledgements

First of all, I would like to thank Prof. Dr. Markus Riederer from the Julius-von-Sachs-Institute for Biosciences, department of Botany II, for supervising this PhD and for providing excellent working conditions. I am deeply grateful for his continuous support and many helpful discussions and suggestions.

Special thanks go to Dr. Markus Burghardt for supporting me with countless discussions and helpful ideas.

My sincere thanks go to Dr. Christian Popp (Syngenta Crop Protection) for co-supervising this PhD and for any support.

I also thank Prof. Dr. Wolfgang Dröge-Laser for co-supervising this PhD and for helpful discussions and ideas.

I would like to express my thanks to Dr. Adrian Friedman (Syngenta Crop Protection) for his support and encouragement.

I would like to acknowledge the financial support from Syngenta Crop Protection.

Finally, I would like to express further thanks to all colleagues of the department of Botany II for any help, support and feedback.

Abbreviations

A	area [m^2]
AI	active ingredient
c	concentration [g m^{-3}]
D	diffusion coefficient [m^2 s^{-1}]
E_A	activation energy [J mol^{-1}]
F	flow rate [g s^{-1}]
J	flux [g s^{-1} m^{-2}]
k	rate constant [h^{-1}] [min^{-1}]
K	partition coefficient
$K_{barrier/solution}$	barrier/solution partition coefficient
$K_{c/w}$	cuticle/water partition coefficient
$K_{o/w}$	*n*-octanol/water partition coefficient
$K_{sc/w}$	seed coat/water partition coefficient
$K_{w/w}$	water/water partition coefficient
L_{hydr}	hydraulic conductivity [g s^{-1} m^{-2} Mpa^{-1}]
M_0	amount initially applied [g]
M_t	amount taken up at time t [g]
$M_{t\rightarrow\infty}$	amount taken up at end of experiment [g]
MV	molar volume [cm^3 mol^{-1}]
MW	molar weight [g mol^{-1}]
P	permeance [m s^{-1}]
PEG	polyethylene glycol
R	universal gas constant (8.314 J K^{-1} mol^{-1})
T	temperature [°C], [K]
WS	water solubility [g l^{-1}]
β	size selectivity [mol cm^{-3}]
Δc	concentration difference [g m^{-3}], [g g^{-1}]
Δx	thickness of barrier [m]
ΔΨ	water potential difference [Pa]
ε	porosity
τ	tortuosity of the diffusional path
Ψ	water potential [Pa]
Ψ_π	osmotic water potential [Pa]

1. Introduction

1.1 Role of the seed coat

Plants developed the ability to produce seeds for reproduction and dispersal about 370 million years ago (Linkies et al. 2010). Since then evolution led to a great variation in seed anatomy between species (Werker 1997). This variability can be seen especially in the variation of seed size between species which ranges from the seeds of the Orchidaceae which are less than 0.01 mm long up to the 30 cm seeds of the palm *Lodoicea maldivica*. In most cases a seed is basically composed of an embryo, a supply of nutrients to help the offspring to establish, and the surrounding seed coat (testa). The seed coat represents the barrier that protects the valuable seed. Protection can be against physical as well as against biological damage (Werker 1997, Black et al. 2006). Depending on the species the seed coat can also feature structures that are helpful for seed dispersal. Examples for this are the development of a sarcotesta in the case of endozoochory or the development of wings or hairs aiding dispersal by wind (Werker 1997, Black et al. 2006). Another function of the seed coat can be to impose dormancy in order to prevent germination under non-favourable conditions (Werker 1997, Black et al. 2006). In the case of water impermeable seed coats, the seed coat maintains a low moisture content in the seed and thus seed viability is preserved over a longer period of time (Black et al. 2006). The exchange of gases also has to be controlled by the seed coat in accordance to the embryo's needs (Werker 1997, Black et al. 2006). Another very important role of the seed coat is the regulation of the uptake of water for seed swelling as well as the exchange of solutes with the environment, which is of significance in several important situations.

1.2 Significance of seed coat permeability

A seed in moist soil can take up or release water or solutes. This exchange with its environment has an influence on the development of the seed and seedling. While the uptake of water across the seed coat causes seed swelling (imbibition) and thus is a prerequisite for germination, the uptake or release of solutes across the seed coat has biological significance as well as economical importance.

1.2.1 Biological significance of seed coat permeability

In several situations naturally taking place in soil, a seed takes up or releases solutes. One example of such an exchange process which has often been described in literature is the leakage of solutes from seeds which can take place at the very beginning of imbibition but stops again soon after (Larson 1968, Simon and Harun 1972, Simon 1974, Powell and Matthews 1979, Duke and Kakefuda 1981, Bewley et al. 2013). These compounds released by imbibing seeds can be different solutes like ions, amino acids, sugars or proteins (Larson 1968, Simon 1978, Duke and Kakefuda 1981, Bewley et al. 2013). It was concluded that these solutes are of cytosolic origin (Bewley 1997, Black et al. 2006, Bewley et al. 2013). If these solutes cross the seed coat and are released to the seed surface and into the adjacent soil, the growth of pathogens can be promoted which might then affect the seed or seedling (Keeling 1974, Bewley et al. 2013). One hypothesis on how the solutes leave the cells was that too rapid uptake of water causes a rupture of the cell membranes (Larson 1968, Powell and Matthews 1978, Duke and Kakefuda 1981). Today it is understood that leakage is caused by a changed membrane phospholipid orientation in the dry embryo as the cell membranes in the dry seed are in a hexagonal configuration (Simon and Harun 1972, Simon 1974, Bewley 1997, Black et al. 2006, Bewley et al. 2013). During early imbibition the cell membranes rearrange to their normal lamellar configuration and leakage stops (Simon and Harun 1972, Simon 1974, Bewley 1997, Black et al. 2006, Bewley et al. 2013).

Another process where seeds exchange solutes with the surrounding soil is the uptake or release of germination inhibitors. When seeds take up germination inhibitors across their seed coats chemical dormancy is caused (Black et al. 2006, Bradford and Nonogaki 2007). In allelopathic interactions of plants, such germination inhibitors can be released by various living parts or litter of the competing vegetation (Evenari 1949, Börner 1960, Friedman and Waller 1983a, Reigosa et al. 1999) or by competing seeds themselves (Börner 1960, Friedman and Waller 1983b, Iqbal and Fry 2012). Once in the soil, allelochemicals can enter seeds and prevent germination (Evenari 1949, Reigosa et al. 1999, Iqbal and Fry 2012). Besides inhibition of germination, allelopathic agents leaching from seeds can also hinder growth of competing vegetation by slowing down germination or reducing root growth of seedlings of other plant species (Reigosa et al. 1999, Suman et al. 2002, Zhang et al.

2011). Allelochemicals can be secondary metabolites from different chemical groups as for example phenolic compounds like ferulic acid, coumaric acid and vanillic acid (Reigosa et al. 1999) or alkaloids like caffeine (Friedman and Waller 1983a). In the case of allelopathic agents taken up or released by seeds in the soil, the substances have to cross the seed coat to reach their target which makes permeation of solutes across seed coats biologically significant.

1.2.2 Economical significance of seed coat permeability

A situation in which seed coat permeability to solutes is of high economic importance is the uptake of agrochemicals by seeds that have undergone seed treatment. In commercial seed treatment or seed dressing, the active ingredient (AI), which in most cases is a fungicide or insecticide, is applied directly to the surface of the dry seed. This leads to a protection of the seed and the young plant from the beginning of the germination process on. Since by the use of the seed as carrier the application is highly targeted, the amount of pesticide needed per area is reduced in comparison to a spraying application in the field (Black et al. 2006). Additional to this environmental advantage, the use of treated seeds is also convenient to the farmers. Therefore, seed treatment is a widely used method. Already in ancient Greek and Roman literature descriptions of seed treatments against diseases with juice of houseleek, olive extracts or chalk are described (Black et al. 2006). In recent agricultural practice seed treatment pesticides are much more sophisticated and effective. In the 1930s synthetic organic fungicides were introduced as seed treatment active ingredients and from the 1970s systemic active ingredients were used in seed treatment applications (Black et al. 2006). For a systemic mode of action, the AI has to be taken up across the seed coat into the embryo. Hereby, the exact amount of AI taken up is critical for the effect of the treatment. Uptake of doses being too low can reduce the protective effect, while the uptake of too much AI can lead to phytotoxicity (Simmen and Gisi 1995, Montfort et al. 1996). Complex seed treatment formulations with various additives or adjuvants are designed to either enhance or slow down release and uptake of the AI (Bardner 1960, Simmen and Gisi 1995, Kanampiu et al. 2009, Angst et al. 2010). The effect of additives like for example surfactants, stickers, humectants or plasticizers has been thoroughly researched in leaf uptake formulations (Schönherr 1993, Buchholz and Schönherr 2000, Hazen 2000). Less research has been published on the effect of additives on seed treatment AI uptake,

though. To further improve the effectiveness of seed treatment formulations, more information is needed on the seed coat's barrier properties, on the underlying uptake mechanism and on the mode of action of additives in seed treatment AI uptake situations.

1.3 Use of *Pisum sativum* as model plant

The anatomy of seeds is highly diverse between species (Werker 1997). The species which was used in the present experiments as a model was *Pisum sativum* (pea). Pea is a widely used model plant and it is closely related to the economically very important legume *Glycine max* (soybean). An advantage of using pea seeds is that the seeds are easy to handle due to their large seed size and simple seed anatomy. The anatomy of a pea seed and seed coat is presented in the following.

1.4 Seed anatomy

1.4.1 Anatomy of *Pisum sativum* seed

In the mature pea seed, the embryo is enclosed by the seed coat (Figure 1.1). The embryo consists of the embryonic axis with radicula, hypocotyl and plumula and of the storage cotyledons. The radicle gives rise to the root and the plumula gives rise to the shoot after germination (Black et al. 2006). The very large storage cotyledons serve as sole storage organs while a storage endosperm is absent in the mature *Pisum sativum* seed (Werker 1997). The massive storage cotyledons consist of enlarged cells which are filled with storage materials (Werker 1997). These storage reserves are mostly starch and protein (Black et al. 2006).

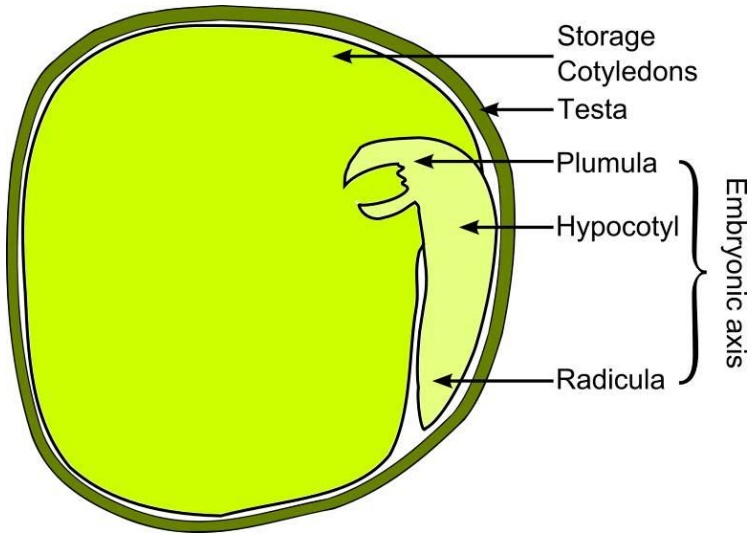

Figure 1.1: Anatomy of a *Pisum sativum* seed.

The embryo develops from the fertilised ovule and thus is combined from maternal and paternal origin. The seed coat on the other hand is maternal tissue which has developed from the integuments surrounding the ovule (Werker 1997).

1.4.2 Anatomy of *Pisum sativum* seed coat

In most species all seed coat cells die upon maturation (Werker 1997, Ranathunge et al. 2010), therefore, solute permeation across the seed coat is a physical process governed by the seed coat's chemical and anatomical properties.

The *Pisum sativum* seed coat is composed of characteristic cell layers. It consists of an outer cell layer of palisade cells with a covering cuticle which is derived from the outer lining of the outer integument, a layer of hourglass cells with large intercellular spaces and as innermost layer a multicellular layer of compressed parenchyma cells (Werker et al. 1979, Werker 1997). Changes in the seed coat structure can be found at the hilum, where the seed was attached to the funiculus, and at the micropyle, which is the gap between the two integuments where the pollen tube entered the embryo sac (Werker et al. 1979, Werker 1997). The hilum and micropyle are located at the ventral side of the legume seed (Meyer et al. 2007). Since the seed coat cells die upon seed maturation (Werker 1997, Ranathunge et al. 2010), intact cell membranes and complete cells are not present in the seed coat. The seed coat therefore consists mainly of cell wall material. Cellulose und pectic substances were detected in *Pisum sativum* seed coats by Werker et al. (1979).

1.4.3 *Pisum sativum* seed coat covering cuticle

The *Pisum sativum* seed coat is covered by a cuticle as outermost layer (Werker et al. 1979, Werker 1997). For leaf and fruit surfaces it was shown that the covering cuticle limits transport of both water and solutes (Schreiber and Schönherr 2009). For soybean seeds the cuticle has also been concluded to determine initial water uptake since it was found that water uptake correlates with the presence of small cracks in the seed coat cuticle (Ma et al. 2004). However, the role of the seed coat covering cuticle on solute sorption and permeation is not yet clear. The seed coat covering cuticle could act as lipophilic sorption compartment and as a barrier on solute uptake similar to leaf and fruit cuticles (Schreiber and Schönherr 2009). Therefore, a detailed description of the seed coat covering cuticle would be of interest. Werker et al. (1979) examined the pea seed coat by light microscopy. A partial chemical analysis of the pea seed coat cuticle was done by Espelie et al. (1979) where the cutin fraction only was examined. A quantification of the complete *Pisum sativum* seed coat lipid fraction including soluble cuticular waxes is lacking.

1.5 Seed swelling process

Prior to germination, the seed undergoes the process of seed swelling or imbibition. The mature seed has a very low water content and low water potential which leads to an inrush of water in a moist environment (Black et al. 2006, Bewley et al. 2013). Depending on the species, very large amounts of water can be taken up. It can be supposed that this process leads to changes in the seed coat, affecting the seed coat's barrier properties. Changes in the barrier properties of the seed coat during the imbibition process have been noticed in several species. For *Zea mays* permeability to water was estimated and it was found that it increased during swelling (Collins et al. 1984). For *Brassica napus*, too, it was found that the seed coat barrier properties towards water inflow change during the seed swelling process (Shaykewich and Williams 1971). A detailed examination of these changes in the barrier properties of seed coats during swelling and a quantification of changes in *Pisum sativum* is lacking, though.

Besides of these structural changes taking place during imbibition, the process of water uptake itself could also directly cause uptake of solutes by the solvent drag mechanism. For synthetic polymers it was shown that a flow of water across the

barrier can drag along dissolved substances across the barrier (Yasuda and Peterlin 1973, Van Bruggen et al. 1982). This mechanism of solvent drag uptake was also shown for apoplastic root uptake (Fiscus 1975, Aloni et al. 1998, Freundl et al. 1998) but it was not yet examined for seed coat uptake of solutes.

Thus, seed imbibition is a complex process which causes changes in the seed coat's barrier properties and which probably influences uptake of solutes by a seed in the soil. The relationships between seed swelling, seed coat barrier properties and solute uptake need to be examined.

1.6 Analysis of solute uptake across the seed coat

1.6.1 Permeation across a barrier

According to Fick's first law of diffusion, a diffusive flow of a solute takes place when a concentration gradient is present as driving force (equation 1.1).

$$J = -D \cdot \frac{\Delta c}{\Delta x} \qquad (1.1)$$

In this equation, J is the flux of solute moving by diffusion [g s^{-1} m^{-2}], D [m^2 s^{-1}] is the diffusion coefficient, Δc [g m^{-3}] is the concentration difference which acts as driving force for the solute flux and Δx [m] is the length of the diffusion path. In the case of a solute flow across a barrier, the permeance P can be used to describe the process (equation 1.2).

$$J = P \cdot \Delta c \qquad (1.2)$$

J is the flux of solute [g s^{-1} m^{-2}] and Δc [g m^{-3}] is the concentration difference. The permeance P [m s^{-1}] describes to what degree the barrier allows the flow of a given solute. P has the unit of a velocity and thus describes the permeation speed of the solute across the specific barrier. P is composed of the partition coefficient $K_{barrier/solution}$ (dimensionless) describing the solute partitioning from the adjacent aqueous solution into the barrier, the diffusion coefficient D [m^2 s^{-1}] within the barrier, and the thickness Δx [m] of the barrier (equation 1.3).

$$P = \frac{K_{barrier/solution} \cdot D}{\Delta x} \quad (1.3)$$

By measuring the permeance P with a set of solutes with different physico-chemical properties information about the uptake mechanism can be obtained. In order to obtain the permeance P from a transport experiment, the flux of solute J [g s^{-1} m^{-2}] divided by the concentration difference Δc [g m^{-3}] as driving force has to be measured (equation 1.4).

$$P = \frac{J}{\Delta c} \quad (1.4)$$

Therefore, for a mechanistic analysis of solute permeation across a seed coat the solute flux across the seed coat driven by a known concentration gradient has to be measured.

1.6.2 Past approaches to examine seed uptake of solutes

Active ingredient (AI) uptake by seeds was examined in the past with different experimental approaches.

1.6.2.1 Biological essays

Active ingredient uptake by seeds was examined indirectly in several experiments by essaying the efficiency of seed treatment on controlling pests or by occurrence of phytotoxic effects (Graham-Bryce et al. 1980, Suzuki et al. 1994, Montfort et al. 1996, Yue et al. 2003, Stevens et al. 2008, Zeun et al. 2012). This approach does not facilitate quantitative description of uptake across the seed coat since no uptake rate is measured directly. Additionally, AI uptake can be across the seed coat or by emerging plant parts after germination. Furthermore, the influence of environmental conditions like temperature or soil moisture on uptake makes the interpretation of results obtained from field studies difficult.

1.6.2.2 Analysis of AI amounts in plants grown from treated seeds

Different parts of plants grown from treated seeds were analysed for their contents of AI and by this the uptake and distribution of the AI was examined (Thielert et al. 1988, Parida et al. 1990, Simmen and Gisi 1996, Querou et al. 1998, Westwood et al. 1998, Laurent and Rathahao 2003). In the experiments performed by Simmen and Gisi (1996) the AI was applied to several sites on a wheat caryopsis and it was found that uptake across the testa is possible. Thielert et al. (1988) kept treated caryopses in a special sample holder in a moist environment to germinate and confirmed AI uptake across the testa.

In these experiments a quantitative measurement of uptake rates over time is not possible. The AI concentration differences as driving forces are unknown and changing. Furthermore, in most of these experiments uptake can take place not only across the seed coat but also by emerging parts of the seedling.

1.6.2.3 Experiments with whole seeds placed into solution

Uptake by whole seeds placed into AI solution was measured in several experiments (Rieder et al. 1970, Scott and Phillips 1971, Phillips et al. 1972, Garcinuño et al. 2003) by a concentration decrease in the donor solution. In these experiments the uptake across the seed coat over the time could be measured. The exact AI concentration difference as driving force across the seed coat was not known, though.

1.6.2.4 Measurement of uptake after incubation of treated seeds

Fluorescent tracers were applied as seed treatment and uptake was examined by fluorescence detection in the embryo after placing the seeds into moist sand for a period of time by (Salanenka and Taylor 2008). The microscopical detection of fluorescence does not allow a quantitative description of uptake, though. Similar experiments were performed by Querou et al. (1997) who treated wheat caryopses with radioactively labelled AI, placed them into moistened soil and combusted the seeds in order to measure uptake. In these experiments the exact concentration gradient as driving force is not known and thus the underlying uptake mechanism cannot be examined.

Therefore, from none of these experiments the permeance P could be obtained. The experiments did not supply the data needed for an analysis of the underlying mechanism for permeation across the seed coat.

1.6.3 Steady-state experimental approach

In order to obtain permeances across the seed coat which can be used for an analysis of the underlying seed coat permeation mechanism, steady-state experiments with controlled environmental conditions would be a suitable method. In such steady-state experiments, the solute flow across a barrier is measured over time under defined conditions with a known concentration gradient as the driving force for permeation. From such experiments the permeance P can be obtained according to equation (1.4) which can then be used to describe the barrier properties to permeation. This approach was used in the past to describe the barrier properties of leaf and fruit cuticles (Kerler et al. 1984, Becker et al. 1986, Popp et al. 2005, Schreiber and Schönherr 2009). From these experiments it was found that leaf and fruit cuticular permeation can take place via a lipophilic or a polar pathway (Popp et al. 2005, Schreiber 2005, Schreiber and Schönherr 2009) (Figure 1.2).

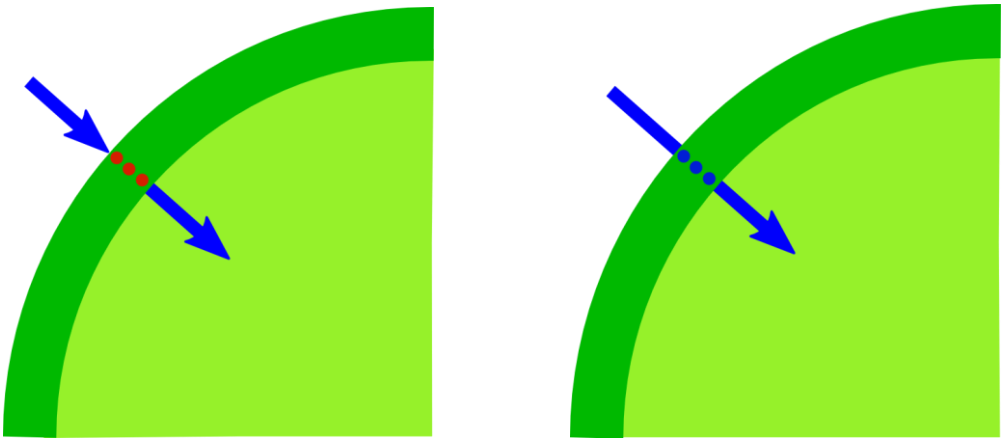

Figure 1.2: Schematic drawing of the lipophilic permeation pathway (left) in comparison to the hydrophilic or aqueous permeation pathway (right).

In the lipophilic permeation pathway, the solute partitions into the lipophilic barrier, moves across the barrier by diffusion, and leaves it on the other side in a second

partitioning step. The permeation process is therefore a combination of solution in and diffusion across the barrier (Stein 1986, Vieth 1991, Cussler 1997). Due to the sorption step of the solute into the lipophilic barrier, permeation via lipophilic pathways depends on the solute's lipophilicity. The higher the solute lipophilicity, the easier can the solute enter the lipophilic barrier. Consequently, lipophilic solutes can cross the barrier at higher rates (Stein 1986, Kerler and Schönherr 1988a, Kerler and Schönherr 1988b). The second possible permeation pathway across leaf cuticles is permeation via an aqueous pathway. In this process, the solute does not partition into the lipophilic compartment of the barrier but stays in its aqueous environment. Therefore, permeation is not influenced by the solute's lipophilicity. Instead, permeation depends on molecular size due to the narrow inner dimensions of the aqueous pathways (Lieb and Stein 1971, Schönherr and Schreiber 2004, Schlegel et al. 2005). Whether in the seed coat uptake process the lipophilic pathway or the hydrophilic pathway or a combination of both dominate permeation processes has not been determined yet.

1.6.4 Uptake by a treated seed in soil

While the steady-state uptake experiments can be used to understand the basic mechanisms underlying solute uptake across the seed coat, the situation of a treated seed in the field cannot be examined with these experiments. In the uptake situation of a treated seed in the field, the situation is much more complex than in the steady-state uptake process. In the moist soil environment, the seed treatment residue dissolves and the AI can move both across the seed coat into the seed and away from the seed into the soil. During this process the seed treatment residue depletes, resulting in a decrease of flow rates over time. Additionally, the seed uptake process has to be assumed to be influenced by seed imbibition (chapter 1.5). Thus, seed treatment AI uptake is a complicated process with many interacting factors playing a role. Experiments simulating AI distribution from a treated seed in the field could help to understand this complex process.

1.6.4.1 Non-steady-state transport processes

By the distribution of the seed treatment AI, the seed treatment residue depletes over time. This leads to a decrease of the driving force which in consequence causes a

continuous decrease in flow rate, resulting in non-steady-state transport kinetics. In such non-steady-state transport situations, transport can be described as a first-order process (equation 1.5) (Schönherr 2001, Schreiber and Schönherr 2009).

$$\frac{M_t}{M_0} = 1 - e^{-k \cdot t} \qquad (1.5)$$

In this equation, M_t is the amount permeated across the barrier at the time t [g], M_0 is the amount initially applied [g], t is the time [h] and k [h^{-1}] is the rate constant. The rate constant describes the velocity of the process for the solute examined. By measuring k for different AIs, the uptake behaviour could be examined in relation to the AI's physico-chemical properties. This approach has been used in the past to examine leaf cuticular permeation in non-steady-state situations (Baur et al. 1996, Schönherr 2001, Buchholz 2006, Schreiber and Schönherr 2009). Thus, a simulation of seed treatment AI uptake in non-steady-state experiments would facilitate the measurement of rate constants which could be used for a description of the uptake process.

1.6.4.2 Experiments simulating seed treatment AI uptake

The prerequisite for simulating the situation of a treated seed in the soil in laboratory experiments is the preparation of treated seed material. The treatment should be reproducible, practicable in a laboratory scale and the applied amount should be as controllable as possible. Commercial seed treatment formulations cannot be used for these experiments since such formulations contain many additives besides the AI. Such additives, which can be for example dispersing agents, frost protection substances, preservatives or surfactants (Backman 1978), would interfere with the transport process and thus complicate the interpretation of the results. For experiments aiming to understand the processes taking place, the seed treatment formulation should therefore contain as few ingredients as possible.

Experiments for the simulation of seed treatment AI distribution could be performed with intact treated seeds or with isolated treated seed coats. The use of isolated treated seed coats could provide a simplified model of the AI dissolution and distribution.

1.7 Aim of the present work

The aim of the present work was to analyse the uptake of solutes across seed coats with the model plant *Pisum sativum* and with a set of model solutes. Several suitable approaches to characterise the seed coat uptake process and the seed coat barrier properties were used in the present study.

- The seed coat as the barrier enclosing the seed was characterised and the lipophilic and hydrophilic fractions of the seed coat were estimated.

- Sorption of solutes by the seed coat was quantified by the determination of seed coat/water partition coefficients. With the measured seed coat/water partition coefficients of the set of model solutes the lipophilic sorption compartment of the seed coat was estimated.

- The complex seed imbibition process was studied. The seed coat barrier properties towards a mass flow of water and changes in these barrier properties during seed swelling were examined. Seed water uptake from liquid water, water saturated air und moist sand was examined in order to analyse the water uptake mechanism.

- An experimental setup was established which was used to measure permeation of a set of model substances with different physico-chemical properties across isolated seed coat halves. Steady-state experiments were performed which allowed the determination of the permeance P. This data were used to analyse the seed coat barrier properties and underlying uptake mechanisms. In addition, the effect of temperature on the permeation process and the effect of a water potential gradient on permeation were examined.

- In order to examine seed coat permeation in the situation of a treated seed in the field, reproducible seed treatment methods at a laboratory scale were established. Isolated treated seed coats as well as whole treated seeds were produced.

- Experimental setups for the study of seed treatment AI distribution with intact treated seeds and isolated treated seed coat halves were established. The processes of seed treatment AI dissolution, movement into the sand and uptake were analysed. Seed material treated with different AIs and additives was used in order to gain information on the effect of the AI's physico-chemical properties and the effect of additives. In order to compare results of different seed treatments, the uptake curves were quantified with the rate constant k.

2. Materials and Methods

2.1 Seed material

Pea (*Pisum sativum* L. cv. Santana) seeds were obtained from Syngenta Seeds B. V., Enkhuizen, Netherlands and stored at 4 °C until further use. Only visibly undamaged seeds were used in the experiments.

2.1.1 Seed coat isolation

In many experiments isolated seed coat halves of dry or swollen pea seeds were used instead of whole seeds. To obtain isolated seed coat halves of dry pea seeds, the seed coat of a seed in its original dry state was cut into halves along the gap between the two cotyledons which were then removed from the seed coat halves (Figure 2.1 A). For the isolation of swollen seed coats, the pea seeds were placed into water over night for swelling before seed coat isolation. Then the seed coat halves were isolated as described for the dry seeds (Figure 2.1 B). Seed coat halves of swollen seeds were used for the experiments directly after their isolation to prevent drying. By this seed coat isolation method, the hilum and micropyle were at the very edge of the isolated seed coat halves.

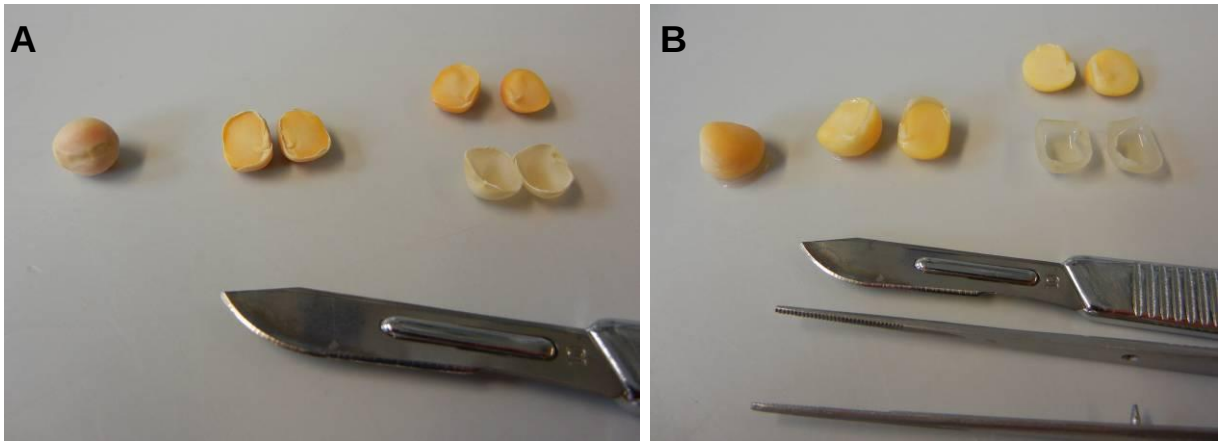

Figure 2.1: Isolation of seed coat halves of *Pisum sativum*. A: dry seed, B: swollen seed. From left to right: whole seed, seed cut into halves along the gap between the two cotyledons, cotyledon halves removed from seed coat halves.

2.1.2 Seed weight and surface area

The weight of whole *Pisum sativum* seeds in their original dry state as well as in their completely swollen state was measured gravimetrically on a balance (SCALTEC SBA 31, SCALTEC Instruments GmbH, Göttingen, Germany). The surface of whole swollen seeds was quickly dried with tissue paper prior to weighing to remove adherent water. The weight of dry and swollen pea seeds was measured with 20 seeds each. To measure the surface area of dry and of completely swollen seeds the seed coat was removed from a seed and cut into small fragments to minimise curving. These fragments were flattened and scanned and the total seed surface area was estimated by comparison with a reference area of known size using imaging software (Adobe Photoshop 7.0, Adobe Systems Incorporated, San José, USA). The surface area of dry and swollen pea seeds was measured with 20 seeds each.

In order to measure the weight of the complete seed coat material of a pea seed, the two seed coat halves of a dry seed were isolated with special care to collect all fragments and crumbs. Then the weight of the seed coat material was measured gravimetrically on a micro-balance (S3D, Sartorius, Göttingen, Germany). The seed coat of 19 individual seeds was examined. To determine the water content of swollen pea seed coats, the weight of isolated seed coat samples was measured before and after swelling gravimetrically on a micro-balance (S3D, Sartorius, Göttingen, Germany) with the difference being the water content. The surface of the swollen seed coat samples was quickly dried with tissue paper prior to weighing in order to remove adherent water. The water content of 100 swollen seed coat samples was determined.

2.1.3 Microscopical characterisation of the seed coat

For a morphological characterisation swollen *Pisum sativum* seed coat halves were embedded in Tissue-Tek O.C.T. Compound (Sakura Finetek, Zoeterwoude, The Netherlands) and cooled to -20 °C. Cross-sections of 15 µm thickness were cut from the frozen seed coat half with a cryo-microtome (Leica CM 1900, Leica Microsystems, Nussloch, Germany). The sections were examined by light microscopy (Leica DMR, Wetzlar, Germany). The average thickness of the pea seed coat was measured for 15 sections cut from five individual pea seed coats using

imaging software (ImageJ 1.44, W. S. Rasband, U. S. National Institutes of Health, Maryland, USA).

2.1.4 Chemical characterisation of seed coat cuticular lipids

For an analysis of lipid compartments in the seed coats the amounts of soluble waxes and cutin were determined. A *Pisum sativum* seed coat isolated from a dry seed was washed with chloroform (Roth, Karlsruhe, Germany) for 30 min in a small glass vial to extract the fraction of soluble waxes. Before analysis of the wax fraction a derivatisation of the samples with bis-N,N-(trimethylsilyl)trifluoroacetamide (Macherey-Nagel, Düren, Germany) in pyridine (Sigma-Aldrich, Taufkrichen, Germany) was performed for 30 min at 70 °C for obtaining the trimethylsilyl derivatives of hydroxyl-containing compounds. For the quantification of waxes a capillary gas chromatograph (GC) with flame ionization detector (FID) (5890 HP Series II; Agilent Technologies, Böblingen, Germany) and on-column injection with a capillary column (30 m × 0.32 mm, DB-1, d f = 0.1 µm, J&W Scientific, Agilent Technologies, Böblingen, Germany) was used. For separation of the wax peaks injection took place at 50 °C followed by 2 min at 50 °C, temperature raise by 40 °C min^{-1} to 200 °C, held for 2 min at 200 °C, raise by 3 °C min^{-1} to 320 °C, and held for 30 min at 320 °C. Carrier gas (H_2) pressure started at 5 kPa and was raised after 5 min by 3 kPa min^{-1} to 50 kPa where it was held for 30 min at 50 kPa. 1-eicosanol (purity > 98 %, Fluka, Neu-Ulm, Germany) was used as internal standard.

Peaks were identified by GC (6890 N, Agilent Technologies, Böblingen, Germany) coupled to a mass spectrometric (MS) detector (*m/z* 50–750, MSD 5973, Agilent Technologies, Böblingen, Germany). Again, the chromatographic conditions described above were used with the exception that helium was the carrier gas. Carrier gas pressure was held at 50 kPa for 5 min, then raised by 3 kPa min^{-1} to 150 kPa, followed by 50 min held at 150 kPa.

After chloroform extraction the de-waxed seed coat samples were further treated with 1 N HCl in 1,4-dioxane (Merck, Darmstadt, Germany) overnight at room temperature to transform epoxy groups into their respective chlorohydrin derivatives and with BF_3-Methanol (~10 %, Fluka, Neu-Ulm, Germany) overnight at 70 °C to depolymerise the cutin polymer and to release the cutin monomers as the corresponding methyl esters. After addition of 1-eicosanol (Fluka, Neu-Ulm, Germany) as internal standard chloroform was added to the vials which subsequently were agitated leading to a

partitioning of the cutin monomers between the polar and the apolar phase. The partitioning treatment was repeated twice and the chloroform supernatants pooled for further analysis. The cutin monomers were quantified by GC-FID using the internal standard and analysed by GC-MS as described above for the wax fraction. In the present case the GC temperature conditions for FID and MS detection were: injection at 50 °C, 1 min at 50 °C, temperature raise by 10 °C min^{-1} to 150 °C, held for 2 min at 150 °C, raise by 3 °C min^{-1} to 300 °C, and held for 30 min at 300 °C. Carrier gas inlet pressure was 50 kPa for 70 min, raised by 10 kPa min^{-1} to 150 kPa, and held for 30 min at 150 kPa. For lipid analyses six isolated seed coats were examined.

2.2 Chemicals used in the experiments

2.2.1 Model solutes

Experiments were performed with a set of model solutes selected for covering a wide range of physico-chemical properties (Table 2.1). These chemicals range in molecular size from 180 to 873 g mol^{-1} and in *n*-octanol/water partition coefficients log $K_{o/w}$ from -7.4 to 4.4. The *n*-octanol/water partition coefficient quantifies the partitioning of a solute between the lipophilic solvent *n*-octanol and water and thus can be used as a measure of a substance's lipophilicity. The substances used are seven active ingredients applied in commercial seed treatment, three sugars as hydrophilic model compounds naturally occurring in seeds, caffeine as an example of a plant-derived allelochemical which inhibits germination when taken up by seeds (Friedman and Waller 1983a), and the dye phloxine b. The active ingredients were obtained from Syngenta Crop Protection Münchwilen AG, Münchwilen, Switzerland. Purity of the AIs was ≥ 94 % w/w (difenoconazole, CAS Registry Number: 119446-68-3), ≥ 95 % w/w (fludioxonil [131341-86-1] and sedaxane [874967-67-6]) and ≥ 98 % w/w (thiamethoxam [153719-23-4]). In the case of ^{14}C-labelled substances radiochemical purity was ≥ 98 % (abamectin [71751-41-2], azoxystrobin [131860-33-8] and metalaxyl-M [70630-17-0]). Glucose and maltose (purity of both ≥ 99 %) were from Fluka, Neu-Ulm, Germany. Maltotriose (purity ≥ 95 %), phloxine b (CAS 18472-87-2, purity ≥ 80 %) and caffeine (purity ≥ 99 %) were from Sigma-Aldrich, Taufkirchen, Germany. Figure 2.2 shows figures of the active ingredients and Figure 2.3 shows figures of the sugars, dye and allelochemical used in the experiments. All solutes are undissociated at neutral pH (calculated by chemicalize.org by ChemAxon, Marvin Version 5.11.5, 2013, http://www.chemicalize.org) except for phloxine b which is partly present in a charged state and thus in the permeation experiments with this solute phosphate buffer (di-sodium hydrogen phosphate, Merck, Darmstadt, Germany and potassium dihydrogen phosphate, Roth, Karlsruhe, Germany) of a 40- fold higher concentration than the phloxine b concentration was used as solvent. Therefore, the difference in ionic strength on both sides of the barrier was very small and the effect of an electrical potential on the permeation process could be neglected (Tyree et al. 1990).

Table 2.1: Physico-chemical properties of the model substances used in the experiments: molecular weight (MW), molar volume (MV), *n*-octanol/water partition coefficient $K_{o/w}$ as a measure of substance lipophilicity, water solubility at 25 °C (WS) and substance group.

No.	Compound	MW [g mol^{-1}]	MV [a] [cm^3 mol^{-1}]	log $K_{o/w}$	WS [mg l^{-1}]	Substance group
1	Fludioxonil	248	153	4.1 [d]	1.8 [d]	fungicide
2	Thiamethoxam	292	181	-0.1 [d]	4100 [d]	insecticide
3	Metalaxyl-M	279	223	1.7 [d]	26000 [d]	fungicide
4	Sedaxane	331	235	3.3 [d]	14 [d]	fungicide
5	Difenoconazole	406	273	4.4 [d]	15 [d]	fungicide
6	Azoxystrobin	403	292	2.5 [d]	6 [d]	fungicide
7	Abamectin	873	668	4.4 [d]	0.007 – 0.01 [d]	insecticide
8	Glucose	180	126	-2.9 [b]	1 x 10^6 [b]	carbohydrate
9	Maltose	342	223	-5.0 [b]	1 x 10^6 [b]	carbohydrate
10	Maltotriose	504	326	-7.4 [b]	1 x 10^6 [b]	carbohydrate
11	Phloxine B	830	450	2.0 [c]	9 x10^4 [b]	dye
12	Caffeine	194	136	0.2 [b]	2632 [b]	allelochemical

[a] calculated according to (Abraham and Mcgowan 1987)

[b] estimated by EPI Suite software (v 4.10. United States Environmental Protection Agency, Washington, DC, USA)

[c] (Levitan 1977)

[d] Syngenta Material Safety Data Sheet

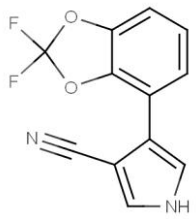

No. 1: Fludioxonil

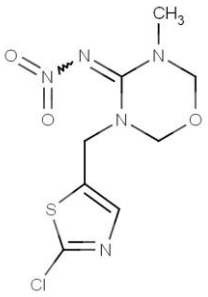

No. 2: Thiamethoxam

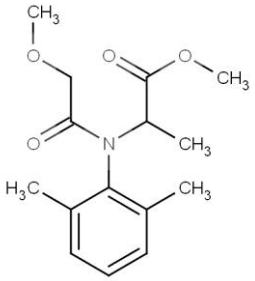

No. 3: Metalaxyl-M

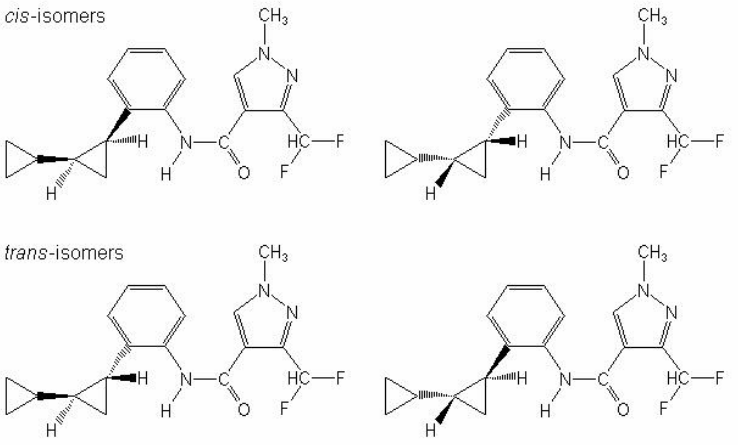

No. 4: Sedaxane

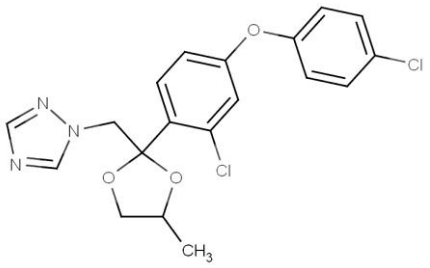

No. 5: Difenoconazole

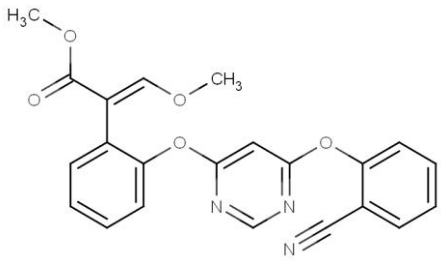

No. 6: Azoxystrobin

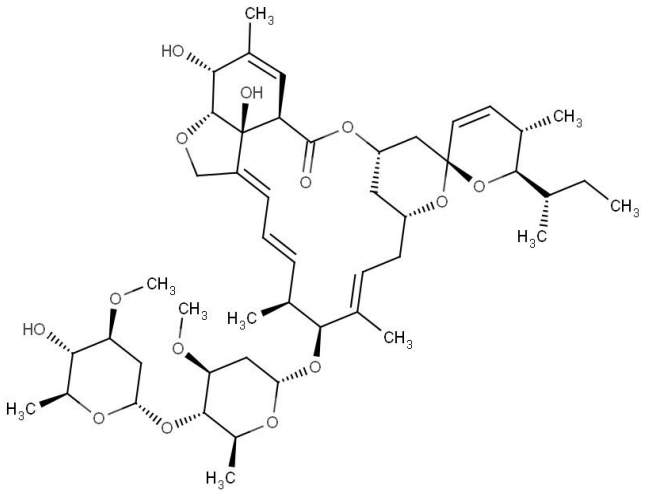

No. 7: Abamectin

Figure 2.2: Figures of the active ingredients used in the experiments.

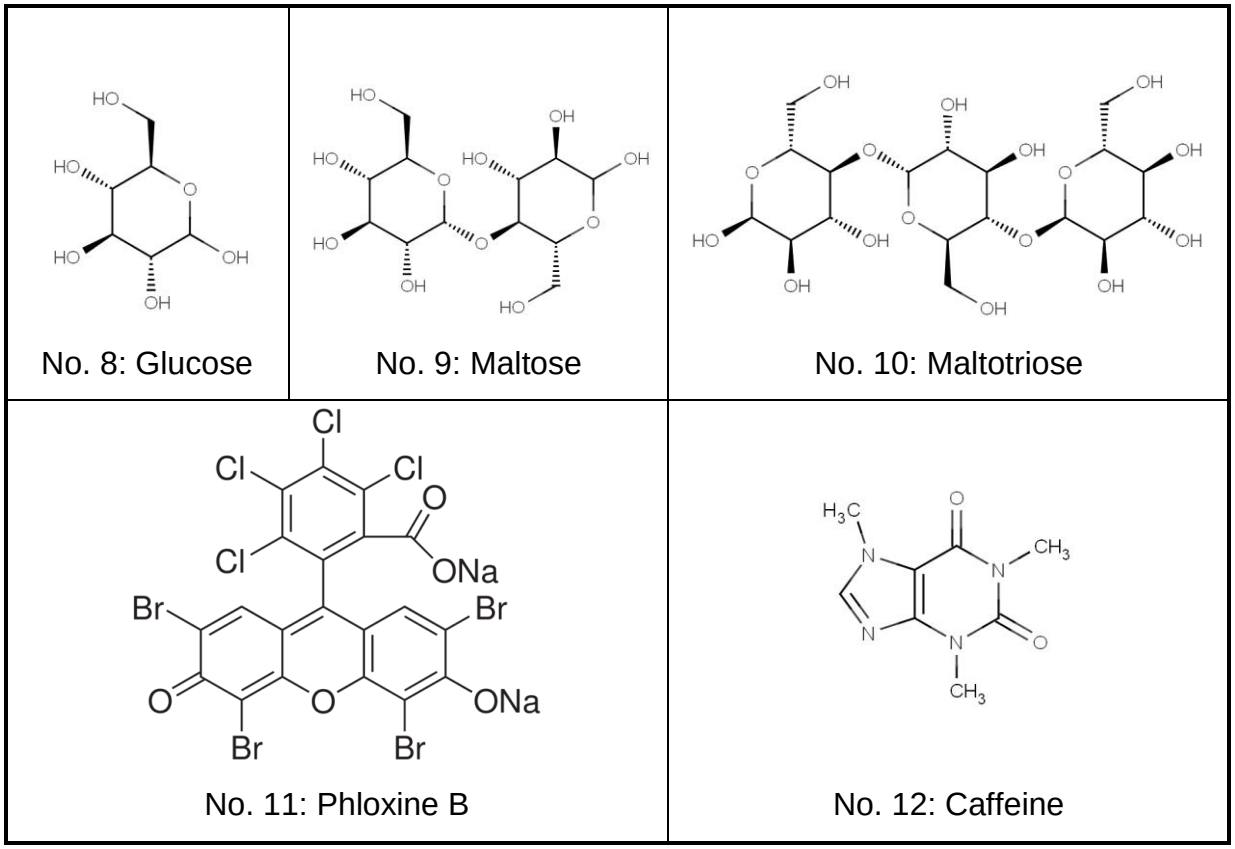

Figure 2.3: Figures of the sugars, dye and allelochemical used in the experiments.

2.2.2 Quantification of the solutes

For quantification of the solutes different detection methods were used. Part of the active ingredients were ^{14}C-labelled (abamectin: specific activity 2.32 MBq mg^{-1}, azoxystrobin: specific activity 2.02 MBq mg^{-1}, metalaxyl-M: specific activity 5.09 MBq mg^{-1}). These compounds were quantified by liquid scintillation counting (Tri Carb 2500, Canberra Packard, Germany) with scintillation cocktail (Ultima Gold XR, Canberra Packard, Germany) added to the samples.

For the non-labelled active ingredients (difenoconazole, fludioxonil, sedaxane, thiamethoxam), HPLC (high performance liquid chromatography) (1100 Series, Agilent Technologies, Böblingen, Germany) with a quaternary pump and a 1040M diode array detector at a wavelength of 220 nm was used for quantification. For sample preparation, the aqueous sample solution was evaporated under a gentle stream of purified air and the residue subsequently dissolved in 50 % acetonitrile

(HPLC grade, Roth, Karlsruhe, Germany) in water. Injection volume of the samples was 5 µl, and separation was achieved on a Nucleodur C-18 column (particle size 3 µm, column length 70 mm, column i.d. 4.6 nm, Macherey-Nagel, Düren, Germany) at 40 °C and with a flow rate of 1.2 ml min^{-1}. The eluent gradient with solvent B: methanol, solvent C: acetonitrile and solvent D: 0.1 % aqueous phosphoric acid started from 10 % B and 90 % D, to 30 % C and 10 % B (4 min), to 35 % C and 10 % B (14 min), to 35 % C and 40 % B (16 min), to 65 % C and 30 % B (19 min, 2 min held), to 90 % C and 5 % B (22 min, 5 min held), and back to initial conditions (27 min, 3 min held). Acetonitrile and methanol were HPLC grade from Roth, Karlsruhe, Germany and phosphoric acid (98 %) was from AppliChem, Darmstadt, Germany. Retention times and integrated peak areas were used for the identification and quantification of the substances. Calibration lines in the concentration range of the samples were linear in the range from 5 to 150 µg ml^{-1}.

The sugars (glucose, maltose, maltotriose) were quantified by HPLC combined with an evaporative light scattering detector (Sedex Model 75, Sedere, Alfortville, France). The column used was a Prevail Carbohydrate ES (5 µm, 250 mm, 4.6 mm, Grace Davison Discovery Sciences, USA). Injection volume was 20 µl and the eluent gradient started from 70 % solvent C (acetonitrile) and 30 % A (water), to 50 % C and 50 % A (7 min) and back to initial conditions (8 min). Again, calibration lines corresponding to the concentration range of the samples were used for identification and quantification of the substances. Calibration lines were linear in the range from 10 to 80 µg ml^{-1}.

The amount of phloxine b was measured photometrically at 570 nm (Multiskan EX, Thermo Labsystems, Vantaa, Finland). For quantification, a calibration line corresponding to the concentration range of the samples was used which was linear in the range from 20 to 400 µg ml^{-1}.

Caffeine was determined by a UV/Vis Spectrometer (Unicam UV4, Unicam, Cambridge, UK) at 273 nm. The calibration line used for quantification was in the concentration range of the samples and was linear from 1 to 20 µg ml^{-1}.

2.2.3 Additives

Two additives, NeoCryl A-2099 and adigor, were used in part of the experiments. These additives are commercially used in plant protection product formulations. Both additives were obtained from Syngenta Crop Protection Münchwilen AG,

Münchwilen, Switzerland. NeoCryl A-2099 is a film-forming mixture of a styrene acrylic polymer and water. It can be used either in overprint varnishes and barrier coating or as a crop safener in agrochemical formulations where it can prevent phytotoxicity in leaf applications (Angst et al. 2010).

Adigor is a commercial tank mix adjuvant based on methyl esters of canola oil fatty acids (Syngenta safety data sheet) and is used in commercial herbicide formulations to enhance effectiveness (Muehlebach et al. 2007). The surface-active additive adigor was examined by surface tensiometry (Tensiometer K8600, Krüss GmbH, Hamburg, Germany) at room temperature. Twelve different concentrations of adigor in deionised water in the range of 5×10^{-5} % to 1 % (w/v) were measured. At the critical micelle concentration, an increase in adigor concentration did not lead to any further reduction of the surface tension.

2.3 Seed imbibition

2.3.1 Seed water uptake from liquid water

To examine the seed water uptake process in the situation of maximal water availability, the imbibition of *Pisum sativum* seeds from liquid water was analysed. Whole pea seeds in their original dry state were weighed (SCALTEC SBA 31, SCALTEC Instruments GmbH, Göttingen, Germany) and placed into a glass of deionised water. At time intervals the seeds were taken out of the water, quickly blotted dry with tissue paper to remove adhering water and weighed again. Then the seeds were immediately returned into the water to continue the imbibition process, keeping the interruption as short as possible. The experiment was conducted at 4 °C. By plotting the weight increase over the time imbibition kinetics was obtained. Water uptake from liquid water was measured with ten seeds.

2.3.2 Seed water uptake from water saturated air

The swelling process of seeds in water saturated air was examined. Dry pea seeds were weighed (SCALTEC SBA 31, SCALTEC Instruments GmbH, Göttingen, Germany) and placed on a grid above deionised water in a tightly closed plastic box. The seeds were not in contact to liquid water and the air volume was as small as possible so that the seeds were surrounded by water saturated air. At time intervals, the seeds were taken out of the box for weight measurement and quickly replaced. The experiment was conducted at room temperature. To obtain imbibition kinetics the seed weight was plotted versus the time. Seed swelling in water saturated air was measured with eight seeds.

2.3.3 Seed water uptake from moist sand

To examine *Pisum sativum* seed imbibition in a situation close to the situation of a seed in the field, water uptake of pea seeds placed in moist sand was analysed. Before beginning of the swelling process the weight of pea seeds in their original dry state was measured gravimetrically on a balance (SCALTEC SBA 31, SCALTEC Instruments GmbH, Göttingen, Germany). Then the seeds were placed in glasses filled with purified sea sand (Merck, Darmstadt, Germany) with a particle size of 0.1 to 0.3 mm with 0.2 g water g^{-1} dry sand. The glasses were tightly closed and kept at

4 °C. The seed weight increase was measured gravimetrically after periods of time of 0.5 h, 1.5 h, 4 h, 8 h, 20 h, 40 h, 60 h and 80 h. The weight increase was plotted over the time to obtain imbibition kinetics. To examine the water uptake from moist sand, ten seeds were weighed at each time point.

2.3.4 Water uptake by isolated seed coats

As in part of the experiments isolated *Pisum sativum* seed coat halves were used, water uptake by these was examined, too. To obtain a swelling kinetics, the weight of isolated seed coat halves was measured gravimetrically on a micro-balance (S3D, Sartorius, Göttingen, Germany) in their original dry state before placing the seed coat halves into deionised water for swelling. In time intervals, the seed coat halves were taken out, quickly blotted dry with filter paper to remove adherent water and the weight increase was measured gravimetrically. The seed coat halves were immediately put back into water to resume swelling. As seed coat water uptake was very fast in the beginning, time intervals between weighing were as short as possible without interrupting the swelling kinetics too often. The weight increase was plotted over the time to obtain swelling kinetics. The swelling process of isolated seed coat halves was measured with 5 seed coat samples.

The mean maximum water uptake capacity by seed coats was measured with 100 samples. The weight of isolated seed coat samples in their original dry state was measured gravimetrically on a micro-balance (S3D, Sartorius, Göttingen, Germany) and then the seed coat samples were placed into liquid water over night. The swollen seed coat samples were taken out again, blotted dry with filter paper and the weight increase was quickly measured gravimetrically.

The maximum water uptake by isolated seed coat halves from water saturated air was also examined. The weight of isolated seed coat samples in their original dry state was measured gravimetrically on a micro-balance (S3D, Sartorius, Göttingen, Germany) and then the seed coat samples were placed into water saturated air over night. The seed coat samples were taken out again and the weight increase was measured gravimetrically. Ten seed coat samples were examined.

2.4 Seed coat hydraulic conductivity

The seed coat hydraulic conductivity L_{hydr} describes the barrier properties of the seed coat which control a hydraulic bulk flow of water. It is defined as the hydraulic bulk water flow F_{bulk}^{water} [g s^{-1}] across a barrier divided by the area involved A [m^2] and the water potential difference $\Delta\Psi$ [MPa] as driving force (equation 2.1).

$$L_{hydr} = \frac{F_{bulk}^{water}}{A \cdot \Delta\Psi} \qquad (2.1)$$

The resulting hydraulic conductivity L_{hydr} has the unit g s^{-1} m^{-2} MPa^{-1}. Alternatively, the flow F_{bulk}^{water} can also be described as a volume with the unit m^3 s^{-1}. Then the resulting unit of the hydraulic conductivity is m^3 s^{-1} m^{-2} MPa^{-1} or after reduction of the fraction m s^{-1} MPa^{-1}.

Two different experimental approaches were taken to examine a hydraulic mass flow of water across the seed coat driven by a known water potential difference as driving force.

2.4.1 Water flow driven by adjusted water potential difference

Water uptake across seed coats of whole, intact *Pisum sativum* seeds driven by a known water potential gradient as driving force was analysed. Whole pea seeds were placed for 24 h into aqueous PEG solutions of 200, 300, 400 and 500 g kg^{-1} PEG 8000 (7000 – 9000 g mol^{-1}, Fluka, Neu-Ulm, Germany) where they took up water until they had reached the same water potential as the outside solutions. The internal water potentials of these solutions were according to Michel (1983) -0.51, -1.09, -1.88 and -2.89 MPa, respectively. These seeds were in a swelling state between dry and completely swollen, so the surface area had to be estimated. Therefore, the seed length, height and width were measured, the mean diameter d calculated from these three parameters, and the surface area A calculated according to equation (2.2) assuming spherical shape of the seeds.

$$A = 4\pi \left(\frac{d}{2}\right)^2 \qquad (2.2)$$

These seeds with adjusted internal water potential were subsequently placed into deionised water for further swelling. For a short time, the water uptake by the seeds was driven by a known water potential gradient, which was the difference between the water potential of free water (0 MPa) and the adjusted internal water potential of the seeds (-0.51, -1.09, -1.88 and -2.89 MPa). The uptake of water by the seeds was measured gravimetrically at time points of 10, 20 and 30 min (SCALTEC SBA 31, SCALTEC Instruments GmbH, Göttingen, Germany). The experiment was performed at 25 °C. Water uptake by seeds with adjusted water potential was analysed with at least ten seeds per water potential. The resulting water inflow data with corresponding water potential difference $\Delta\Psi$ [MPa] was used to calculate the seed coat hydraulic conductivity L_{hydr} according to equation (2.1).

2.4.2 Measurement of the water potential difference during seed swelling

By measurement of the *Pisum sativum* seed water potential at different time points during the imbibition process it was possible to examine the seed coat hydraulic conductivity development during swelling. Dry seeds were placed into deionised water for swelling at room temperature. At time points of 1 h to 8 h ten seeds each were taken out of the water, quickly blotted dry with filter paper to remove adherent water and the seed water potential was measured by dewpoint potentiometery (WP4C dewpoint potentiometer, UMS, Munich, Germany). As the imbibition kinetics would have been interrupted for too long by the measurement, the seeds were not replaced into water and instead new seeds were taken out of the water at each time point. Consequently no nested samples could be obtained. Seed water potential measurement data are based on 2 to 10 replicates. The difference $\Delta\Psi$ [MPa] between the measured water potential of the seeds and the water potential of free water represents the driving force for water uptake across the seed coat. The hydraulic water flow F_{bulk}^{water} [g s^{-1}] driven by this water potential difference was measured in an imbibition experiment at room temperature as described in 2.3.1 with a sample size of n=7. As for the calculation of the seed coat hydraulic conductivity the area involved is needed, the seed length, height and width was measured with a sample of 20 seeds per swelling state and the seed surface area was calculated as described in 2.4.1. These data were used to calculate the pea seed coat hydraulic conductivity according to equation (2.1) for the different time points during imbibition.

2.5 Determination of seed coat/water partition coefficients

In analogy to the *n*-octanol/water partition coefficient $K_{o/w}$ which describes the partitioning of a solute between *n*-octanol and water, the seed coat/water partition coefficient $K_{sc/w}$ describes the partitioning behaviour of a solute between the pea seed coat and water. Therefore, $K_{sc/w}$ is a measure of the affinity of a substance to the seed coat. $K_{sc/w}$ is defined as the quotient of the equilibrium concentration of solute in the seed coat $c_{seed\ coat}$ [g g^{-1}] and the equilibrium concentration of solute in the aqueous phase c_{water} [g g^{-1}] (equation 2.3):

$$K_{sc/w} = \frac{c_{seed\ coat}}{c_{water}} \qquad (2.3)$$

To determine seed coat/water partition coefficients, a *Pisum sativum* seed coat sample with known swollen weight was incubated in an aqueous solution of the examined solute. The concentrations of the solutions ranged from 0.1 to 0.3 µg ml^{-1} for the radio-labelled substances. In the case of abamectin which has low water solubility a solution with a solid residuum was used to avoid total depletion of the solution and to obtain measurable solute amounts in the seed coat. The concentration of the abamectin solution was 0.025 µg ml^{-1}. In the case of the non-radio-labelled solutes concentrations ranged from 1 to 800 µg ml^{-1} except for phloxine b which had a concentration of 20 mg ml^{-1}.

To achieve equilibrium of the partitioning of the solute between water and seed coat material the sample was kept on a shaker for 24 h at 25 °C. After reaching equilibrium concentrations of the solute in water and seed coat material, the seed coat sample was taken out of the solution and carefully blotted dry with tissue paper. Care was taken to remove all solution adhering to the seed coat surface. To determine the solute amount in the seed coat sample, an extraction of the seed coat material was necessary. This was achieved by shaking the seed coat sample in 1 ml of 50 % acetonitrile in water for 1 h followed by treatment in an ultrasonic bath (Bandelin Sonorex Super RK 514 BH, Bandelin electronic, Germany) for 15 min. Then the solute concentration in the extract was measured as described in 2.2.2. To calculate the solute concentration in the seed coat sample $c_{seed\ coat}$ prior to extraction, the total solute amount extracted was divided by the swollen weight of the seed coat sample. The concentration of the solute in the aqueous solution c_{water} was also

measured and the seed coat/water partition coefficient $K_{sc/w}$ was calculated according to equation (2.3). For measurement of seed coat/water partition coefficients, at least six seed coat samples were used per substance.

The seed coat extraction procedure was tested for efficiency for azoxystrobin (number of samples n= 4), fludioxonil (n= 8), metalaxyl-M (n= 3), sedaxane (n=5) and thiamethoxam (n= 6). For this, the concentration of AI in the aqueous solution was measured before start of the experiment and the total amount of AI used in the experiment was calculated. After the experiment, the total amount of AI still left in the aqueous solution plus the total AI amount extracted from the seed coat sample were summed up to obtain the AI amount retrieved after the experiment. A difference between total solute amount before and after the experiment would hint at an insufficient seed coat extraction. The percentage of retrieved solute (recovery rate) was calculated for the five solutes tested.

2.6 Steady-state solute permeation across isolated seed coat halves

An experimental setup was devised for performing steady-state permeation experiments with isolated seed coat halves. In these experiments, the solute flow driven by a known concentration gradient from a donor solution across the seed coat into a receiver solution was recorded over time. An aqueous donor solution of the respective compound was added to the well of a 96-well microtiter plate. An isolated swollen pea seed coat half was placed on the well with the outer side of the seed coat half in contact to the donor solution. As receiver solution deionised water was pipetted into the seed coat half (Figure 2.4). The solute then permeates from the donor solution across the seed coat half into the receiver solution.

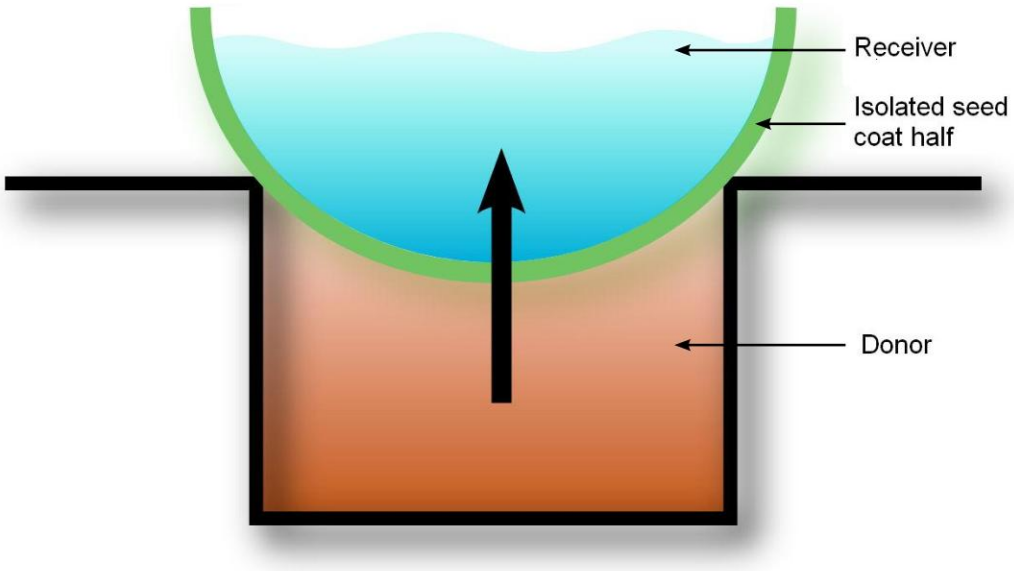

Figure 2.4: Experimental setup for permeation experiments. A seed coat half is placed onto a well of a microtiter plate which is filled with a donor solution of the substance studied. The seed coat half is filled with deionised water as receiver solution. Solute permeation takes place across the seed coat into the receiver solution which is removed for analysis and replaced by fresh solution at given time intervals.

The experiment was performed for all examined substances at 25 °C in an incubator (Memmert, Schwabach, Germany). To prevent dehydration of the pea seed coat halves the microtiter plate was covered with a lid and water was added to unused

wells. The donor concentrations in the experiments ranged from 0.1 to 0.4 µg ml^{-1} for the radio-labelled substances. In the case of abamectin which has low water solubility a solution with a solid residuum was used to avoid depletion of the donor (Kerler et al. 1984). The concentration of the abamectin solution was 0.025 µg ml^{-1}. Donor concentrations were 10 to 950 µg ml^{-1} for the non-labelled substances. In the case of lipophilic substances with *n*-octanol/water partition coefficients $K_{o/w} > 1$ the lipophilic sorption compartments in the seed coat were saturated prior to the experiment to prevent hold-up times in the transport kinetics (Kerler et al. 1984). To saturate the seed coat halves, they were placed onto a well filled with a solution of the substance. The seed coat was filled with receiver solution, and the solute amount reaching the receiver was monitored. When the solute amount moving into the receiver solution per time was constant, saturation of the seed coat was assumed. Then the seed coat was placed onto fresh donor solution to start the experiment. In time intervals of 0.5 to 1.5 h, according to the permeation speed, the solute amount permeated into the receiver solution was quantified. By taking the complete receiver solution for analysis and replacing it with fresh solution the concentration in the receiver compartment was kept close to zero. Permeated solute amounts were very small in relation to the amounts in the donor solution so that donor concentrations did not change significantly during the experiments and, thus, experiments were done under steady-state conditions. By summing up the permeated solute amounts for each time point linear transport kinetics was obtained for all model compounds.
By plotting the amount of solute permeated ΔM [g] over the time Δt [s] the flow rate F [g s^{-1}] was obtained from the regression line (equation 2.4):

$$F = \frac{\Delta M}{\Delta t} \tag{2.4}$$

The permeance P [m s^{-1}] was calculated from the flow rate F [g s^{-1}] divided by the area A [m^2] exposed and the concentration gradient Δc [g m^{-3}] which is the driving force for permeation (equation 2.5):

$$P = \frac{F}{A \cdot \Delta c} \tag{2.5}$$

For measuring the contact area A, seed coat halves were placed onto wells filled with 0.5 % (w/v) Evan's Blue (Sigma-Aldrich, Taufkirchen, Germany) solution for 30 min which led to an exact staining of the exposed area of the seed coat halves. Afterwards the stained parts of the seed coats were cut out, divided into preferably planar fragments, and scanned. The combined area of the fragments was calculated by comparison with a reference area of known size (Adobe Photoshop 7.0, Adobe Systems Incorporated, San José, USA). The contact area A amounted to 0.670 cm^2 (± 0.048) (n=23). In the permeation experiments all data obtained are based on at least eight replications.

2.6.1 Effect of temperature on permeation of thiamethoxam

To examine the effect of temperature on steady-state permeation the steady-state permeation experiment with isolated pea seed coats as described in chapter 2.6 was repeated with thiamethoxam at 20 °C, 25 °C, 30 °C and 35 °C in an incubator (Memmert incubator, Schwabach, Germany). By measuring permeation at all temperatures with the same seed coats nested samples were obtained. For each temperature, the permeance P was calculated according to equations (2.4) and (2.5).

2.6.2 Effect of a water potential gradient on solute permeation

In order to analyse the effect of a water potential gradient across the seed coat on solute permeation, experiments with 500 g kg^{-1} PEG 8000 (Fluka, Neu-Ulm, Germany) added to the receiver solution were performed. The donor solution was again an aqueous solution without PEG added and therefore had a water potential of 0 MPa. PEG of molecular weights of ≥ 4000 do not cross pea seed coats (Manohar 1966) and thus a water potential gradient of 2.89 MPa (Michel 1983) could be applied across the seed coat. The permeation experiments with isolated pea seed coats as described in 2.6 were performed without and with water potential gradient with glucose and with sedaxane as solutes.

2.7 Simulation of seed treatment AI distribution in moist soil

For the analysis of the seed coat permeation process in a more practical context, the situation of a treated seed in the soil was examined. Uptake by a treated seed in soil is different from the steady-state transport situation examined in the steady-state experiments. Treated seeds take up the AI from a seed treatment residue which dissolves in the moist soil environment and is depleted over time. The AI concentration difference as driving force thus changes over time and non-steady-state transport conditions are present. To simulate this process, a soil material had to be chosen which could be used to simulate the field environment. The process was analysed both with whole treated seeds and in a simplified model also with isolated treated seed coats, so methods for the treatment of both test objects had to be established. Additionally, experimental setups which could be used to analyse the processes taking place when a treated seed is placed into a moist soil environment were established.

2.7.1 Establishment of seed treatment methods

2.7.1.1 Treatment of whole seeds

For the treatment of whole pea seeds, 20 seeds each were placed with the treatment solution into a 100 ml beaker and treated by stirring. To obtain a uniform covering of the seeds they were stirred with the solution for 2 min at medium speed on a magnetic stirrer (IKA RCT basic, Ika Labortechnik, Staufen, Germany). The application amount of seed treatment solution had to be high enough to ensure homogeneous treatment of all seeds but too much solution would prevent rapid drying of the seeds after treatment. The optimal amount of treatment solution was found to be 60 - 100 µl. After treatment, the seeds were placed onto aluminium foil for drying, and the seed surface dried within minutes (Figure 2.5).

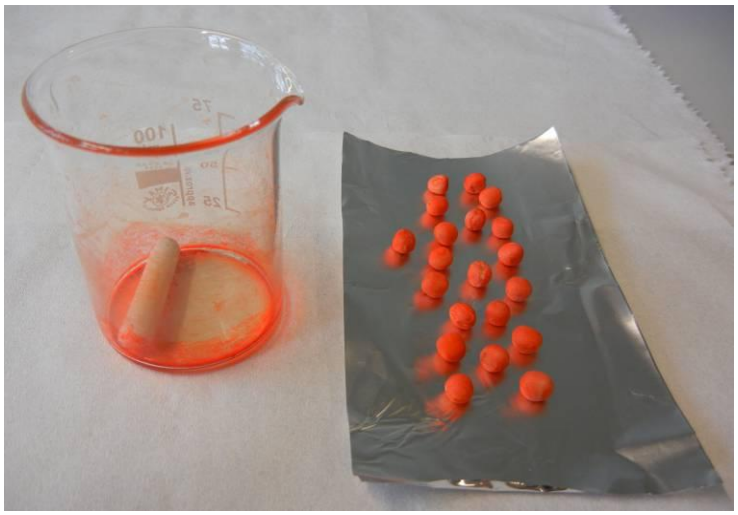

Figure 2.5: Result of seed treatment of whole seeds. For visualisation purposes, treatment was performed with a dye solution instead of AI treatment solution. 20 seeds are treated by stirring for two minutes with the seed treatment solution in a beaker. Afterwards the seeds are placed on aluminium foil for drying.

For treatment with metalaxyl-M a solution of 5 mg ml^{-1} of metalaxyl-M in water was used. To apply a covering layer of NeoCryl A-2099 above the AI layer, the treatment with AI was followed by two treatments with 30 µl of 2 % NeoCryl A-2099 solution, with thorough drying in between the treatments. The seed treatment solution for treatment with sedaxane contained 20 mg ml^{-1} sedaxane dissolved in 50 % acetonitrile in water. To obtain treated seeds with sedaxane with adigor, the treatment solution contained 20 mg ml^{-1} sedaxane and additionally 200 mg ml^{-1} adigor in 50 % acetonitrile in water.

To measure the applied solute amount, 10 of the 20 seeds treated per charge were subjected to extraction of the seed coats. The seed coats of the treated seeds were removed and all fragments obtained from a single seed were placed into a reaction tube. 1 ml of 50 % acetonitrile in water was added to each seed coat, and the solute was extracted by 1 h of shaking followed by 15 min treatment in an ultrasonic bath. Then the AI amount per seed was determined as described in chapter 2.2.2.

2.7.1.2 Treatment of isolated seed coat halves

To obtain isolated treated *Pisum sativum* seed coat halves, seed coat halves were removed from dry pea seeds as described in chapter 2.1.1. Only intact seed coat

samples without visible fractures were used. These isolated seed coat halves were treated with a seed treatment solution by applying an exact volume of the solution to the outer surface of the seed coat half with a pipette (Figure 2.6).

Figure 2.6: Isolated seed coat half directly after application of treatment solution with a pipette. Before start of the experiment, the treatment solution dried completely.

Different variations of the treatment were applied. For treatment with metalaxyl-M each seed coat half was treated with 6 µl solution with 5 g l^{-1} metalaxyl-M in water. To obtain treated seed coat halves with metalaxyl-M with a covering layer of NeoCryl A-2099, 6 µl of a 4 % NeoCryl A-2099 solution were applied over the metalaxyl-M layer after thorough drying of the AI treatment solution over night. To treat seed coat halves with sedaxane 5 µl treatment solution with 3 g l^{-1} sedaxane in 50 % acetonitrile in water were applied to each seed coat half. For experiments with treated seed coats with sedaxane and adigor, a treatment solution with 3 g l^{-1} sedaxane and 30 g l^{-1} adigor in 50 % acetonitrile in water was used. Again 5 µl were applied to each seed coat half. In the case of thiamethoxam treatment, each seed coat was treated with 10 µl of treatment solution containing 2.5 µg AI per µl deionised water. Seed coat halves were treated either without additive or with a covering layer of NeoCryl A-2099. In the case of NeoCryl A-2099 addition, a second treatment with 6 µl of 4 % NeoCryl A-2099 was applied on the seed coat half after the AI treatment solution was completely dry.

All treated seed coat halves were left over night for thorough drying before they were used for experiments.

2.7.2 Soil material

For the simulation of the situation of a treated seed in the field, a suitable soil material had to be chosen. Instead of field soil which is a complex and varying mixture of components, sand with known water content was used as simplified soil material. Purified sea sand (Merck, Darmstadt, Germany) with a particle size of 0.1 to 0.3 mm was used in all experiments with 0.2 g deionised water g^{-1} dry sand added. The sand water potential was determined for eight sand samples by dewpoint potentiometry (WP4C dewpoint potentiometer, UMS, Munich, Germany). To estimate the field capacity of the sand, an amount of sand was saturated with water and left in a chute covered with a lid and with a bit of filter paper at the bottom so that all excess water could drain away. An amount of this water saturated sand was measured gravimetrically on a balance (SCALTEC SBA 31, SCALTEC Instruments GmbH, Göttingen, Germany) and it was measured again in its completely dry state. By dividing the water content in g by the sand weight in g the field capacity was calculated.

The total sand amount needed for an experiment was prepared one day before the experiment by addition of the required amount of water to the sand and keeping the sand in a tightly closed container over night for allowing even distribution of the water throughout the sand.

2.7.3 Establishment of experimental setup

2.7.3.1 Distribution of AI from whole treated seeds

Experiments with whole treated seeds were performed in order to examine the process of seed treatment residue dissolution and movement of the seed treatment AI into the surrounding soil or across the seed coat into the embryo. By using whole seeds, the effect of water uptake by the swelling seed was included in the analysed process. Whole treated *Pisum sativum* seeds were placed into 25 ml glass vials filled with moist sand. In the moist sand environment the seed treatment residue dissolved. The solute then either stayed on the seed coat surface, or moved into the seed coat tissue or across the seed coat into the embryo, or it moved away from the seed surface into the surrounding moist sand. The experiment was performed with treated seeds with metalaxyl-M without additive or with a covering layer of NeoCryl A-2099 applied over the metalaxyl-M treatment. The experiment was also performed with

treated seeds with sedaxane without additive and with sedaxane combined with adigor. The samples were kept at 4 °C in moist sand for periods of time of 0.5 h, 1.5 h, 4 h, 8 h, 20 h, 40 h, 60 h and 80 h. At the chosen temperature of 4 °C, no germination of the seeds or rupture of the seed coat was visible throughout the time span of the experiment. After the incubation time, the seed was taken out of the sand, and the seed coat was removed from the seed. Prior to measurement of the AI amounts in sand and seed coat samples, an extraction in 50 % acetonitrile in water by 1 h of shaking and 15 min treatment in an ultrasonic bath followed by filtration or centrifugation to remove particles (Schlatter and Beste 2005, Bourgin et al. 2009) was performed. To calculate the amount of solute taken up after the time period t of the experiment, $M_t^{\text{taken up}}$, the solute amount in the sand M_t^{sand} and seed coat $M_t^{\text{seed coat}}$ were subtracted from the applied amount M_0 which had been determined after seed treatment for each treatment charge as described in 2.7.1.2 (equation 2.6):

$$M_t^{\text{taken up}} = M_0 - M_t^{\text{seed coat}} - M_t^{\text{sand}} \qquad (2.6)$$

For part of the samples treated with sedaxane the uptake amount was also measured directly by extraction of the embryo. With sedaxane high recovery rates could be obtained in embryo extraction and both direct measurement and calculation with equation (2.6) gave the same results. To extract the AI from the embryo, the embryo was cut into thin slices and the material was extracted three times with 4 ml of fresh solvent (50 % acetonitrile in water) each time by 1 h of shaking and 15 min treatment in an ultrasonic bath followed by filtration or centrifugation to remove particles. The AI amounts measured in the three fractions were summed up to obtain the total AI amount extracted from the embryo. Direct measurement of uptake was performed for part of the seeds treated with sedaxane without additives at 20 h (n= 12) and 40 h (n= 6) as well as for part of the seeds treated with sedaxane with adigor at 40 h (n= 10) and 60 h (n= 5). For the samples where AI amounts in the embryo were measured directly, recovery rates were calculated. The recovery rate is the total percentage of applied AI that can be recovered at the end of the experiment by extraction of the seed coat, sand and embryo fractions. For metalaxyl-M treated seeds, extraction of cotyledons from treated seeds can give low recovery rates (Singh 1989). A reason could be metabolisation of metalaxyl-M by the embryo into the more polar acid derivative (Gupta et al. 1985, Owen and Donzel 1986, Zadra et

al. 2002) and subsequent covalent binding to embryo organic matter (Senesi 1992, Gevao et al. 2000, Sigler et al. 2003). Consequently, for metalaxyl-M in all samples uptake was determined according to equation (2.6). For each type of seed treatment ten to 20 seeds were used for each time point.

2.7.3.2 Distribution of AI from isolated treated seed coat halves

Experiments with isolated treated seed coats were performed in order to examine the process of seed treatment residue dissolution and diffusive movement from the seed treatment residue either into the soil adjacent to the treated seed or across the seed coat into a receiver solution. The experiments with isolated treated seed coats were performed at room temperature on 96-well microtiter plates. The wells were filled with sand with a moisture content of 0.2 g water g^{-1} dry sand. The treated seed coat half was placed with the treated outer side of the seed coat in contact to the moist sand onto the well and the seed coat half was immediately filled with water as receiver solution to start the experiment (Figure 2.7).

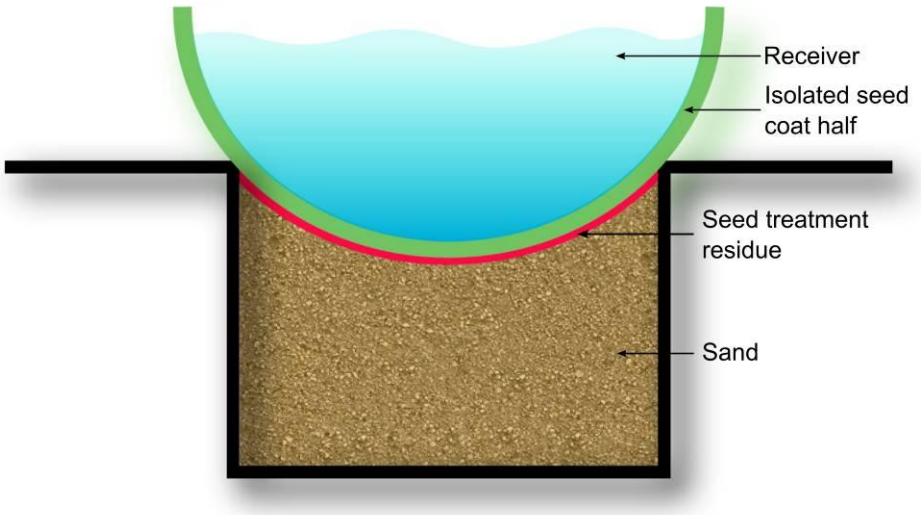

Figure 2.7: Experimental setup for the simulation of the situation of a treated seed in the soil with an isolated, treated seed coat. An isolated, treated seed coat half is placed onto a well of a microtiter plate which is filled with moist sand. The seed coat half is filled with deionised water as receiver solution. The seed treatment residue dissolves and the solute moves either into the sand or across the seed coat into the receiver solution. Receiver solution and sand are taken for analysis at time intervals.

Upon contact to water, the seed coat swelled, the seed treatment residue dissolved and the solute either remained associated with the seed coat or moved into the sand or across the seed coat into the receiver solution. In time intervals of 2 min the seed coat half was placed onto fresh sand and the receiver solution was taken for analysis and replaced by fresh water. The amount of solute in the receiver solution was measured as described in 2.2.2. To be able to measure the AI amounts in sand and seed coat samples, an extraction in 50 % acetonitrile in water by 1 h of shaking and 15 min treatment in an ultrasonic bath followed by filtration or centrifugation to remove particles (Schlatter and Beste 2005, Bourgin et al. 2009) was performed. The total accumulated amount of solute measured after the experiment in the receiver solution, sand samples and seed coat extract was summed up to obtain the exact amount applied M_0. In order to calculate the solute amount still remaining associated with the seed coat $M_t^{seed\ coat}$ at a given time point t, the accumulated solute amount at that time point in the receiver $M_t^{receiver}$ and in the sand M_t^{sand} were subtracted from the solute amount applied M_0 (equation 2.7):

$$M_t^{seed\ coat} = M_0 - M_t^{receiver} - M_t^{sand} \quad (2.7)$$

Three different AIs were examined in these experiments both without and with additive. The experiment was performed with treated seed coats with metalaxyl-M without additive and with a covering layer of NeoCryl A-2099 applied over the metalaxyl-M layer after drying. The experiment was also performed with treated seed coats with sedaxane without additive and in combination with adigor. As third AI, thiamethoxam was examined without additive and with a layer of NeoCryl A-2099 applied above the AI layer. Six parallels were examined for each type of treatment.

2.7.4 Quantification of uptake kinetics

To be able to compare uptake curves obtained from the experiments with treated seeds or treated seed coat halves the curves had to be described quantitatively.

As in these non-steady-state experiments the concentration difference as driving force is reduced over time, uptake is a first-order process. At the beginning of AI distribution the AI concentration on the seed coat is high and consequently the resulting uptake rate in this phase is high. Over the time the AI reservoir is depleted

and thus the uptake rate slows down. The curve converges to the final relative uptake amount $\frac{M_{t\to\infty}}{M_0}$ which is actually taken up across the seed coat at the end of the experiment. The remaining fraction of M_0 is the amount which is washed off into the sand or remains associated with the seed coat. The uptake percentages were plotted versus the time and a curve fit of a nonlinear regression (exponential rise to maximum, two parameters, equation 2.8) was performed on the data with SigmaPlot 12.0 (Systat Software, Inc., San José, USA).

$$\frac{M_t}{M_0} = \frac{M_{t\to\infty}}{M_0} \cdot (1 - e^{-kt}) \qquad (2.8)$$

In this description of the uptake kinetics, M_t is the AI amount taken up at the time t, M_0 is the AI amount which was initially applied, $M_{t\to\infty}\ M_0^{-1}$ in % is the fraction of applied AI which is taken up at the end of the experiment, k in h^{-1} or min^{-1} is the rate constant which describes the uptake speed and t is the time in h or min.

2.8 Statistics

Results are given as means with 95 % confidence intervals. For graphs and statistical analyses SigmaPlot 12.0 (Systat Software, Inc., San José, USA) was used. For statistical analyses, results were tested for normal distribution by the Shapiro-Wilk test. The unpaired t-test was used to test for statistical significance of differences in the case of normal distribution and otherwise the Mann-Whitney rank sum test was used.

3. Results

3.1 Characterisation of the seed material

3.1.1 Seed weight and surface area

Whole seeds of *Pisum sativum* had a weight of 0.316 g (± 0.014) when in their original dry state and 0.617 g (± 0.030) when completely swollen. The seeds increased their weight by a factor of 1.95 during imbibition. The measured surface area of whole dry seeds was 1.68 cm^2 (± 0.05) and of swollen seeds 2.70 cm^2 (± 0.17). In part of the experiments isolated *Pisum sativum* seed coat halves were used. These seed coat halves could be isolated from dry as well as from swollen pea seeds. The total isolated testa material of an individual pea seed had a dry weight of 23.03 mg (± 1.47). When placed in water isolated seed coat samples increased their weight by a factor of 2.29; they took up 1.29 mg (± 0.03) water per mg of dry seed coat material.

3.1.2 Microscopical characterisation of the seed coat

The *Pisum sativum* seed coat sections viewed by light microscopy consisted of several characteristic cell layers (Figure 3.1).

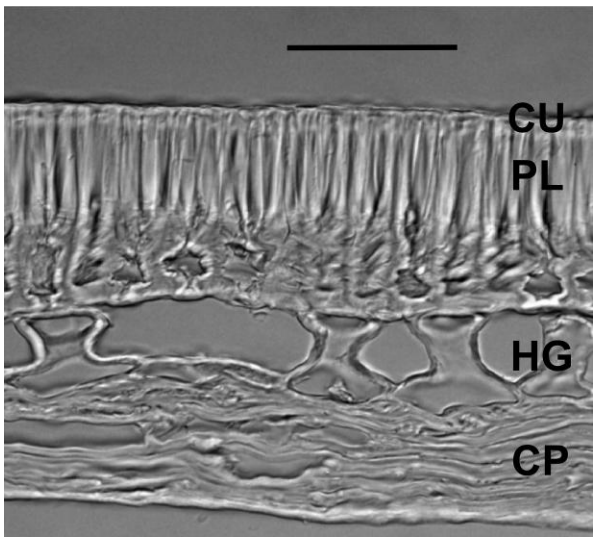

Figure 3.1: Section through an isolated pea seed coat. Visible cell layers are the palisade cell layer (PL) with the covering cuticle (CU), the hourglass cell layer (HG) and the layer of compressed parenchyma cells (CP). Scale bar represents 100 µm.

The visible cell layers of pea seed coats were palisade cells with a covering cuticle as outermost layer, hourglass cells and the cell wall material of crushed, compressed parenchyma cells as innermost layer. The average thickness of isolated swollen *Pisum sativum* seed coats was 185.8 µm (± 22.1).

3.1.3 Chemical characterisation of seed coat lipids

The total amount of lipids extractable from *Pisum sativum* seed coats with chloroform was 15.9 µg (± 4.3) per seed coat. The amount of typical cuticular waxes identified in the soluble fraction extracted from pea seed coats was 3.62 µg (± 1.75) per seed coat (Table 3.1). This results in a mean wax coverage of swollen pea seed coats of 1.34 µg cm^{-2}. The dominating aliphatic cuticular compound in the soluble wax fraction was hentriacontan (2.97 µg (± 1.53) per seed coat). Besides typical cuticular wax compounds the fraction extracted with chloroform also contained a large amount of short chain free fatty acids (C16 – C20, 6.49 µg (± 2.49) per seed coat) and β-sitosterol (0.185 µg (± 0.107) per seed coat). The total amount of lipids obtained by BF_3-MeOH transesterification from pea seed coats was 304.4 µg (± 34.9) per seed coat. The most important substances in this lipid fraction were hexadecanoic acid (21.8 µg (± 3.8); Table 3.1) and octadecanoic acid (19.4 µg (± 2.3)), 16-hydroxy hexadecanoic acid (17.4 µg (± 5.4)), 7- hydroxy hexadecan-dioic acid or 8-hydroxy hexadecan-dioic acid (13.7 µg (± 1.4)) and 9,16-dihydroxy hexadecanoic acid (25.0 µg (± 3.9)) as well as β-sitosterol (49.9 µg (± 9.3)). The sum of the amounts of soluble lipids and lipids obtained after transesterification taken together gives a lipid fraction of 320.3 µg (± 37.0) per seed coat.

Table 3.1: Substances in the extractable lipid fraction and lipid fraction released by transesterification of *Pisum sativum* seed coats, amounts and percentages per fraction given as means with 95 % confidence intervals.

Fraction	Compound			Amount extracted per seed coat [µg]	Amount of fraction [%]
Extractable lipids	Aliphatic cuticular waxes	Alkanes	C27	0.0987 ± 0.0194	0.634 ± 0.123
			C29	0.177 ± 0.051	1.12 ± 0.19
			C31	2.97 ± 1.53	18.2 ± 7.1
		Primary alcohols	C26	0.154 ± 0.061	0.966 ± 0.288
			C28	0.222 ± 0.101	1.38 ± 0.46
	Short chain free fatty acids		C16	2.28 ± 0.84	14.1 ± 2.6
			C18	4.11 ± 1.62	25.3 ± 5.2
			C20	0.0947 ± 0.0388	0.582 ± 0.135
	β-sitosterol			0.185 ± 0.107	1.12 ± 0.50
	not identified			5.62 ± 1.32	32.7 ± 7.7
Lipids released by trans-esterification	Fatty acids		C16	21.8 ± 3.8	7.16 ± 0.92
			C18	19.4± 2.3	6.39 ± 0.46
	OH-fatty acids		16-OH C16	17.4 ± 5.4	5.72 ± 1.60
			7/8-OH-1,16- C16	13.7 ± 1.4	4.51 ± 0.43
			9,16-diOH C16	25.0 ± 3.9	8.20 ± 0.78
	β-Sitosterol			49.9 ± 9.3	16.3 ± 1.5
	Others			58.6 ± 8.7	19.2 ± 1.0
	Not identified			98.6 ± 9.6	32.5 ± 2.5

3.2 Seed imbibition

3.2.1 Seed water uptake from liquid water

Water uptake by whole *Pisum sativum* seeds placed into deionised water followed specific kinetics (Figure 3.2). After a short lag phase, the seeds rapidly increased their weight. Between 2 h and 6 h weight increase was nearly linear. In this linear phase the slope of the uptake curve represents a seed water uptake of 0.10 g water per g dry weight per h. After 7 hours the water uptake rate slowed down again and at the end a plateau phase was reached where the weight remained constant. After seed imbibition the final seed weight was nearly twice the initial seed weight.

A small percentage of the pea seed lot showed the phenomenon of hardseededness (Werker 1997, Meyer et al. 2007). These seeds did not increase their weight when exposed to water, even after overnight incubation in water. Such hard seeds were discarded and were not used in the experiments.

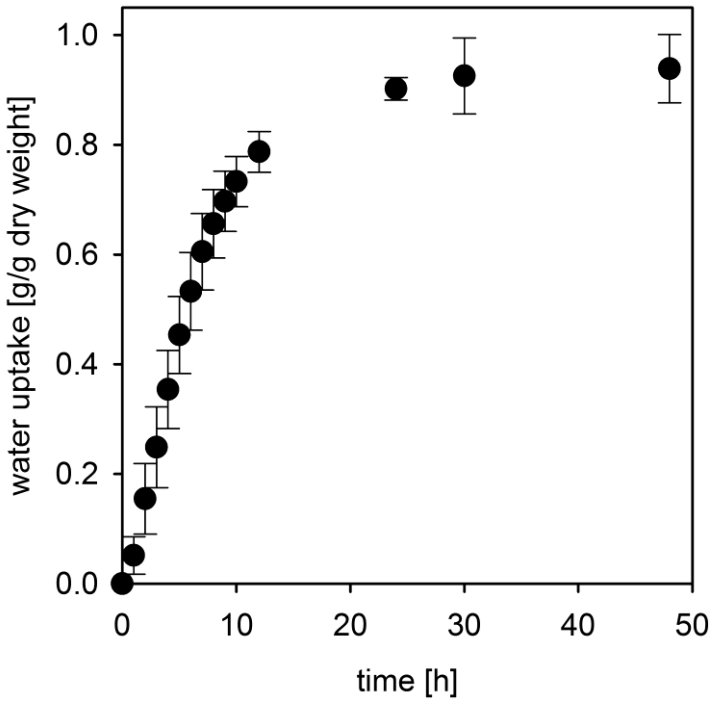

Figure 3.2: Weight increase of whole dry *Pisum sativum* seeds placed into liquid water at 4 °C. Results are given as means with 95 % confidence intervals.

3.2.2 Seed water uptake from water saturated air

Pisum sativum seeds were able to take up water from surrounding water saturated air (Figure 3.3). In the first two days in water saturated air the seeds showed the fastest water uptake. In this phase of the water uptake kinetics the slope of the kinetics is 3.25 x 10^{-3} g water per g dry weight per h, which is by a factor of 30 slower than water uptake by seeds placed into liquid water (Figure 3.2). In the following time the uptake rate slowed down. After 14.75 days the seeds had taken up 0.25 g water per g dry seed weight. At this time point the maximum seed swelling state as shown by swelling seeds in liquid water was not yet reached but if the seeds were left for longer periods of time in water saturated air germination and growth of microbial contaminants could start.

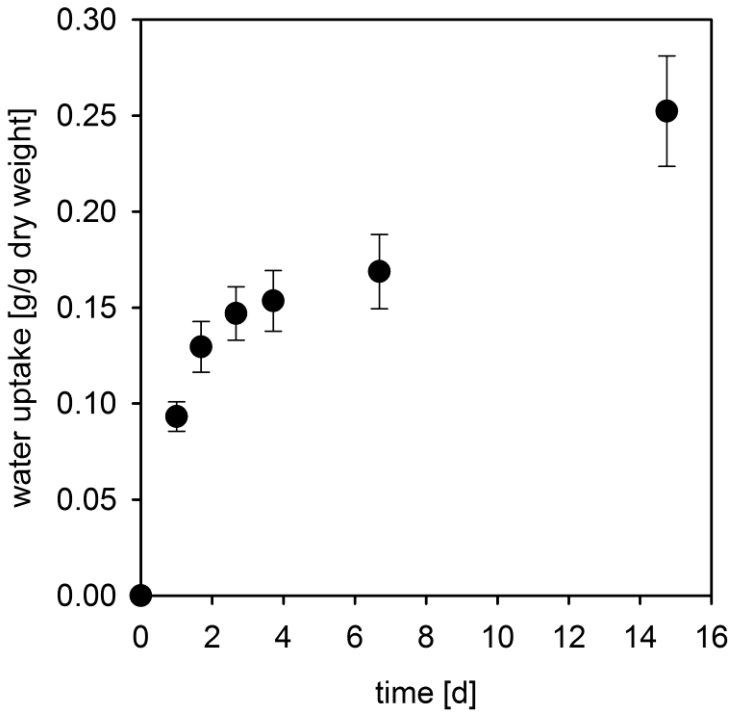

Figure 3.3: Weight increase of whole dry *Pisum sativum* seeds placed into water saturated air at room temperature. Results are given as means with 95 % confidence intervals.

3.2.3 Seed water uptake from moist sand

Pisum sativum seeds placed into sand with a moisture content of 0.2 g water per g of dry sand at 4 °C showed distinct imbibition kinetics. After a short lag phase during the first hours, water uptake by pea seeds placed into moist sand was nearly linear between 4 and 20 hours. In this fastest water uptake phase the seeds took up 0.020 g water per g dry weight per hour, which is by a factor of 5 slower than the maximum water uptake rate reached by seeds placed in liquid water (Figure 3.2) and 6 times faster than the maximum water uptake rate from water saturated air (Figure 3.3). After 40 hours, water uptake continued slightly slower until after 60 hours a plateau is reached. After 60 hours the seeds did not increase their weight anymore and imbibition was complete. At 4 °C, no visible germination processes took place during the experiment. In all cases the seed coats surrounding the seeds remained intact.

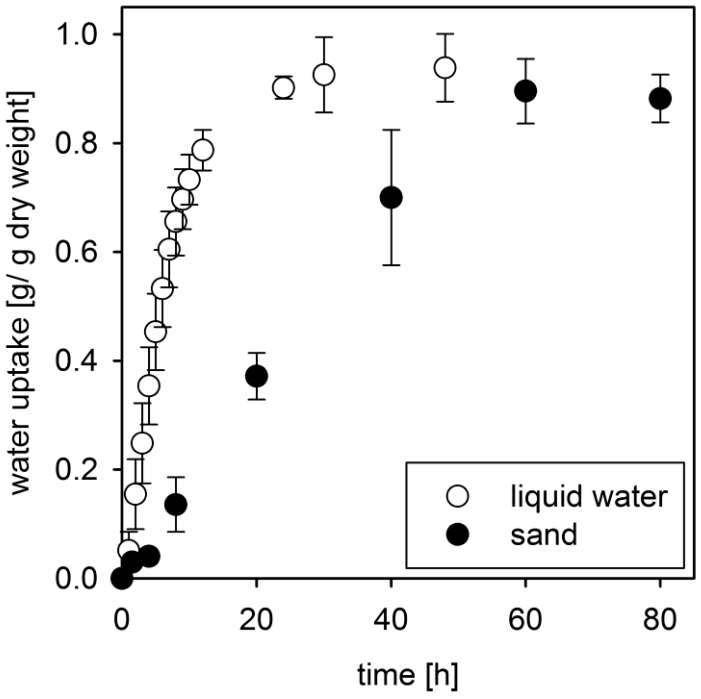

Figure 3.4: Uptake of water by whole dry *Pisum sativum* seeds at 4 °C. Shown is the water uptake by pea seeds placed into moist sand with a moisture content of 0.2 g water g^{-1} dry sand (black symbols) in comparison with pea seed water uptake from liquid water (white symbols). Results are given as means with 95 % confidence intervals.

3.2.4 Water uptake by isolated seed coats

As for some experiments isolated seed coat halves of *Pisum sativum* seeds were used instead of whole intact seeds, water uptake kinetics by such seed coat halves was examined. When dry isolated pea seed coat halves were placed into liquid water, initial water uptake was very fast (Figure 3.5). The seed coat halves took up 0.96 g water per g dry seed coat weight within the first two minutes of the swelling kinetics. This water uptake is nearly ten times faster than the maximum water uptake rate by whole pea seeds in liquid water. In the following minutes the swelling process continued much slower as the seed coats took up only 0.01 to 0.03 g water per g dry weight per minute. After 20 min the uptake kinetics reached a plateau phase.

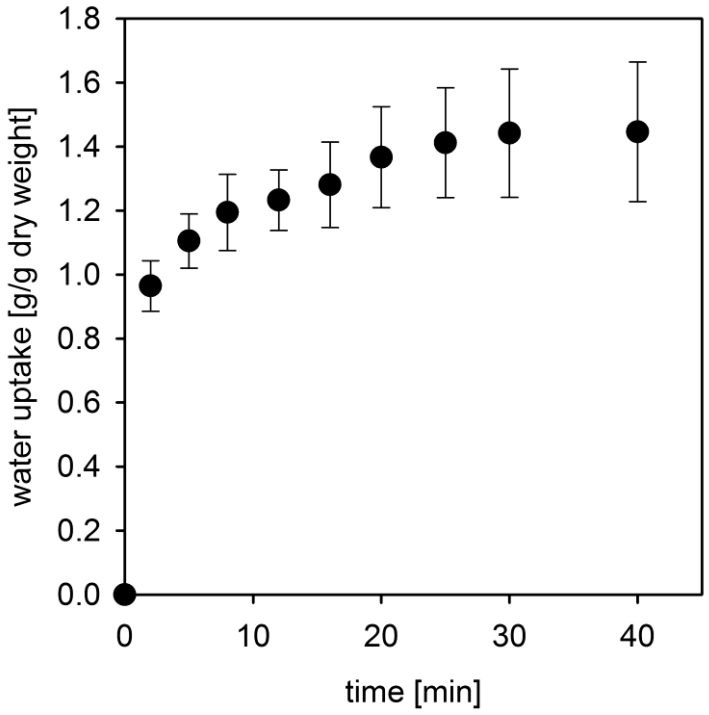

Figure 3.5: Water uptake by dry isolated *Pisum sativum* seed coat halves placed into liquid water at room temperature. Results are given as means with 95 % confidence intervals.

When placed into water saturated air over night, isolated seed coat halves took up 0.80 mg (± 0.07) water mg^{-1} of dry weight. The mean maximum seed coat water uptake capacity from liquid water was 1.61 fold higher.

3.3 Seed coat hydraulic conductivity

To describe the seed coat barrier properties towards inflowing water, the seed coat hydraulic conductivity L_{hydr} was determined. For this purpose, the water uptake of whole pea seeds was measured in correlation to the water potential gradient as the driving force. Two different approaches were used to measure L_{hydr}, which are a water inflow into seeds with adjusted internal water potential and a direct measurement of the seed water potential and water uptake at different time points during imbibition.

3.3.1 Water flow driven by adjusted water potential difference

In PEG solutions with known water potential, whole *Pisum sativum* seeds took up water until the water potential between seed interior and surrounding solution was equal. In these solutions the seeds reached an intermediate swelling state and remained in this state. The seeds did not complete imbibition in the PEG solutions. When these seeds with adjusted internal water potential were placed into liquid deionised water they continued the imbibition process. Subsequent water uptake by these seeds correlated linearly with increasing water potential gradient between seed interior and surrounding water (Figure 3.6). An increase in water potential gradient between adjusted seed interior and surrounding liquid water from -0.5 to -2.9 MPa led to an increase in water influx across the seed coat from 0.048 g s^{-1} m^{-2} to 0.122 g s^{-1} m^{-2}.

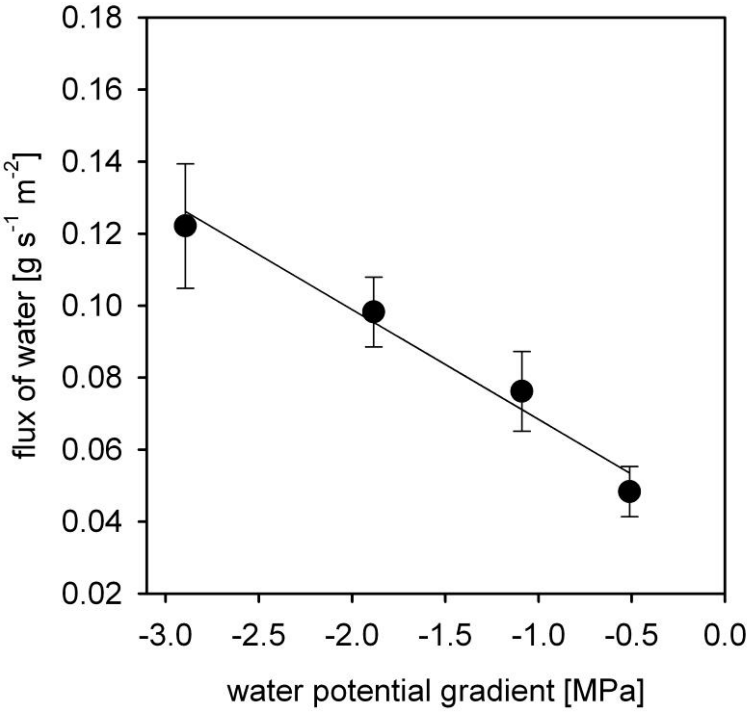

Figure 3.6: Uptake of water by *Pisum sativum* seeds with adjusted internal water potential placed into deionised water at room temperature, plotted versus the water potential gradient. Results are given as means with 95 % confidence intervals. The regression line is given by the equation y = 0.0305 x + 0.0379 (R^2 = 0.68), with the slope representing the hydraulic conductivity L_{hydr} (g s^{-1} m^{-2} MPa^{-1}) of *Pisum sativum* seed coats.

The slope of the regression line in the plot of flux versus water potential gradient as the driving force (Figure 3.6) represents the mean hydraulic conductivity L_{hydr} of the pea seed coats measured in the swelling experiment (equation 2.1). It amounts to 0.0305 g s^{-1} m^{-2} MPa^{-1} (± 0.0060) or if the water flux is described in the unit of a volume 3.05 x 10^{-8} m s^{-1} MPa^{-1}.

3.3.2 Direct measurement of water potential difference

To observe the seed coat hydraulic conductivity in more detail during the process of seed imbibition, the seed water potential was measured directly at different time points during the swelling process of whole *Pisum sativum* seeds. By this approach the driving force for water inflow at each time point was obtained. Thus, for each examined time point during the swelling process the hydraulic conductivity (equation 2.1) could be calculated. During the *Pisum sativum* seed imbibition process, the water flow increased after a short lag phase and slowed down again after 6 h (Figure 3.7 A). The seed water potential was initially -152 MPa but increased rapidly to -3.92 MPa during the first hour of imbibition (Figure 3.7 B). The seed water potential converged to 0 towards the end of the kinetics. The resulting calculated seed coat hydraulic conductivity L_{hydr} changed during seed swelling (Figure 3.7 C). L_{hydr} increased with increasing water content of the seed. In the nearly dry state at the beginning of seed swelling the hydraulic conductivity was 0.0019 g s^{-1} m^{-2} MPa^{-1}. After a short lag phase in the first 2 hours the hydraulic conductivity increased faster and reached values of 0.18 g s^{-1} m^{-2} MPa^{-1} after 4 hours and 0.46 g s^{-1} m^{-2} MPa^{-1} after 6 hours. At 8 h, when the seed imbibition process was nearly completed, the hydraulic conductivity was 0.69 g s^{-1} m^{-2} MPa^{-1}.

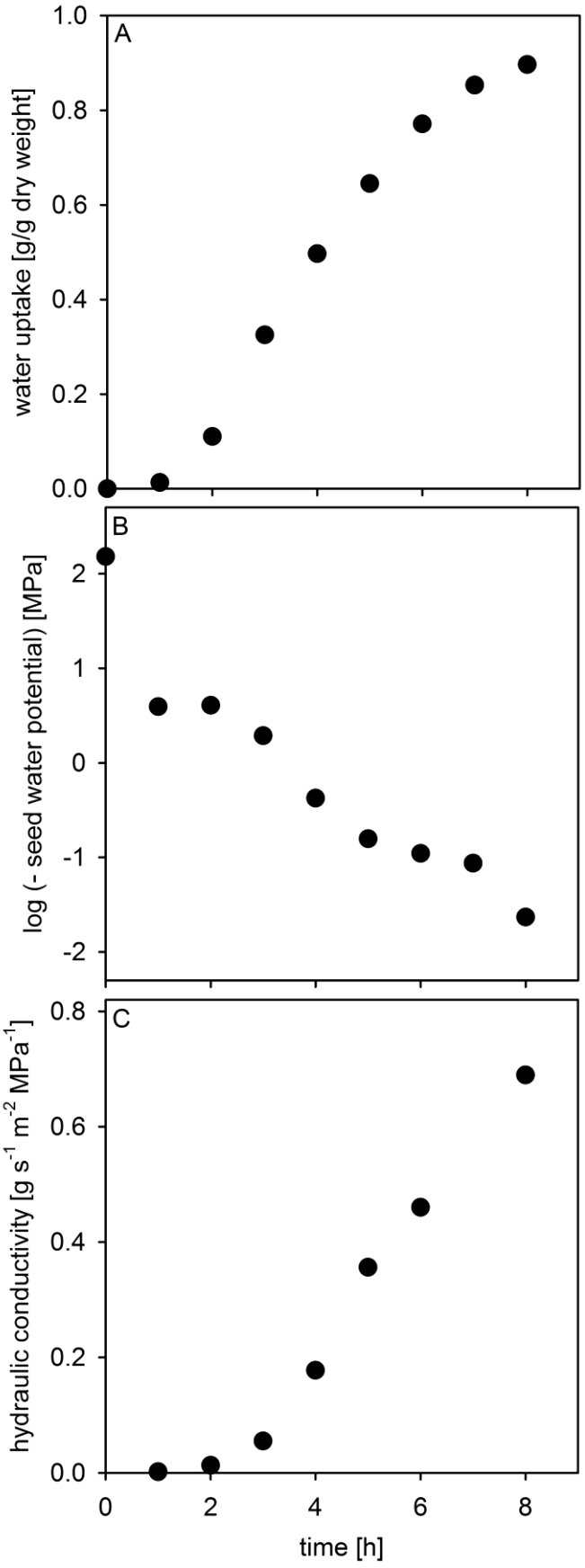

Figure 3.7: Uptake of water by dry *Pisum sativum* seeds (A), seed water potential (B) and hydraulic conductivity of the seed coat (C) during the swelling process at room temperature in liquid water. Results are given as means.

3.4 Determination of seed coat/water partition coefficients

Seed coat/water partition coefficients $K_{sc/w}$ were measured for the analysis of sorption of AIs in the seed coat. To measure the AI amounts absorbed by the seed coat samples, the seed coat samples had to be extracted after the incubation time. An insufficient seed coat extraction would lead to mistakes in determined seed coat/water partition coefficients. Therefore, the method used to extract the seed coat material was tested for efficiency with a range of AIs.

3.4.1 Validation of seed coat extraction method

The seed coat extraction method which was used in order to quantify the solute amount in the *Pisum sativum* seed coat at the end of the seed coat/water partition coefficient experiments was efficient as nearly the total solute amount initially applied in the experiment could be located again at the end of the experiment. By summing up the solute amount measured in the water plus seed coat extracts at the end of the experiment the recovery rate was obtained. The mean recovery rate was 97.8 % of the initial amount (Table 3.2). For the different extracted solutes the recovery rate ranged from 92 % to 103 % which means that hardly any non-extracted solute was left associated with the seed coats after seed coat extraction.

Table 3.2: Percentage of the initial solute amount detectable in water plus *Pisum sativum* seed coat extract (recovery rate) after the seed coat/water partition coefficient experiments, given as means with 95 % confidence intervals.

No.	Compound	Recovery rate after seed coat extraction
1	Fludioxonil	91.7 ± 2.7
2	Thiamethoxam	97.9 ± 0.4
3	Metalaxyl-M	103.1 ± 3.8
4	Sedaxane	95.9 ± 3.1
6	Azoxystrobin	100.2 ± 3.2

3.4.2 Seed coat/water partition coefficients

The seed coat/water partition coefficients ($K_{sc/w}$) of the set of model compounds measured with *Pisum sativum* seed coats covered only two orders of magnitude while the corresponding *n*-octanol/water partition coefficients cover a much broader range (Table 2.1). The seed coat/water partition coefficients ranged from 0.316 for the hydrophilic sugar maltotriose to 83.8 for the lipophilic AI abamectin (Table 3.3) and the values increased with increasing solute lipophilicity.

Table 3.3: Seed coat/water partition coefficients $K_{sc/w}$ of the substances studied, measured with isolated *Pisum sativum* seed coats, given as means with 95 % confidence intervals.

No.	Compound	$K_{sc/w}$
1	Fludioxonil	53.2 ± 3.2
2	Thiamethoxam	0.707 ± 0.043
3	Metalaxyl-M	0.858 ± 0.052
4	Sedaxane	5.64 ± 0.56
5	Difenoconazole	58.4 ± 4.0
6	Azoxystrobin	2.99 ± 0.21
7	Abamectin	83.8 ± 11.5
8	Glucose	0.634 ± 0.072
9	Maltose	0.443 ± 0.058
10	Maltotriose	0.316 ± 0.036
11	Phloxine B	0.723 ± 0.035
12	Caffeine	1.99 ± 0.11

3.5 Steady-state solute permeation across isolated seed coat halves

3.5.1 Validation of established experimental setup

An experimental setup was developed (Figure 2.4) which made the determination of permeances of *Pisum sativum* seed coats feasible. In the transport experiments, steady-state conditions could be achieved as shown by linear transport kinetics (Figure 3.8) and nearly constant donor concentrations during experiments. Permeances could be obtained for a set of model solutes with different physico-chemical properties. An advantage of the established experimental setup was that nested samples could be taken at a sequence of time points with a single seed coat half.

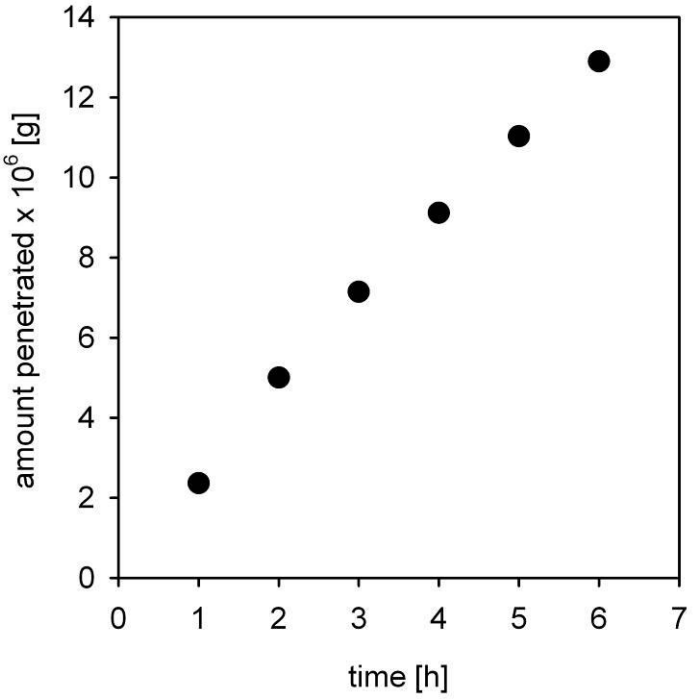

Figure 3.8: Typical transport kinetics of solute permeation across a swollen isolated *Pisum sativum* seed coat. Shown is thiamethoxam permeation in g plotted versus the time in h.

3.5.2 Permeances across *Pisum sativum* seed coats

With the steady-state experiments it was observed that isolated *Pisum sativum* seed coats were permeable to all of the examined model solutes. Permeances could be measured for each solute. The permeances measured in the steady-state permeation experiments across isolated swollen *Pisum sativum* seed coats at 25 °C with a set of model compounds ranged from 3.34 x 10^{-8} m s^{-1} for abamectin to 18.9 x 10^{-8} m s^{-1} for caffeine (Table 3.4). Therefore, the permeance of the fastest and the slowest solute differed by a factor of 5.7.

Table 3.4: Permeances P [m s^{-1}] of the substances studied across swollen isolated *Pisum sativum* seed coats at 25 °C, given as means with 95 % confidence intervals.

No.	Compound	P [x 10^{8} m s^{-1}]
1	Fludioxonil	14.1 ± 1.8
2	Thiamethoxam	15.7 ± 1.2
3	Metalaxyl-M	12.9 ± 0.9
4	Sedaxane	12.4 ± 0.7
5	Difenoconazole	8.14 ± 1.70
6	Azoxystrobin	12.5 ± 0.3
7	Abamectin	3.34 ± 0.75
8	Glucose	13.9 ± 2.0
9	Maltose	10.7 ± 1.1
10	Maltotriose	8.09 ± 0.82
11	Phloxine B	6.52 ± 0.40
12	Caffeine	18.9 ± 1.7

3.5.3 Effect of temperature on permeation of thiamethoxam

In the examined temperature range from 20 to 35 °C there was a linear relationship between permeation of thiamethoxam across isolated *Pisum sativum* seed coats and temperature. When the temperature at which the steady-state experiment with isolated pea seed coats was performed was increased by 15 °C, a 1.7 - fold increase in permeance followed (Table 3.5).

Table 3.5: Permeances P [m s^{-1}] of thiamethoxam across isolated *Pisum sativum* seed coats obtained at a temperature range from 20 °C to 35 °C, given as means with 95 % confidence intervals.

Temperature	P [x 10^8 m s^{-1}]
20 °C	11.6 ± 1.4
25 °C	14.1 ± 1.9
30 °C	15.8 ± 2.3
35 °C	19.6 ± 3.2

3.5.4 Effect of a water potential gradient on solute permeation

The use of a 500 g kg^{-1} PEG 8000 solution as receiver solution in the steady-state experiments with isolated *Pisum sativum* seed coats had an effect on solute flow. By the PEG solution in the receiver compartment, a water potential gradient was applied across the seed coat and solute flow from the donor across the seed coat to the receiver was increased. This increase in flow could be observed both for the hydrophilic solute glucose and for the lipophilic AI sedaxane (Figures 3.9 and 3.10). The resulting permeance of sedaxane was increased by a factor of 2.16 (± 0.89). The permeance of glucose was increased by a factor of 1.69 (± 1.00).

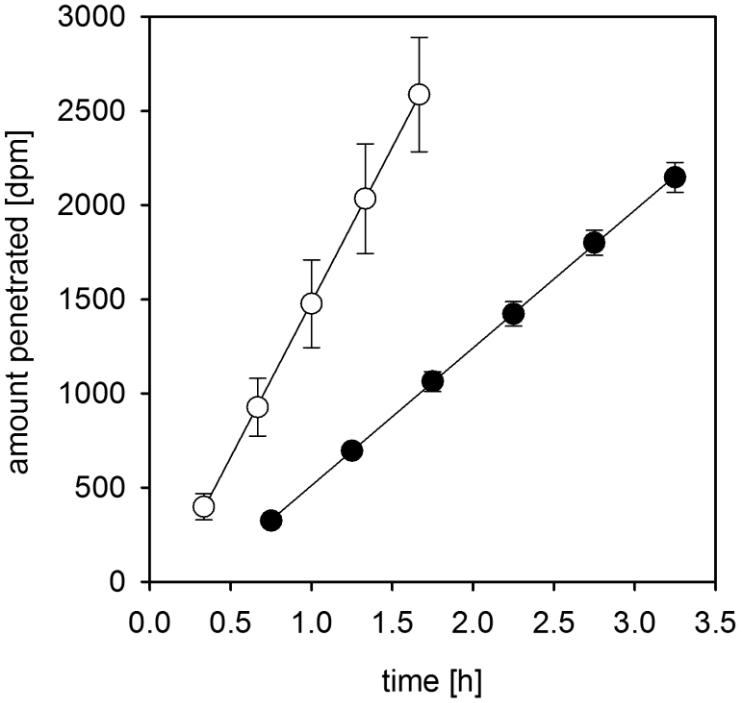

Figure 3.9: Flow of sedaxane across isolated *Pisum sativum* seed coats at 25 °C. The black symbols represent flow with deionised water as receiver solution and the white symbols represent flow with a water potential gradient applied by using a 500 g kg^{-1} PEG solution as receiver. Results are given as means with 95 % confidence intervals. The regression line for the kinetics without water potential applied is given by y = 730.8 x - 218.8 (R^2 = 0.99) and with water potential applied by y = 1645.6 x - 160.8 (R^2 = 0.90).

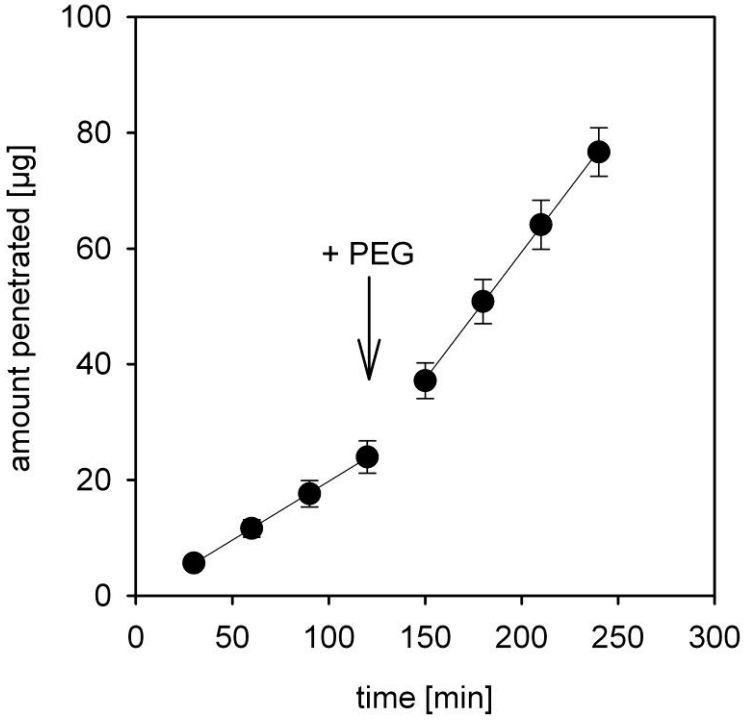

Figure 3.10: Flow of glucose across isolated *Pisum sativum* seed coats at 25 °C. At the first four time points, deionised water was used as receiver solution, followed by four time points with a water potential gradient applied by using a 500 g kg^{-1} PEG solution as receiver. Results are given as means with 95 % confidence intervals. The regression line for the first part of the kinetics is given by y = 0.203 x - 0.552 (R^2 = 0.93) and for the second part of the kinetics by y = 0.440 x - 28.5 (R^2 = 0.95).

3.6 Simulation of seed treatment AI distribution in moist soil

Experimental setups were developed for the examination of the distribution of AIs from seed treatment residues in moist soil. In these experiments the AI is applied as seed treatment to the surface of whole seeds or isolated seed coat halves. In a moist soil environment the seed treatment residue dissolves and the AI can move either across the seed coat or into the soil. As the AI is present in a limited dose, the driving force for AI distribution changes over time and a non-steady-state transport situation is caused. Additionally, the seed coat barrier properties change during seed swelling (Figure 3.7). Therefore, no linear uptake kinetics can be expected.

3.6.1 Establishment of seed treatment methods

As prerequisite for experiments simulating the seed treatment AI distribution in a moist soil environment treated seeds or treated isolated seed coat halves had to be produced. In the treatment of whole seeds by stirring in a beaker the application of a precise solute amount to the seed surface was difficult because a varying fraction of the treatment solution was lost on the inner surface of the beaker (Figure 2.5). The exact amount of solute applied to the surface of whole seeds varied between each treatment charge. Solute coverage of whole *Pisum sativum* seeds treated with metalaxyl-M without additives varied between treatment charges from 2.60 µg (± 0.37) to 4.98 µg (± 0.17) solute per seed. With metalaxyl-M with a covering layer of NeoCryl AI coverage ranged from 1.93 µg (± 0.09) to 5.42 µg (± 0.55) metalaxyl-M per seed. Whole seeds treated with sedaxane without additives carried 22.92 µg (± 3.43) to 32.86 µg (± 4.26) of solute per seed and seeds treated with sedaxane in combination with adigor carried 15.82 µg (± 1.80) to 27.06 µg (± 1.70) sedaxane per seed. In the treatment of isolated seed coat halves the required amount of solute could be directly applied with a pipette, resulting in a homogeneous loading of the individual seed coats.

3.6.2 Characterisation of additives

In the experiments with seed treatments, the effects of two additives were examined. NeoCryl A-2099 is a polymer which is not surface-active and adigor is an oil-surfactant blend. Addition of adigor to deionised water led to a maximal measured

surface tension reduction to 33.5 mN m^{-1}. The critical micelle concentration of adigor was reached at 82.3 mg l^{-1}.

3.6.3 Characterisation of soil material

Instead of field soil, moist purified sea sand with 0.2 g deionised water per g dry sand was used in the experiments as simplified and homogeneous soil material. The measured field capacity of the sand was 0.22 g g^{-1}. The sand moisture content used in the experiments therefore is equivalent to 91 % field capacity. The moist sand with 0.2 g water per g dry sand had a water potential of -0.31 MPa (± 0.09).

3.6.4 Experiments with whole treated seeds

To analyse the seed treatment AI distribution in an experimental setup close to the real situation in the field and to include the aspect of seed swelling, experiments were performed with whole treated seeds. During the course of the experiments with whole treated seeds, the distribution of relative AI amounts into the sand as well as the relative amounts still associated with the seed coat were measured. The relative amount of AI taken up into the embryo was either calculated (equation 2.6) or directly measured. Thus, relative amounts of the applied AI in three compartments were plotted.

3.6.4.1 Validation of the embryo extraction method

Part of the data for sedaxane uptake was measured directly following embryo extraction. To check for sufficient thoroughness of the extraction method, the recovery rate was calculated, which is the sum of the percentages of initially applied amount that was located again at the end of the experiment in all fractions. The mean recovery rate measured was 100.9 % (Table 3.6). Therefore, the method used for extraction of seed coat material and embryos was efficient.

Table 3.6: Percentage of the initially applied solute amount detectable after extraction in sand, seed coat plus embryo samples (recovery rate), measured for several sets of samples, given as means with 95 % confidence intervals.

Treatment type	Time point [h]	Recovery rate [%]
Sedaxane without adigor	20	101.9 ± 7.7
	40	102.7 ± 6.9
Sedaxane with adigor	40	101.7 ± 4.8
	60	97.2 ± 14.7

3.6.4.2 Distribution of metalaxyl-M from whole treated seeds

The relative AI amount left associated with the seed coat of *Pisum sativum* seeds treated with metalaxyl-M without additives decreased within 20 h in moist sand to 13.0 % of the applied amount (Figure 3.11 A). After 80 h, only 0.9 % of the applied metalaxyl-M amount was left associated with the seed coat. When a layer of NeoCryl A-2099 was added in the seed treatment, the relative AI amount associated with the seed coat decreased slower than on the seeds treated without additives (Figure 3.11 D). After 20 h, 24.4 % of the applied amount was still associated with the seed coat. The percentage left on and in the seed coat after 80 h was 6.1 %. The relative AI amounts associated with the seed coat of seeds treated with metalaxyl-M without and with NeoCryl A-2099 were statistically different (P- value ≤ 0.05) at all time points except for 8 h.

The relative amount of metalaxyl-M washed off into the sand from seeds treated with metalaxyl-M without additives reached values of 42.7 % to 50.2 % of the applied amount after 20 h (Figure 3.11 B). When NeoCryl A-2099 was added in the seed treatment, the percentage of Metalaxyl-M washed off into the sand reached slightly lower values between 34.1 % and 41.2 % after 20 h (Figure 3.11 E). The relative AI amounts in the sand around seeds treated with metalaxyl-M without and with NeoCryl A-2099 were statistically different at 1.5 h, 4 h, 20 h, 60 h and 80 h (P- value

≤ 0.05). At the remaining time points, the differences in the relative solute amounts were not statistically significant.

Seeds treated with Metalaxyl-M without additives took up 32.1 % of the applied amount within 4 h and the final relative uptake amount after 80 h was 53.4 % (Figure 3.11 C). The percentage of metalaxyl-M taken up by seeds treated with Metalaxyl-M with NeoCryl A-2099 was after 4 h 30.2 % which was slightly lower. The final percentage taken up after 80 h in moist sand was 54.3 % (Figure 3.11 F). The differences in the relative metalaxyl-M amounts taken up by seeds treated with metalaxyl-M without and with NeoCryl A-2099 were statistically significant only at the time point of 60 h (P- value ≤ 0.05). In all other cases, the differences in the relative solute amounts were not statistically significant.

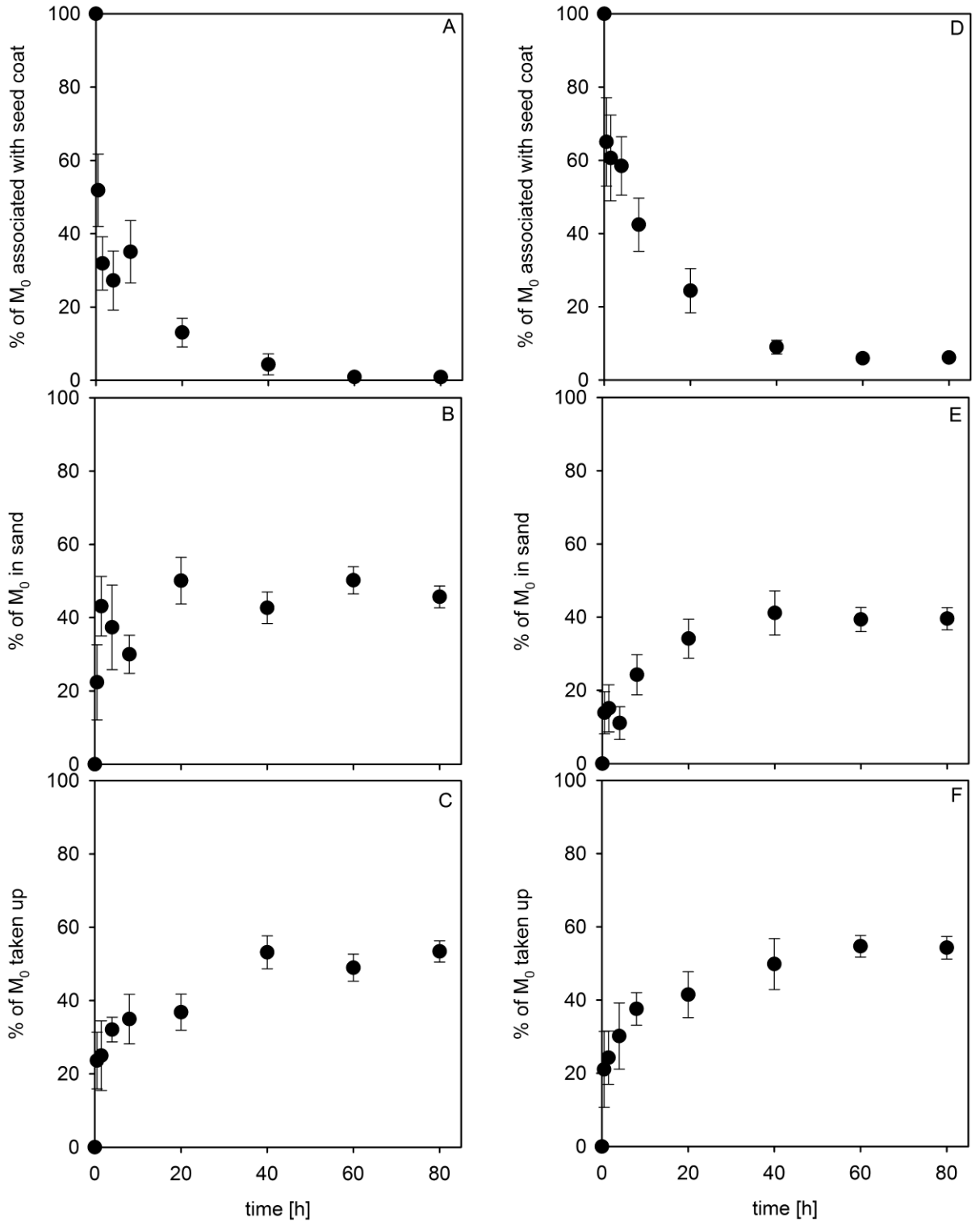

Figure 3.11: Percentages of applied AI in different compartments at time intervals after placing whole treated seeds of *Pisum sativum* into moist sand for different periods of time at 4 °C. Seeds were treated with metalaxyl-M without additive (left hand side, A – C) or treated with two covering layers of NeoCryl A-2099 above the AI layer (right hand side, D – F). Results are given as means with 95 % confidence intervals.

3.6.4.3 Distribution of sedaxane from whole treated seeds

When *Pisum sativum* seeds treated with sedaxane without additive were placed into moist sand, the relative AI amount remaining associated with the seed coat decreased to 77.6 % of the applied amount within the first 0.5 h (Figure 3.12 A). The decrease continued to a percentage of 29.4 % at 80 h. With an addition of adigor to the treatment solution, the relative amount of sedaxane remaining associated with the seed coat of whole treated seeds decreased faster. At 0.5 h only 68.0 % of the applied AI amount remained on and in the seed coat (Figure 3.12 D). After 80 h in moist sand, 25.3 % of the initial sedaxane amount was remaining associated with the seed coat. The differences in sedaxane percentages remaining on and in the seed coat of seeds treated with sedaxane without and with additive were statistically significant at 1.5 h and 4 h (P- value ≤ 0.05). In all other cases the differences in relative solute amounts were not statistically significant.

The relative sedaxane amount washed off into the sand from seeds treated with sedaxane without additive reached values between 27.7 and 30.5 % of the applied amount after 20 h (Figure 3.12 B). With addition of adigor in the seed treatment, the relative amount of sedaxane washed off into the sand reached similar to slightly higher values between 26.5 and 37.0 % after 20 h (Figure 3.12 E). The percentages of sedaxane washed off into the sand from seeds treated without and with additive were significantly different at 1.5, 4, 8 and 60 h (P- value ≤ 0.05). In all other cases the differences in relative solute amounts were not statistically significant.

The relative AI amount taken up by seeds treated with sedaxane without additive was 7.4 % of the applied amount after 4 h (Figure 3.12 C). After 60 h in moist sand the relative amount taken up was 42.4 % of the applied AI amount and this value did not increase any more after 80 h. When adigor was added in the seed treatment solution the relative amount taken up after 4 h in moist sand was 16.0 % and after 8 h 11.4 % (Figure 3.12 F). After 80 h in moist sand a relative uptake amount of 48.8 % of the applied AI was reached. The difference between percentages of sedaxane taken up by seeds treated with sedaxane without and with additive was statistically not significant except for the time points of 4 h and 60 h (P- value ≤ 0.05).

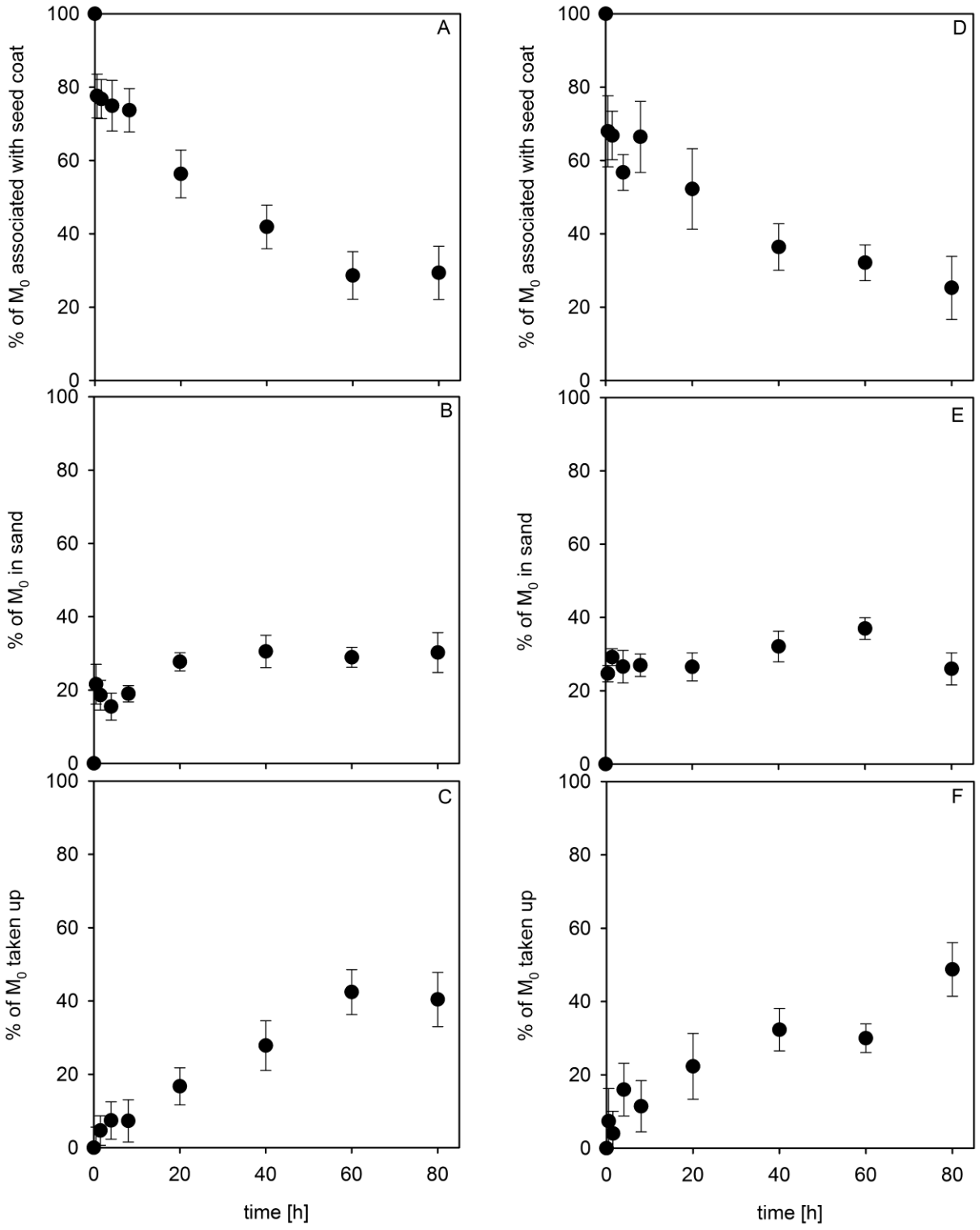

Figure 3.12: Percentages of applied AI in different compartments at time intervals after placing whole treated seeds of *Pisum sativum* into moist sand for different periods of time at 4 °C. Seeds were treated with sedaxane without additive (left hand side, A – C) or treated with sedaxane in combination with adigor (right hand side, D – F). Results are given as means with 95 % confidence intervals.

3.6.4.4 Quantification of uptake kinetics by whole treated seeds

In order to quantify the kinetics of AI uptake by whole treated seeds, a curve fit of a nonlinear regression was performed (equation 2.8 and Figure 3.13).

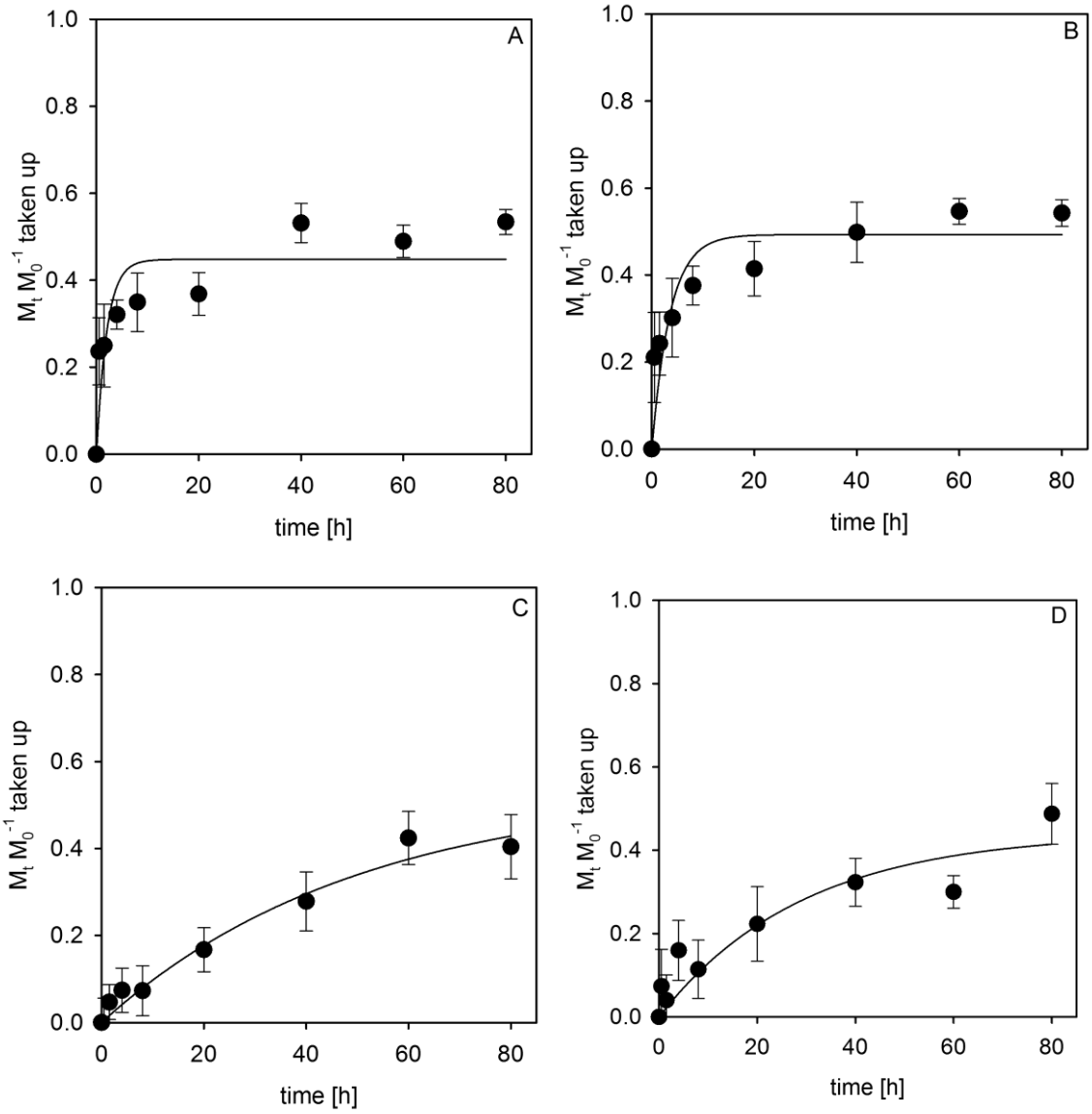

Figure 3.13: Relative amounts of AI taken up across the seed coat after placing whole treated seeds of *Pisum sativum* into moist sand at 4 °C. Seeds were treated with metalaxyl-M without additive (A), with metalaxyl-M with two covering layers of 2 % NeoCryl A-2099 (B), with sedaxane without additive (C) or with sedaxane with adigor (D). Results are given as means with 95 % confidence intervals. The regression line is given by the equation $y = 44.8 (1 - e^{-0.493 x})$ (A), $y = 49.3 (1 - e^{-0.281 x})$ (B), $y = 53.8 (1 - e^{-0.0200 x})$ (C), $y = 44.3 (1 - e^{-0.0343 x})$ (D), with y representing the relative amount taken up and x the time in h.

From the regression line describing the uptake kinetics, the rate constant k and the final relative uptake amount $M_{t\rightarrow\infty}\ M_0^{-1}$ for each uptake curve were obtained and can be used to quantify and compare the kinetics (equation 2.8 and Table 3.7).

Table 3.7: Rate constant k [h^{-1}] and final relative AI amount taken up $M_{t\rightarrow\infty}\ M_0^{-1}$ obtained from the AI uptake kinetics describing uptake by whole treated seeds placed into moist sand. Results are given as means with 95 % confidence intervals.

Seed treatment	k [h^{-1}]	$\frac{M_{t\rightarrow\infty}}{M_0}$ [%]
Metalaxyl-M without additive	0.493 ± 0.191	44.8 ± 2.7
Metalaxyl-M with NeoCryl A-2099	0.281 ± 0.088	49.3 ± 3.2
Sedaxane without additive	0.0200 ± 0.0111	53.8 ± 17.3
Sedaxane with adigor	0.0343 ± 0.0182	44.3 ± 9.1

Addition of NeoCryl A-2099 in the treatment of whole seeds with metalaxyl-M leads to a reduction in the rate constant k (Table 3.7) which is not significant (P- value = 0.0620) and to a slight but significant increase in final relative AI amount taken up $M_{t\rightarrow\infty}\ M_0^{-1}$ (P- value = 0.030). In the case of whole seeds treated with sedaxane, the addition of adigor in the seed treatment leads to an increase in the rate constant k and a decrease in the final relative AI amount taken up $M_{t\rightarrow\infty}\ M_0^{-1}$, but the differences are not significant (P- values = 0.189 and 0.334, respectively).

The rate constant k for AI uptake by seeds treated with sedaxane without additive is 25 times smaller than k for AI uptake by seeds treated with metalaxyl-M without additive (P- value ≤ 0.001) while the final relative amount taken up is not significantly different (P- value = 0.267).

3.6.5 Experiments with isolated treated seed coat halves

During the course of the experiments with isolated treated seed coats, the relative amount of AI in the receiver solution and in the sand was measured and the respective relative AI amount remaining on or in the seed coat half was calculated (equation 2.7). Thus, the relative amounts of applied AI in three compartments were plotted versus the time.

3.6.5.1 Distribution of metalaxyl-M from isolated treated seed coat halves

When placing isolated *Pisum sativum* seed coat halves treated with metalaxyl-M without additive with their outer side in contact to moist sand (Figure 2.7), the percentage of metalaxyl-M left associated with the isolated seed coat half decreased within minutes. After 2 min 48.6 % of the applied AI remained associated with the seed coat and after 10 min this percentage decreased to 1.1 % of the applied amount (Figure 3.14 A). Only a small percentage of the applied AI was washed off into the sand. The relative AI amount in the sand was only 4.4 % of the applied amount after 10 min (Figure 3.14 B). The majority of the applied metalaxyl-M was taken up across the seed coat into the receiver solution (Figure 3.14 C). Within 2 min, 50.2 % of the applied metalaxyl-M amount was taken up into the receiver compartment. At the end of the experiment the AI percentage in the receiver reached 94.5 % of the applied metalaxyl-M amount.

Application of a layer of the polymer additive NeoCryl A-2099 covering the metalaxyl-M layer on the isolated seed coat half led to changes in the AI distribution. When a covering layer of NeoCryl A-2099 was applied above the AI layer, a higher percentage of AI remained associated with the seed coat half. The relative amount remaining associated with the isolated seed coat half after 10 min was 37.9 % (Figure 3.14 D). The percentage of AI washed off into the sand after 10 min was not changed as clearly, it amounted to 3.9 % of the applied amount (Figure 3.14 E). The relative amount taken up across the seed coat was reduced by the polymer layer. The AI percentage in the receiver solution was 32.2 % after 2 min and 58.2 % after 10 min (Figure 3.14 F).

The differences between both treatment types were statistically significant (P- value ≤ 0.05) for the AI percentages associated with the seed coat and in the receiver solution at all time points but not for the solute percentages washed off into the sand.

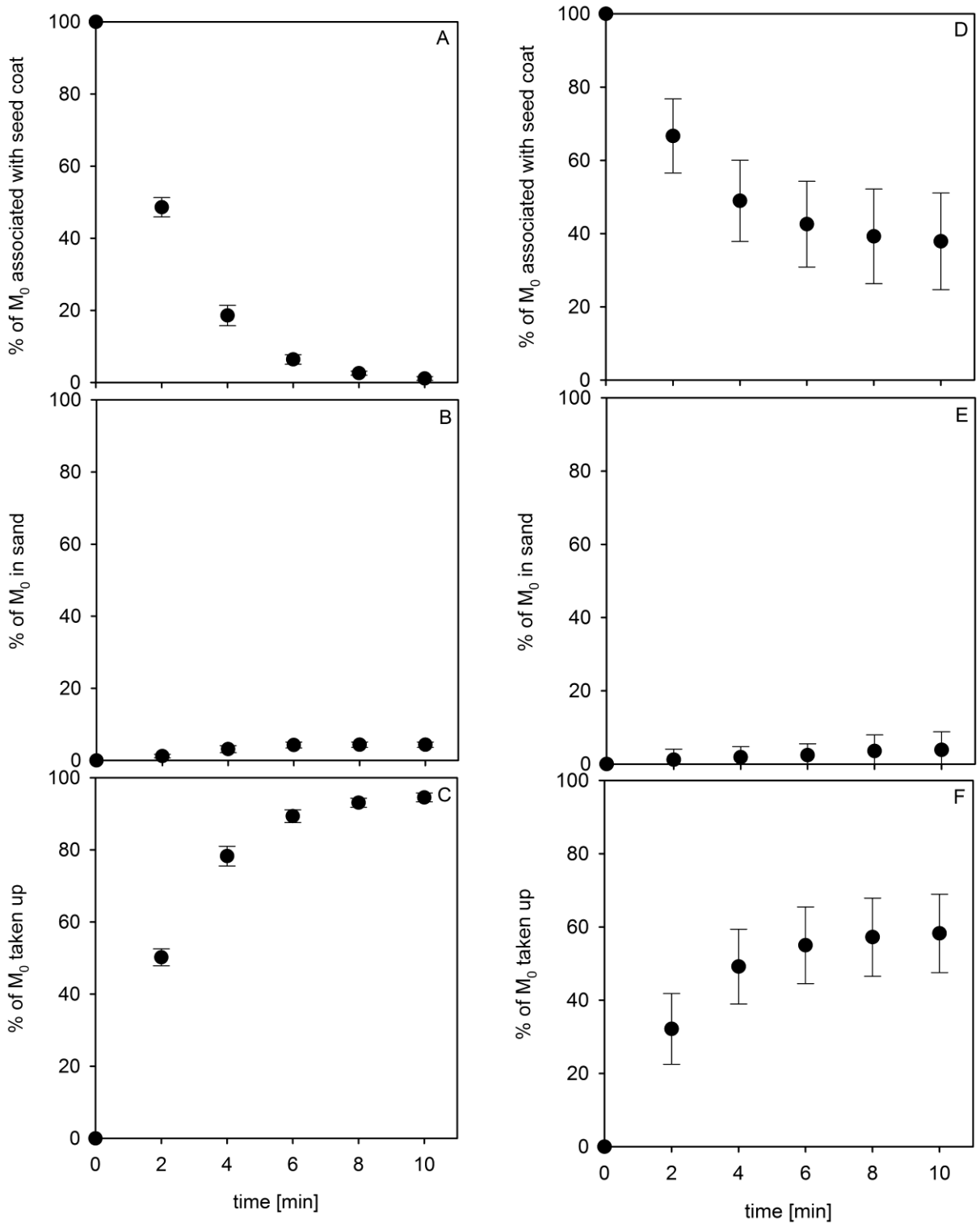

Figure 3.14: Percentages of applied AI in different compartments at time intervals after placing isolated seed coat halves of *Pisum sativum* treated with metalaxyl-M without additive (left hand side, A – C) or treated with a covering layer of NeoCryl A-2099 above the AI layer (right hand side, D – F) at room temperature with the outer side in contact to moist sand. The sand as well as the receiver solution in the seed coat half were taken for analysis and replaced at each time point. Results are given as means with 95 % confidence intervals.

3.6.5.2 Distribution of sedaxane from isolated treated seed coat halves

When placing isolated *Pisum sativum* seed coat halves treated with 15 µg sedaxane without additive with their outer side in contact to moist sand the relative sedaxane amount remaining associated with the seed coat half decreased by 2.8 % during the first two minutes. It was still 77.8 % after 10 min (Figure 3.15 A). Only 2.8 % of the applied sedaxane amount was washed off into the sand after 2 min (Figure 3.15 B). The percentage of AI that was washed off increased to 18.5 % of the applied amount after 10 min. The final relative amount of AI taken up across the seed coat after 10 min was 3.7 % (Figure 3.15 C).

An addition of the surface-active additive adigor to the seed treatment solution led to a reduction of the relative AI amount remaining associated with the seed coat half, which was 47.1 % of the applied amount after 10 min (Figure 3.15 D). Addition of adigor in the treatment led to an increased relative amount of AI being washed off into the sand. The relative sedaxane amount in the sand was 28.7 % after 2 min and reached 50.0 % after 10 min (Figure 3.15 E). The percentage of AI taken up across the seed coat into the receiver solution was not increased by the addition of adigor. It amounted to only 2.9 % of the applied amount after 10 min (Figure 3.15 F).

The differences between seed coat halves treated without and with adigor were statistically significantly different at all time points in the case of sedaxane percentages in the seed coat and sand compartment (P- value ≤ 0.05) but not in the case of sedaxane percentages in the receiver compartment.

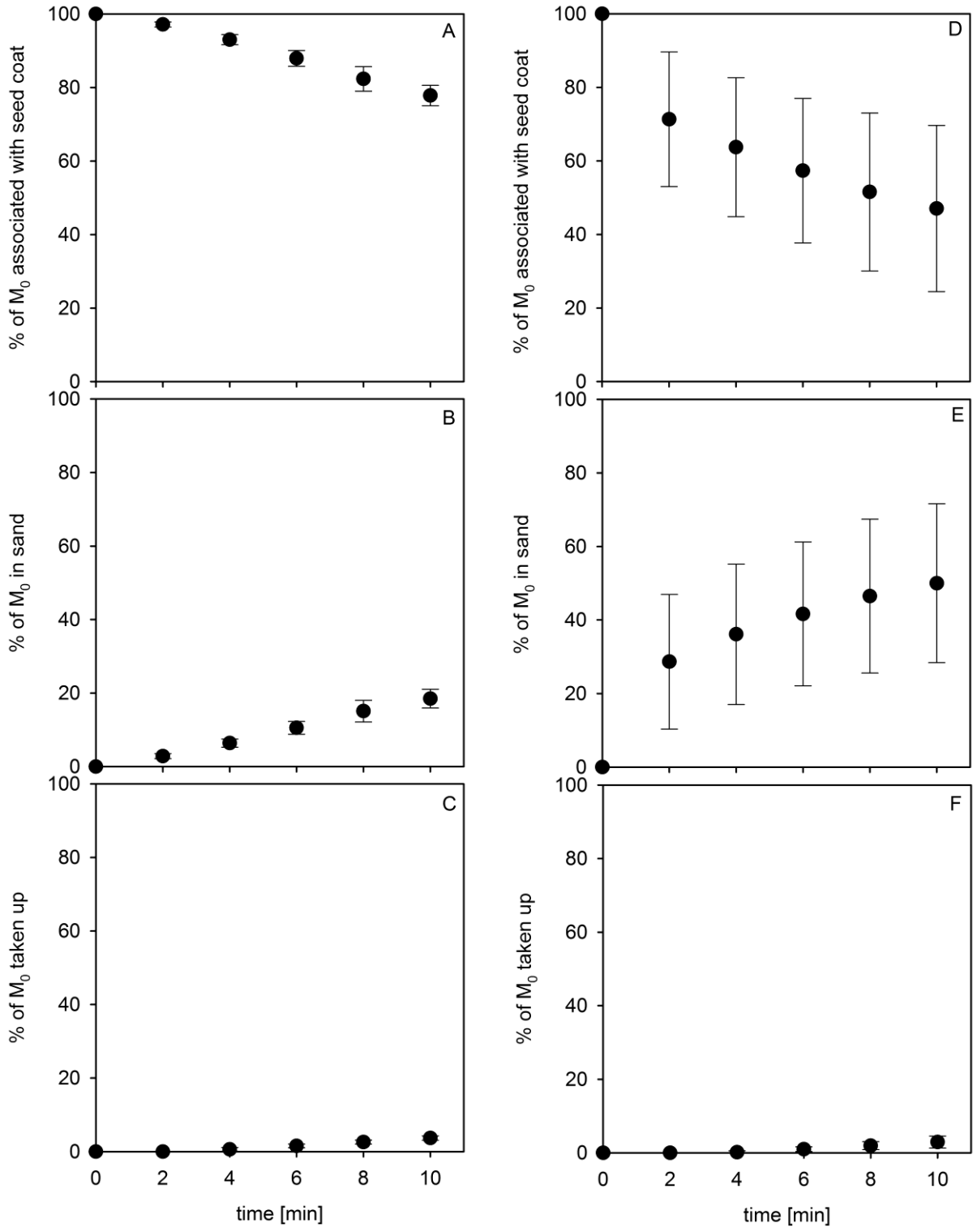

Figure 3.15: Percentages of applied AI in different compartments at time intervals after placing isolated seed coat halves of *Pisum sativum* treated with sedaxane without additive (left hand side, A – C) or with a treatment solution with sedaxane in combination with adigor (right hand side, D – F) at room temperature with the outer side in contact to moist sand. The sand as well as the receiver solution in the seed coat half were taken for analysis and replaced at each time point. Results are given as means with 95 % confidence intervals.

3.6.5.3 Distribution of thiamethoxam from isolated treated seed coat halves

When placing isolated *Pisum sativum* seed coat halves treated with 25 µg thiamethoxam without additive with their outer side in contact to moist sand, the relative AI amount remaining associated with the seed coat decreased to 42.9 % of the initially applied amount within 2 min and after 10 min only 1.7 % remained associated with the seed coat half (Figure 3.16 A). The relative thiamethoxam amount washed off into the sand reached 2.7 % after 10 min (Figure 3.16 B). The majority of the applied AI amount was taken up across the seed coat into the receiver solution. 55.8 % of the applied AI amount was taken up across the seed coat after 2 min and 95.6 % of the applied thiamethoxam amount after 10 min (Figure 3.16 C).

When a layer of the polymer additive NeoCryl A-2099 was applied above the AI layer, the relative thiamethoxam amount which remained associated with the seed coat half was slightly increased. After 2 min 46.3 % of the applied amount remained associated with the seed coat half and after 10 min 7.0 % of the applied amount remained on or in the seed coat (Figure 3.16 D). The thiamethoxam percentage washed off into the sand was smaller when NeoCryl A-2099 was applied above the thiamethoxam layer and reached only 0.9 % after 10 min (Figure 3.16 E). The relative amount of AI in the receiver solution was slightly decreased by the addition of NeoCryl A-2099. The percentage of thiamethoxam taken up was 53.4 % after 2 min and reached 92.1 % after 10 min (Figure 3.16 F).

The differences between AI distribution from seed coat halves treated without and with NeoCryl A-2099 were statistically significant in the case of thiamethoxam percentages in all compartments at all time points (P- value ≤ 0.05) except for the percentages in the seed coat and receiver compartment at 2 and 4 min.

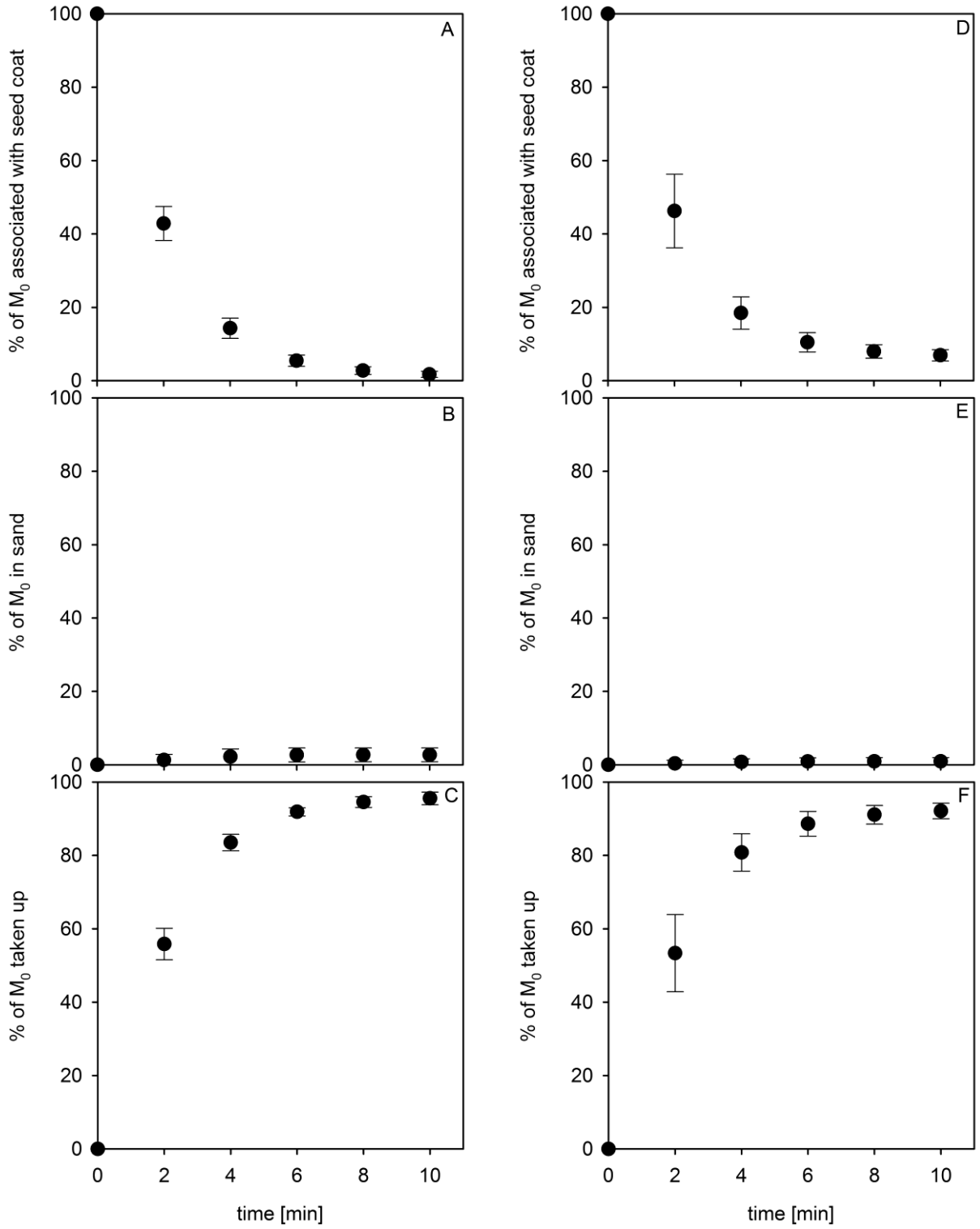

Figure 3.16: Percentages of applied AI in different compartments at time intervals after placing isolated seed coat halves of *Pisum sativum* treated with thiamethoxam without additive (left hand side, A – C) or treated with a covering layer of NeoCryl A-2099 above the AI layer (right hand side, D – F) at room temperature with the outer side in contact to moist sand. The sand as well as the receiver solution in the seed coat half were taken for analysis and replaced at each time point. Results are given as means with 95 % confidence intervals.

3.6.5.4 Quantification of uptake kinetics by isolated treated seed coat halves

In order to quantify the kinetics of AI uptake across isolated treated seed coat halves a curve fit was performed (equation 2.8 and Figure 3.17). For sedaxane uptake this curve fitting did not converge towards the measured uptake curve since the uptake rate did not decrease at the end of the experiments.

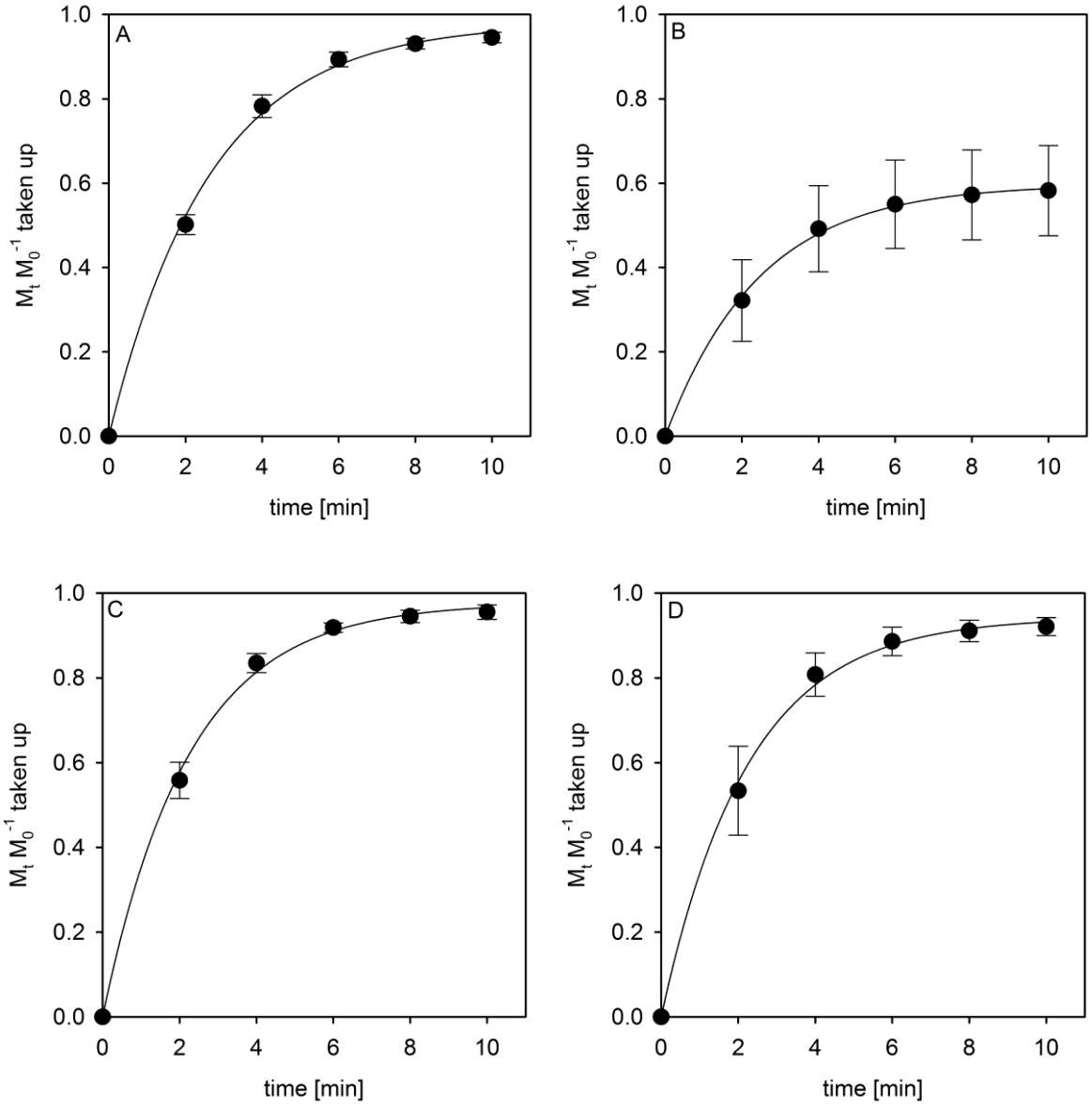

Figure 3.17: Percentages of applied AI taken up across isolated treated seed coats with the outer side in contact to moist sand. Treatment was with metalaxyl-M (A), metalaxyl-M and NeoCryl A-2099 (B), thiamethoxam (C) or thiamethoxam and NeoCryl A-2099 (D). The regression line is given by $y = 97.9\ (1 - e^{-0.381\ x})$ (A), $y = 59.8\ (1 - e^{-0.407\ x})$ (B), $y = 97.7\ (1 - e^{-0.447\ x})$ (C), $y = 94.3\ (1 - e^{-0.444\ x})$ (D).

From the regression line describing the uptake kinetics, the rate constant k and the final relative amount taken up $M_{t\rightarrow\infty}\ M_0^{-1}$ were obtained for uptake across isolated seed coat halves treated with metalaxyl-M and with thiamethoxam without and with additive (equation 2.8 and Table 3.8). These values can be used to quantify and compare the uptake kinetics.

Table 3.8: Rate constant k [min^{-1}] and percentage taken up $M_{t\rightarrow\infty}\ M_0^{-1}$ obtained from the AI uptake kinetics describing uptake across isolated treated *Pisum sativum* seed coats placed onto moist sand. Results are given as means with 95 % confidence intervals.

Seed coat treatment	k [min^{-1}]	$\frac{M_{t\rightarrow\infty}}{M_0}$ [%]
Metalaxyl-M without additive	0.381 ± 0.023	97.9 ± 1.8
Metalaxyl-M with NeoCryl A-2099	0.407 ± 0.160	59.8 ± 6.7
Thiamethoxam without additive	0.447 ± 0.030	97.7 ± 1.8
Thiamethoxam with NeoCryl A-2099	0.444 ± 0.063	94.3 ± 3.5

The rate constant k for AI uptake across isolated seed coat halves treated with metalaxyl-M without additive is slightly smaller than the rate constant for uptake across seed coat halves treated with metalaxyl-M with additive (Table 3.8), but the difference is not significant (P- value = 0.746). The final relative amount taken up $M_{t\rightarrow\infty}\ M_0^{-1}$ is decreased by addition of NeoCryl A-2099 by 38 % (P- value < 0.001). For isolated seed coat halves treated with thiamethoxam, the addition of NeoCryl A-2099 has neither a significant effect on the rate constant k nor on the final relative uptake amount $M_{t\rightarrow\infty}\ M_0^{-1}$ (P- values = 0.930 and 0.084, respectively).

In order to compare the uptake curves of isolated seed coat halves treated with sedaxane with the uptake curves obtained with treatments with metalaxyl-M and thiamethoxam, the slopes of the uptake curves at the fastest AI uptake phase were obtained from the plots. These were for metalaxyl-M without additive 25.1 ± 2.50 % of

the applied AI min^{-1} and for thiamethoxam without additive 27.9 ± 4.58 % of the applied AI min^{-1}. In the linear uptake phase of sedaxane across isolated seed coat halves treated with sedaxane without additive, 0.515 ± 0.0931 % of the applied AI were taken up per minute. Maximum sedaxane uptake was therefore by a factor of 49 and 54 slower than maximum uptake of metalaxyl-M and thiamethoxam, respectively. With adigor added in the seed coat treatment this rate was 0.462 ± 0.181 % of the applied AI min^{-1}. Sedaxane uptake was not significantly influenced by addition of adigor.

4. Discussion

Although uptake of seed treatment active ingredients and leaching of seed metabolites across the seed coat is a well-known phenomenon (see chapter 1.2), the seed coat barrier properties and the mechanisms of seed coat permeation are not well understood. In the present work, therefore, the *Pisum sativum* seed imbibition process was studied and the seed coat was characterised. The basic mechanisms of solute permeation were examined in steady-state experiments and as a further step the permeation process in the more applied situation of uptake of seed treatment AIs was analysed.

To put the information obtained in the present study into perspective, the permeation process across seed coats can be compared with the permeation process across leaf and fruit cuticles. These are likewise important interfaces between plants and the environment, but much better investigated (Kerler and Schönherr 1988b, Popp et al. 2005, Schreiber 2005, Riederer and Friedmann 2006, Schreiber and Schönherr 2009). This comparison helps to interpret the results and to clarify important differences.

4.1 Characterisation of the imbibition process

When a dry seed comes into contact to water, the dynamic process of seed imbibition takes place. Several experiments were made to analyse the mechanisms of water uptake and to examine the changes the seed coat undergoes during imbibition.

4.1.1 Role of the seed coat in the swelling process

An important role of the seed coat is to control water uptake during seed imbibition. The control mechanism can take place by preventing (respectively delaying) as well as by regulating water uptake. A prevention of water uptake for a period of time can inhibit germination until environmental conditions allow the seedling to grow and produce offspring (Vleeshouwers et al. 1995) or promote seed longevity and preserve a reserve of the species in soil (Rolston 1978) from which fractions can germinate at successive times (Williams and Elliott 1960). When seeds do not readily take up available water they are called hard seeds (Arechavaleta-Medina and Snyder

1981, Mullin and Xu 2001) or physically dormant (Finch-Savage and Leubner-Metzger 2006). The barrier which prevents water uptake by hard legume seeds is an intact outer cuticle on the seed coat surface (Arechavaleta-Medina and Snyder 1981, Ma et al. 2004). In the *Pisum sativum* seed lot used in the present work, only a small fraction of the seeds showed hard seededness and did not take up water. These seeds were not used in the experiments and discarded. Thus, all seed coats examined in the present experiments were permeable to water and did not possess an intact continuous cuticle on their surface which would prevent imbibition.

Another mechanism by which the seed coat controls water uptake is a regulation of the rate at which water is taken up into the embryo. If water reaches the embryo too fast, imbibition damage and loss of vigour of the embryo can occur (Larson 1968, Powell and Matthews 1978, Duke and Kakefuda 1981). Such imbibition damage of the embryo was proposed to be cell damage, cell rupture or leakage of cell components before the cell membranes have regained their normal hydrated state (Larson 1968, Powell and Matthews 1978, Simon 1978, Duke and Kakefuda 1981). An intact seed coat surrounding the embryo can prevent such damage of the embryonic tissue (Powell and Matthews 1978, Duke and Kakefuda 1981, Koizumi et al. 2008) by slowing down the water flow rate towards the embryo (Meyer et al. 2007, Koizumi et al. 2008). To examine this regulation of imbibition water inflow by the seed coat, the hydraulic conductivity L_{hydr} of *Pisum sativum* seed coats was measured at several time points during seed imbibition (Figure 3.7). It was found that L_{hydr} is low at the beginning of imbibition and increases during swelling. At the end of the experiment, pea seed coat hydraulic conductivity values of about 0.69 g s^{-1} m^{-2} MPa^{-1} were found, which are similar to the hydraulic conductivities of water permeable fully swollen soybean seed coats measured with two different methods by Meyer et al. (2007) which were 0.32 g s^{-1} m^{-2} MPa^{-1} and 0.67 g s^{-1} m^{-2} MPa^{-1}. Parallel to the increase of the seed coat hydraulic conductivity, the driving force for water uptake, which is represented by the difference in the involved water potentials, also changes during seed swelling. At the beginning of the seed swelling process, the driving force is extremely high as the seed water potential is -152 MPa (Figure 3.7 B), which would lead to a very high inrush of water if it was not for the still low seed coat hydraulic conductivity at this early stage of germination (Figure 3.7 C). The *Pisum sativum* seed coat therefore prevents imbibition damage by a slowing down of water uptake

by the desiccated seed. With proceeding seed swelling, the driving force for water uptake is reduced and the seed coat hydraulic conductivity is increased so that a regulated and steady water uptake is facilitated. The increase of the seed coat hydraulic conductivity during seed swelling might be caused either by a formation of new pathways for water inflow or by enlargement of existing pathways. Pathways for water flow could be formed by cracks in the seed coat, the lumen of the dead seed coat cells or intercellular spaces between hourglass cells (compare Figure 3.1), which become water-filled during seed swelling. Another possible pathway for water flow could be formed by the cell wall material of the swollen seed coat. Hydraulic flow of water through plant cell wall material has been described for example for apoplastic water flow through root tissues (Steudle and Frensch 1996, Steudle and Peterson 1998). It was shown by Steudle and Boyer (1985) that the hydraulic conductivity of cell wall material can increase with increasing water content due to water uptake by pores of the cell wall material.
Pathways which allow bulk flow of water across the seed coat could also be used for diffusive permeation of solutes. Consequently, it can be assumed that parallel to the increase of the hydraulic conductivity of the seed coat during imbibition, permeability for diffusive Al uptake across the seed coat could also increase.

Additionally to restriction of water passage to the embryo, the seed coat can have another role during seed imbibition. It can also act as a water reservoir in the case of short time spans of moisture availability and thus prolong water availability to the embryo (Manz et al. 2005). This has been observed in tobacco seeds, where the seed coat material had a high water-holding capacity and thus increased water availability for the embryo during swelling (Manz et al. 2005). The swelling experiment with isolated *Pisum sativum* seed coats (Figure 3.5) showed that the pea seed coat can also rapidly take up water and hold 1.29-fold their weight in water (chapter 3.1.1). Therefore, the pea seed coat could also regulate water uptake by this mechanism in field situations.

4.1.2 Water uptake mechanism

Two different uptake mechanisms for water uptake across barriers are possible, which are diffusive water uptake and water uptake by mass flow (Refojo 1965, Fernández-Pineda and Mengual 1977, Beyer et al. 2005). In the diffusive water

uptake process, single water molecules reach the outer surface and diffuse across the barrier, driven by the water concentration difference (Fernández-Pineda and Mengual 1977). This was the case with pea seeds swelling in water saturated air (Figure 3.3), where the seed was surrounded by single water molecules in air. Seed imbibition in water saturated air is extremely slow in comparison to imbibition in liquid water. While seeds placed in liquid water reached the maximum water uptake capacity of about 0.95 g g^{-1} dry weight within one day, in water saturated air only about one quarter of this uptake capacity is reached after two weeks.

The driving force for seed water uptake depends on the water concentration in the seed coat. Seed coat samples placed into water saturated air took up nearly as much water as seed coat samples placed into liquid water (chapter 3.2.4). The water content of seed coats in liquid water is only 1.6 times higher than the water content of seed coats in water saturated air, yet the water uptake rate in liquid water is by a factor of 30 (Figures 3.2 and 3.3) higher. Thus, the driving force is similar, but the resulting water uptake is different. This implies that the water uptake mechanisms must be different. While in seeds swelling in water saturated air single water molecules are taken up and hence the uptake is diffusive, the seeds placed in liquid water take up a bulk flow of water. Viscous mass flow or bulk flow of water describes movement of a volume of water as a whole instead of movement of single molecules by diffusion (Fernández-Pineda and Mengual 1977). Viscous mass flow can only take place when water is available in form of an aqueous continuum (Beyer et al. 2005), which was given by the surrounding liquid water. Thus, water uptake by seeds can take place both by diffusion and by mass flow, depending on the available form of water.

4.1.3 Water uptake from moist sand

Seed imbibition in moist sand is similar to the natural case of seed imbibition in the field. Depending on the moisture content and structure of the soil, water in soil can be present not only as free water but also as water bound to various degrees in soil pores or as water in form of water vapour (Nobel 1991, Bewley et al. 2013). In the present experiments the soil was represented by sand with 91 % field capacity. A sandy soil is composed of large particles and large pore sizes and thus can contain comparably high amounts of water (Frey and Lösch 2010). As pore sizes are larger than in other soils, in sandy soils matric forces are smaller than in other soils

(Schaetzl and Anderson 2005). Thus in sand a high amount of water can be available in large pores and a comparably small amount of water is bound in small pores (Frey and Lösch 2010). Though water availability in moist sand is high in comparison for example to water availability in clay, there is still less free water available to the seed than in the extreme case of seed imbibition in liquid water (Figure 3.2). This was seen in the swelling kinetics of pea seeds in moist sand (Figure 3.4) where water uptake was much slower than water uptake from liquid water. On the other hand, imbibition in moist sand was still much faster than imbibition in water saturated air (Figure 3.3). Therefore, water uptake by seeds in moist sand is a combined process. Available liquid water in pores adjacent to the seed is taken up by mass flow and in the case of air-filled pores adjacent to the seed water uptake is by diffusion from air humidity. The combination of both water uptake mechanisms results in water uptake slower than that obtained by seed imbibition in liquid water but faster than imbibition in water saturated air.

4.2 Analysis of the lipophilic fraction of seed coats

The *Pisum sativum* seed coat is covered by a cuticle (Figure 3.1, (Werker et al. 1979)) which could play an important role for permeation of solutes. The lipid compartment of seed coats including the cuticle was therefore examined in more detail.

In the fraction of soluble lipids which were extracted from the seed coat with chloroform, typical plant cuticular wax compounds were detected. The main pea seed coat cuticular wax component was hentriacontane (Table 3.1) which is also the main component of pea leaf cuticular wax (Gniwotta et al. 2005). Primary alcohols of C26 and C28 chain length which constitute over 30 % of the pea leaf cuticular wax (Gniwotta et al. 2005) could be found in the pea seed coat cuticular wax in smaller percentages (Table 3.1). The main wax components of pea leaf wax can thus also be found in pea seed coat wax. However, the amount of typical cuticular wax compounds on pea seed coat surfaces is very low in comparison to the wax amount on pea leaf surfaces. The wax coverage of swollen pea seed coats is only 1.34 µg cm^{-2} which is ten- to 18fold smaller than the wax coverage of pea leaves (Gniwotta et al. 2005). A lower seed coat wax coverage in comparison to leaf wax coverages was also found in soybean (Shao et al. 2007). Additional substances in the chloroform-soluble lipid fraction were free short chain fatty acids and β-sitosterol, which might originate from remains of the dead cells of the seed coat. Sitosterols are typical plant sterols and regulate cell membrane fluidity (Hartmann 1998).

In the fraction of bound lipids, typical cutin compounds like 7- hydroxy hexadecan-dioic acid or 8-hydroxy hexadecan-dioic acid (Holloway 1982) were detected. The main components of the pea seed coat cutin examined by Espelie et al. (1979) were 16-hydroxy hexadecanoic acid and a di-hydroxy hexadecanoic acid which were also detected in high percentages in the present pea seed coat cutin (Table 3.1). Additionally in the bound lipid fraction, short chain fatty acids and β-sitosterol were found which might be remains of the seed coat cells. Shao et al. (2007) made the suggestion that cell membrane components could become incorporated into the cutin polymer of the seed coat cuticle during seed coat cell senescence.

Taking all lipid substances extracted from pea seed coats together leads to a total lipid amount of 320 µg per seed coat which is only 0.61 % of the weight of a swollen seed coat. In contrast to this, the water content of a swollen *Pisum sativum* seed coat is 56 % of its weight (chapter 3.1.1). Therefore, the lipophilic fraction of swollen seed coats is very small while the water content is very high. This is in contrast to plant cuticles which are mainly lipophilic barriers with a varying small fraction of hydrophilic compounds like carbohydrates (Marga et al. 2001, Takahashi et al. 2012).

4.3 Sorption of solutes in the seed coat

The first step of a permeation process across a barrier is movement of the solute into the barrier. This has also been described for permeation across leaf and fruit cuticles where the permeating solute has to partition into the lipophilic cuticular material as first step (Riederer and Schönherr 1984, Kerler and Schönherr 1988b, Schreiber and Schönherr 1992). This sorption of a solute in cuticles can be quantified by the solute's cuticle/water partition coefficient $K_{c/w}$ (Riederer and Schönherr 1984, Kerler and Schönherr 1988a, Popp et al. 2005). The plant cuticle acts as an efficient lipophilic sorption compartment for lipophilic solutes and cuticle/water partition coefficients can have values similar to the corresponding *n*-octanol/water partition coefficients (Kerler and Schönherr 1988a).

To examine sorption of solutes in the seed coat, seed coat/water partition coefficients $K_{sc/w}$ have been determined in the present work. An aspect which has to be kept in mind in the measurement of partition coefficients is that in some cases a concentration dependency could be found. In the determination of cuticle/water partition coefficients, at high solute concentration partition coefficients can decrease and thus sorption isotherms are not linear (Riederer and Schönherr 1984, Riederer and Schönherr 1986). The decrease of the partition coefficient at higher donor concentrations indicates that the sorption sites are saturated and no further solute can be sorbed by the cuticle (Schreiber and Schönherr 2009). For donor concentrations of 4-nitrophenol up to 140 µg ml^{-1} and of atrazine up to 20 µg ml^{-1} linear sorption isotherms in plant cuticles have been determined (Riederer and Schönherr 1986, Chamel and Vitton 1996). In the present measurement of seed coat/water partition coefficients, most of the donor concentrations were below this range where non-linear sorption isotherms were observed for sorption of other solutes in plant cuticles. Only in some cases of solutes with high water concentrations this concentration range was exceeded. But in the partitioning of these hydrophilic solutes into the seed coat it can be assumed that they occupy preferentially the water fraction in the seed coat. As long as the donor solution concentration is well below water saturation, the solute located in the seed coat water fraction at equilibrium would also be below water saturation and no saturation in the seed coat water fraction is expected. Therefore, in the measurement of seed coat/water partition coefficients, linear sorption isotherms have been assumed.

4.3.1 Effect of solute lipophilicity on sorption in the seed coat

When plotting the measured log seed coat/water partition coefficients versus the corresponding log *n*-octanol/water partition coefficients (Figure 4.1) it shows that the seed coat/water partition coefficients cover a much smaller range than the corresponding *n*-octanol/water partition coefficients. While the *n*-octanol/water partition coefficients of the lipophilic solutes have values of 50.1 to 25119, the corresponding seed coat/water partition coefficients range only from 0.723 to 83.8 (Tables 2.1 and 3.3). This is in contrast to sorption of solutes in leaf cuticles, where cuticle/water partition coefficients of lipophilic solutes can reach values similar to the corresponding *n*-octanol/water partition coefficients (Kerler and Schönherr 1988b, Schreiber and Schönherr 2009). This indicates that the seed coat is a less efficient sorption compartment for lipophilic solutes than *n*-octanol and than a leaf cuticle.

The second fact shown by the plot of the partition coefficients (Figure 4.1) is that hydrophilic (log $K_{o/w}$ < 0) compounds show different sorption behaviour in *Pisum sativum* seed coats than lipophilic (log $K_{o/w}$ > 0) compounds. In the plot of log seed coat/water partition coefficients versus log *n*-octanol/water partition coefficients (Figure 4.1) the regression line for the lipophilic solutes has a steeper slope of 0.77 while the slope for the hydrophilic solutes is only 0.05. This shows that for hydrophilic solutes lipophilicity has no pronounced influence on sorption behaviour which is plausible as the hydrophilic solutes hardly partition into the lipophilic sorption compartment of the seed coat. The slight increase of the seed coat/water partition coefficient for the sugars (numbers 10 to 8) correlates with decreasing solute size and could be caused by steric hindrances in solute accommodation in the seed coat material. All seed coat/water partition coefficients of hydrophilic solutes are smaller than 1, indicating that not the total seed coat material is suitable for holding solutes.

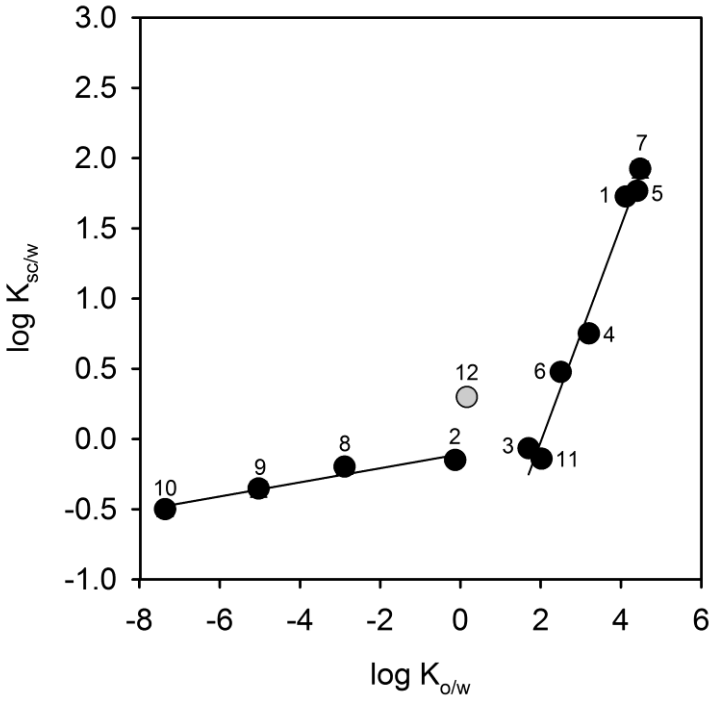

Figure 4.1: Logarithm of the seed coat/water partition coefficients ($K_{sc/w}$) plotted versus logarithm of the corresponding *n*-octanol/water partition coefficient ($K_{o/w}$) as a measure of substance lipophilicity. Numbers refer to Table 2.1. Results are given as means with 95 % confidence intervals. In most cases the error bars are smaller than the symbols. The regression line for the hydrophilic solutes (log $K_{o/w} < 0$) is given by y = 0.050 x - 0.108 ($R^2 = 0.81$) and for the lipophilic solutes (log $K_{o/w} > 0$) by y = 0.770 x - 1.561 ($R^2 = 0.69$).

4.3.2 Lipophilic and hydrophilic fractions of the seed coat

The increase in $K_{sc/w}$ for lipophilic solutes shows that a lipophilic sorption compartment is present in the seed coat. As the increase in $K_{sc/w}$ is much smaller than the increase in the corresponding *n*-octanol/water partition coefficients, this lipophilic compartment represents only a fraction of the seed coat material. The seed coat therefore is composed of a lipophilic fraction $f_{lipophilic}$ which is suitable for sorption of lipophilic solutes and a polar fraction f_{polar} (equation 4.1):

$$f_{lipophilic} + f_{polar} = 1 \quad (4.1)$$

The size of the lipophilic fraction $f_{lipophilic}$ of seed coats can be calculated from the measured seed coat/water partition coefficients $K_{sc/w}$ by equation (4.2), where $K_{w/w}$ is the water/water partition coefficient which amounts to 1.

$$K_{sc/w} = K_{o/w} \cdot f_{lipophilic} + K_{w/w} \cdot f_{polar} \quad (4.2)$$

Calculation of the lipophilic fraction of seed coats (equation 4.2) from the measured seed coat/water partition coefficients of the highly lipophilic solutes with $K_{o/w} > 2$ gives a value of 0.37 % ± 0.21 of the total swollen seed coat. In comparison to this, the lipid amount determined in the lipid analysis was slightly larger and amounted to 0.61 % of the weight of a swollen seed coat. Calculation of the lipophilic fraction with the seed coat/water partition coefficient data led to a smaller value since not the total lipid amount is available for sorption of solutes. Therefore, the actual partition coefficient in the lipophilic fraction of the seed coat is smaller than $K_{o/w}$. This is similar to plant cuticles where not all constituents have the same sorption capacities (Riederer and Schönherr 1984, Popp et al. 2005, Schreiber and Schönherr 2009).

The small lipophilic fraction of the *Pisum sativum* seed coat and consequently inefficient sorption of solutes in the seed coat are in contrast to the sorption of solutes in leaf cuticles (Kerler and Schönherr 1988b, Schreiber and Schönherr 2009). This is a first hint that the permeation process of solutes across seed coats might be different than permeation across leaf and fruit cuticles where the lipophilic fraction dominates in the barrier.

4.4 Characterisation of the permeation process

During seed maturation and drying in legume species like pea and soybean all the seed coat cells die (Werker 1997, Ranathunge et al. 2010). Thus, permeation across the mature seed coat is a physical process which is governed solely by anatomical and chemical properties of the seed coat and physico-chemical properties of the permeating solute. This is similar to the process of AI permeation of solutes across leaf and fruit cuticles (Bukovac and Petracek 1993, Buchholz 2006).

4.4.1 Method for permeation measurement

Diffusive solute permeation across a barrier can be described with the permeance P (Hartley and Graham-Bryce 1980). The permeance P has the unit of a velocity (m s^{-1}) and therefore describes permeation speed of the solute (Hartley and Graham-Bryce 1980, Schreiber and Schönherr 2009). By measurement of permeances of a barrier with a set of different solutes, correlations of permeances with the substances' lipophilicities and molar volumes can be established and thus the process of permeation across the barrier can be characterised (Kerler and Schönherr 1988b, Schreiber and Schönherr 2009). In leaf and fruit cuticular permeation research, this approach led to the identification of two different pathways for solute permeation across plant cuticles which are the lipophilic and the hydrophilic pathway (Popp et al. 2005, Schlegel et al. 2005, Schreiber and Schönherr 2009). Once the dependency of the permeance on the solutes' physico-chemical properties is established, a prediction equation can be obtained which can be used to calculate the permeance for any other solute with known physico-chemical properties (Kerler and Schönherr 1988b, Schreiber and Schönherr 2009).

For the determination of permeances, steady-state permeation across the barrier has to be measured (Hartley and Graham-Bryce 1980). With whole seeds, steady-state uptake experiments are very difficult. When whole seeds are used for uptake experiments, the seed has to be digested prior to measuring the uptake amount. In the case of measurement of radioactively labelled solutes, the digestion solution has to be compatible with the scintillation cocktail. In the case of solute quantification by HPLC with diode array detection, the peaks obtained from the digested mixture of seed components could interfere with the peak of the solute of interest and thus

hinder quantification. A laborious purification of the sample would be necessary. Therefore, the measurement of solute amounts taken up by digestion of whole seeds is difficult. An option besides digestion of the seed could be indirect uptake measurement by measurement of concentration decrease of a donor solution (Rieder et al. 1970, Scott and Phillips 1971, Phillips et al. 1972). But in such experiments still the problem of unknown driving forces remains. Upon solute uptake there is an unknown and changing concentration of the solute in the seed interior since the rate of solute distribution within the seed or the rate of metabolism of the solute are not known.

These difficulties are circumvented in the present study by the use of isolated seed coat halves instead of whole seeds in uptake experiments. In the established experimental setup for steady-state experiments with isolated *Pisum sativum* seed coats (chapter 2.6) the seed coat separates a donor solution from a receiver solution. Permeation of the solute across the seed coat is measured by analysing concentration changes in the solutions. With this experimental setup, permeances for solutes can be measured under controlled steady-state conditions with a known concentration gradient as driving force. Thus, the experiments can be comparable and highly reproducible. Further advantages of the established experimental setup are that the receiver is easily accessible and nested samples are obtained by repetitive sample taking from one seed coat half. Thus, the established experimental setup could be used to perform steady-state experiments with isolated *Pisum sativum* seed coat halves in order to examine the underlying transport mechanisms and the seed coat barrier properties.

In steady-state experiments with watery solutions on both sides of a barrier, the difference in concentration gradient leads to a diffusive flow of solute (Kerler et al. 1984, Schreiber and Schönherr 2009). The difference in solute concentration also causes an osmotic potential difference between donor and receiver solution but in the present experiments this was small enough to be neglected. With the van 't Hoff Relation (equation 4.3) the osmotic water potential of this donor solution can be calculated (Nobel 1991).

$$\Psi_{\Pi} = c \cdot R \cdot T \qquad (4.3)$$

Ψ_π is the osmotic water potential in Pa, c is the concentration in the solution in mol m^{-3}, R is the universal gas constant (8.314 J mol^{-1} K^{-1}) and T the absolute temperature in K. The maximum donor concentrations were about 4 mol m^{-3}. According to equation (4.3) this results in a maximum osmotic water potential of the donor solutions of only 0.01 MPa. Thus, the concentration difference between donor and receiver was taken to be the only factor driving transport processes and permeances were obtained from the steady-state experiments which could be used to characterise the barrier properties of the seed coat.

4.4.2 Effect of solute lipophilicity on permeation

In lipophilic pathways across lipophilic membranes as for example biomembranes or plant cuticles, the permeation process is a combination of solution and diffusion (Stein 1986, Vieth 1991, Cussler 1997). The molecule dissolved in an outside medium enters the membrane in a first partitioning step, diffuses across the membrane and leaves it in a second partitioning process on the other side. Since lipophilic solutes have a higher solubility in a lipophilic barrier than polar solutes, partitioning of lipophilic solutes into the barrier is favoured. Therefore, substances with higher lipophilicity can permeate lipid barriers at a higher rate than polar ones (Stein 1986). The correlation between permeance and lipophilicity can be described by equation (4.4) (Lieb and Stein (1971).

$$P = \frac{D \cdot K}{\Delta x} \qquad (4.4)$$

In this equation, P is the permeance via lipophilic pathways [m s^{-1}], D [m^2 s^{-1}] is the diffusion coefficient in lipophilic pathways in the barrier, K (dimensionless) is the partition coefficient between the lipid barrier and water and Δx [m] is the thickness of the barrier. For cuticular permeation it was shown that the *n*-octanol/water partition coefficient $K_{o/w}$ makes a good approximation instead of the partition coefficient between the lipophilic cuticular barrier itself and water (Kerler and Schönherr 1988a, Kerler and Schönherr 1988b). $K_{o/w}$ describes the lipophilicity of a solute (Leo et al. 1971). Hydrophilic solutes have a $K_{o/w} < 1$ and for lipophilic solutes the *n*-octanol/water partition coefficient is > 1. For different substances $K_{o/w}$ can vary over several orders of magnitude. The high importance of solute lipophilicity on

permeation via lipophilic pathways has been demonstrated for plant cuticles where the permeances to lipophilic organic solutes also vary by several orders of magnitude due to the wide range of magnitudes covered by the $K_{o/w}$ (Kerler and Schönherr 1988b, Schreiber and Schönherr 2009), (Figure 4.2).

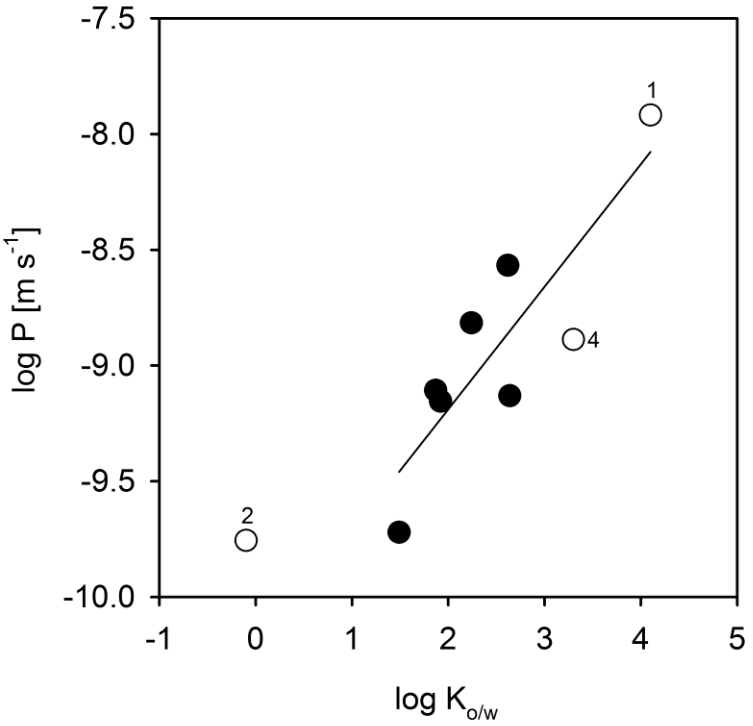

Figure 4.2: Permeation of solutes across isolated *Prunus laurocerasus* leaf cuticles. Data are taken from (Kirsch et al. 1997), permeances for three AIs (white symbols, numbers refer to Table 2.1) were measured (n=1, unpublished results) according to (Kirsch et al. 1997). Results are given as means. The regression line is represented by the equation y = 0.530 x - 10.2 (R^2 = 0.74). The hydrophilic AI thiamethoxam (number 2) was excluded from the regression line.

The permeances of swollen pea seed coats for the set of organic model compounds used in this study cover only one order of magnitude (Table 3.4). This is a clue for a minor importance of solute lipophilicity on the permeation process across pea seed coats. This is confirmed when the measured permeances across *Pisum sativum* seed coats are plotted versus their corresponding *n*-octanol/water partition coefficients as

a measure for substance lipophilicity since in this graph no correlation between these two properties can be seen (Figure 4.3).

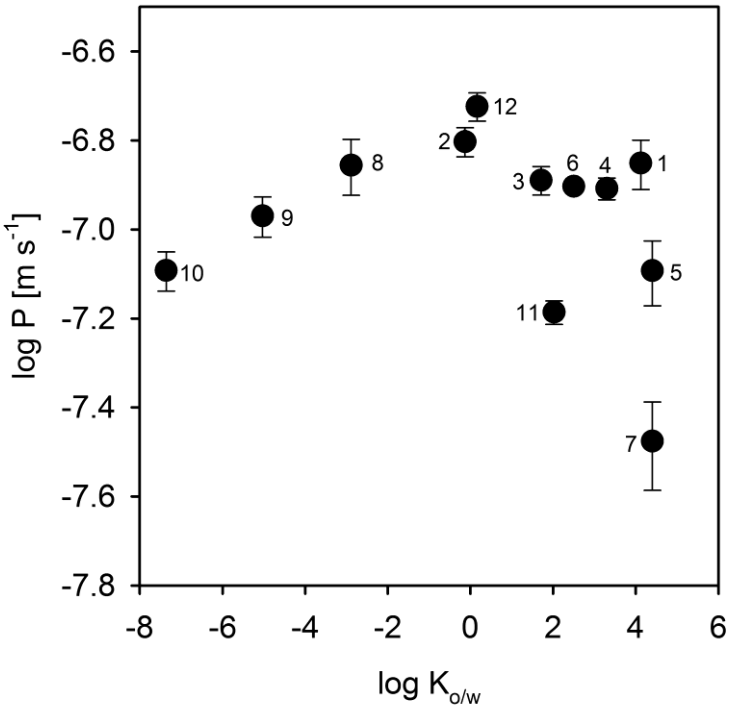

Figure 4.3. Logarithm of the permeance (P) across pea seed coats plotted versus the logarithm of the *n*-octanol/water partition coefficient ($K_{o/w}$) as a measure for the lipophilicity of the model compounds, given as means with 95 % confidence intervals (R^2 = 0.04). Numbers refer to Table 2.1.

Since a plot of the measured permeances across seed coats and the *n*-octanol/water partition coefficient gave no correlation (Figure 4.3), a plot of the permeances and the measured seed coat/water partition coefficients ($K_{sc/w}$) (Table 3.3) was examined. $K_{sc/w}$ represents the actual solute sorption in the pea seed coat measured in the present study and therefore in this plot the correlation between permeances and the actual solute sorption in the seed coat is analysed (Figure 4.4).

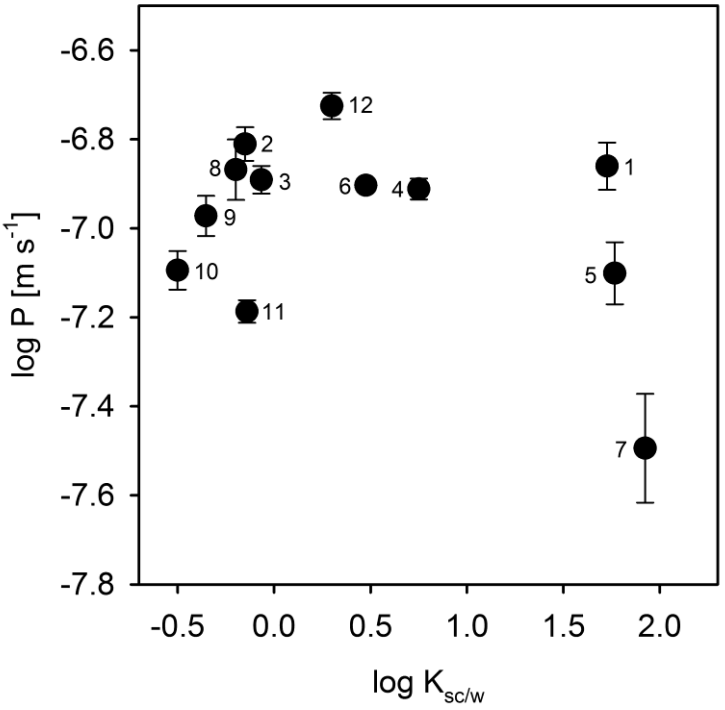

Figure 4.4. Logarithm of the permeance (P) across pea seed coats, given as means with 95 % confidence intervals, plotted versus the logarithm of the seed coat/water partition coefficient ($K_{sc/w}$) (R^2 =0.15). Numbers refer to Table 2.1.

The measured permeances do not correlate with the solute amounts sorbed into the seed coat material (Figure 4.4). The lipophilic solutes are sorbed in higher concentrations in the seed coat (Figure 4.1) but this does not influence permeation. Consequently, permeation of solutes across swollen pea seed coats does not take lipophilic pathways. The presence of aqueous pathways has to be postulated for explaining solute permeability of seed coats.

The fact that permeation across the *Pisum sativum* seed coat takes aqueous pathways might confuse since the seed coat is covered by a lipophilic cuticle (Table 3.1). However, the lipophilic fraction of pea seed coats is very small (chapter 4.2), suggesting a minor importance of this fraction which was confirmed by the results (Figures 4.3 and 4.4). Since lipophilic solutes partition into the seed coat lipophilic fraction (Figure 4.1) but permeation across the seed coat is not influenced by this partitioning into the lipophilic seed coat compartment (Figure 4.4) the lipophilic sorption compartment in the seed coat does not form a continuous lipophilic barrier

enclosing the whole seed. For soybean seeds it was found that the seed coat covering cuticle of water permeable seed coats has cracks facilitating water inflow (Ma et al. 2004). Such cracks could also be present in the *Pisum sativum* seed coat covering cuticle and enable permeation of solutes via aqueous pathways across the seed coat. Therefore, the cuticle covering seed coats of *Pisum sativum* seeds is no all-over barrier and solute permeation can take place via aqueous pathways.

4.4.3 Effect of solute size on permeation

In aqueous pathways permeation takes place via a continuous aqueous phase between the medium at the outer and the inner side of the testa. Thus, there is no phase change of the solute from the aqueous solution into lipid compartments of the barrier and back again to the aqueous phase on the opposite side. Instead, the solute diffuses from the aqueous donor compartment via continuous aqueous pathways across the testa into the aqueous receiver compartment on the other side of the barrier. As no partitioning step is involved, substance lipophilicity has no impact on permeation. Instead, the permeance for a solute diffusing via aqueous pathways through a porous barrier depends mainly on the molar volume of the permeating solute due to narrow inner dimensions of the pathway.

4.4.3.1 Stokes-Einstein model of size dependence

One approach to describe the size dependence of diffusion of a molecule in a medium is by the Stokes-Einstein equation (equation 4.5) which describes diffusion in a simple liquid (Lieb and Stein 1971).

$$D = \frac{k \cdot T}{6 \cdot \pi \cdot r \cdot \eta} \qquad (4.5)$$

In this equation, D is the diffusion coefficient [m^2 s^{-1}], *k* is the Boltzmann constant [J K^{-1}], T is the absolute temperature [K], r is the molecule radius [m] and η is the viscosity of the medium [Pa s]. According to Lieb and Stein (1971), diffusion in a simple liquid like water is given if in a plot of log D or log P versus log MV a linear regression line with a slope of 0.5 to 0.3 is obtained.

The plot of the logarithms of permeances for the set of model compounds across swollen pea seed coats versus the logarithms of their molar volumes (MV) [$cm^3\,mol^{-1}$] shows a good linear correlation (Fig. 4.5). The larger the permeating solute, the slower does it permeate across the seed coat. The fact that permeation across *Pisum sativum* seed coats depends on molar volume instead of lipophilicity strongly supports the hypothesis that aqueous pathways are the route taken by the solutes across the seed coat.

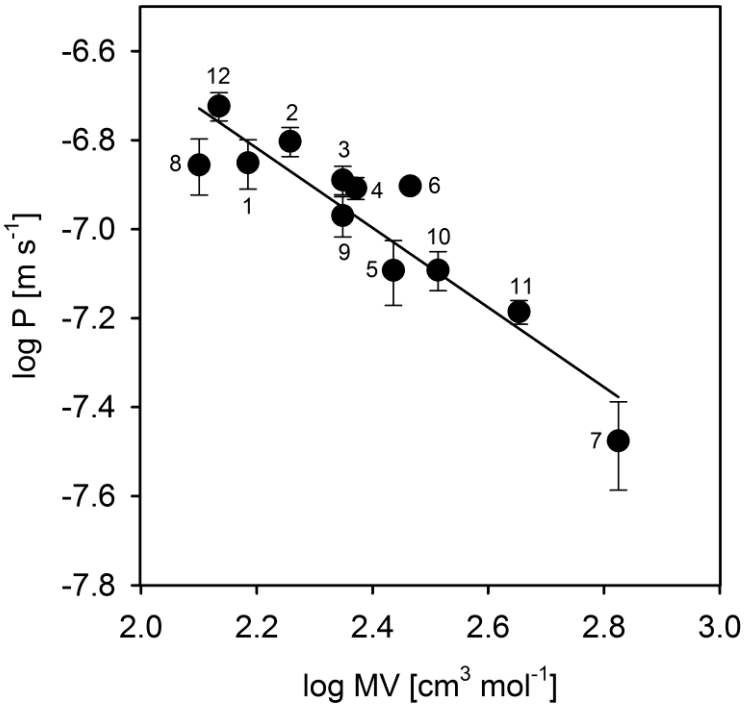

Figure 4.5: Logarithm of the permeance (P) across pea seed coats plotted versus the logarithm of the molar volume (MV) of the model compounds, given as means with 95 % confidence intervals. The regression line is described by y= -0.895 x - 4.85 (R^2 = 0.83). Numbers refer to Table 2.1.

The regression line (R^2 = 0.83) can be used for estimating seed coat permeances for other compounds (equation 4.6) from the molar volume in $cm^3\,mol^{-1}$.

$$\log P = -0.895 \cdot \log MV - 4.85 \qquad (4.6)$$

From the slope of the regression line of the plot of the logarithm of permeances for the set of model compounds versus the logarithm of the corresponding molar volumes (Figure 4.5), the size selectivity of permeation across pea seed coats can be obtained. It amounts to -0.9 (taken from a plot of log P versus log MV, thus dimensionless). This size selectivity is slightly steeper than the size selectivity for diffusion in free water where values of -0.3 to -0.5 are obtained (Lieb and Stein 1971). Therefore, a size dependence is given, but the size selectivity for permeation across seed coats is slightly larger than for diffusion in free water. This could be caused by structural constraints or tortuosity slowing down permeation via aqueous pathways across the seed coat. The size selectivity for permeation across the pea seed coat is much smaller than size selectivity for diffusion of organic compounds via lipophilic pathways in barley leaf wax which amounts to -2.9 to -15 (Schreiber and Schönherr 1993). This highlights again the difference between typical cuticular permeation via lipophilic pathways and permeation across the *Pisum sativum* seed coat via hydrophilic pathways.

4.4.3.2 Free volume theory of size dependence

A second approach which is often used for the interpretation of size dependency of permeation (Baur et al. 1996, Schönherr and Schreiber 2004, Schlegel et al. 2005) is based on the free volume theory describing diffusion in a polymer network instead of in a simple liquid (Cohen and Turnbull 1959, Lieb and Stein 1971, Potts and Guy 1992). In this theory, diffusion is assumed to be a movement through holes or free volumes in the polymer which open transiently due to thermal motion of the polymer material (Lieb and Stein 1971). As larger holes open less frequently than smaller holes, molecular size has a much greater effect on diffusion in this approach (Lieb and Stein 1971). This high importance of molecular size on diffusion is described by equation (4.7) as a first-order correlation (Potts and Guy 1992, Burghardt et al. 2006).

$$D = D_0 \cdot \exp^{-\beta \cdot MV} \qquad (4.7)$$

In this equation, D_0 [cm^2 s^{-1}] is the diffusion coefficient of a fictive solute having a molar volume of 0 cm^3 mol^{-1}, β is the size selectivity of diffusion [mol cm^{-3}] and MV is

the molar volume [cm^3 mol^{-1}] of the diffusing solute. The plot of the logarithm of measured permeances for the set of model compounds across swollen pea seed coats versus their molar volumes MV [cm^3 mol^{-1}] shows a good linear correlation (Figure 4.6).

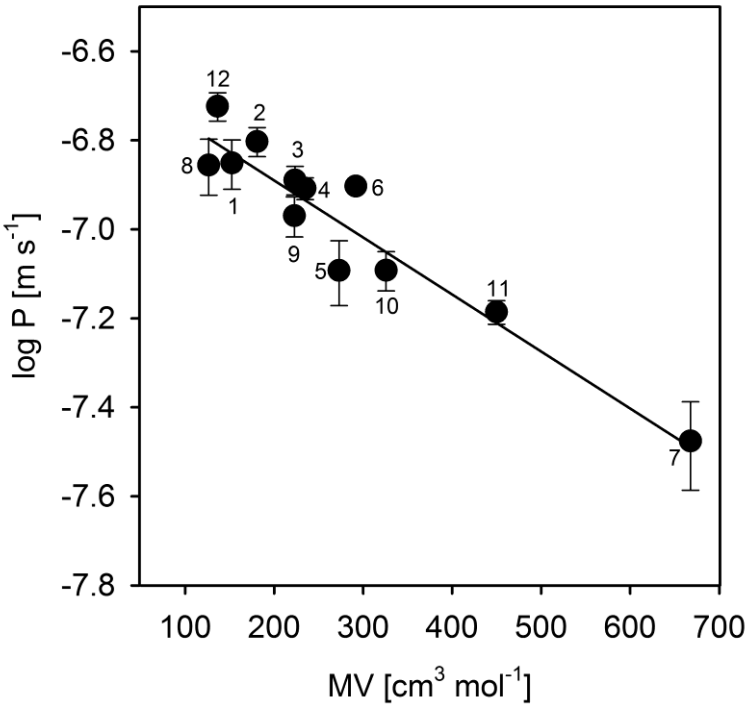

Figure 4.6: Logarithm of the permeance (P) across pea seed coats plotted versus molar volume (MV) of the model compounds, given as means with 95 % confidence intervals. The regression line is described by y = - 0.00128 x - 6.63 (R^2 = 0.90). Numbers refer to Table 2.1.

The regression line (R^2 = 0.90) can be used for estimating seed coat permeances for other compounds with known molecular size (equation 4.8):

$$\log P = -0.00128 \cdot MV - 6.63 \qquad (4.8)$$

The slope of the regression line (equation 4.8) represents the size selectivity of permeation across pea seed coats. It amounts to -0.00128 mol cm^{-3} (taken from a plot of log P versus MV).

From the literature, size selectivities for movement across biomembranes or leaf cuticles are available (Stein 1986, Potts and Guy 1992, Baur et al. 1996, Schönherr and Schreiber 2004, Schlegel et al. 2005). Size selectivities amount to -0.052 and -0.037 mol cm^{-3} for permeation across mammalian and plant cell membranes (Stein 1986) and to -0.011 mol cm^{-3} for permeation across human skin (Potts and Guy 1992). In leaf cuticular desorption experiments measurement of rate constants led to size selectivities of about -0.012 to -0.009 mol cm^{-3} for solute movement via lipophilic pathways (Baur et al. 1996). Size selectivities for movement via polar cuticular pathways are much lower. They amount to values in the range of -0.0028 to -0.0012 mol cm^{-3} (Schönherr and Schreiber 2004, Schlegel et al. 2005). The size selectivity for permeation across pea seed coats is in the lower range of size selectivities in polar leaf cuticular pathways. It is about 10-fold smaller than typical size selectivities in lipophilic leaf cuticular pathways and 50-fold smaller than size selectivities in cell membrane permeation. This agrees with the finding that permeation across pea seed coats is different from permeation via lipophilic pathways.

To compare the size selectivity of permeation across isolated *Pisum sativum* seed coats with the size selectivity of diffusion across a layer of free water of the same thickness as the seed coat, fictive permeances for the model compounds were calculated. The diffusion coefficient D_{water} of a solute in free water can be calculated according to Mitragotri (2003) by equation (4.9).

$$D_{water} = \frac{2.6 \cdot 10^{-5}}{r} \qquad (4.9)$$

In this equation D_{water} [m^2 s^{-1}] is the solute diffusion coefficient in water and r [m] is the solute radius. The solute radius was estimated from the molar volume by assuming spherical shape. With the diffusion coefficient known, the permeance across a layer of free water was calculated with equation (4.10),

$$P = \frac{D}{\Delta x} \qquad (4.10)$$

where P is the calculated permeance across a layer of free water [m s^{-1}], D [m^2 s^{-1}] is the diffusion coefficient in free water and Δx is the thickness of the layer of free water

[m]. Figure 4.7 shows the calculated permeances for the set of model compounds across a layer of free water of equal thickness to the seed coat (185.8 µm, chapter 3.1.2) in comparison to the measured permeances across isolated pea seed coats.

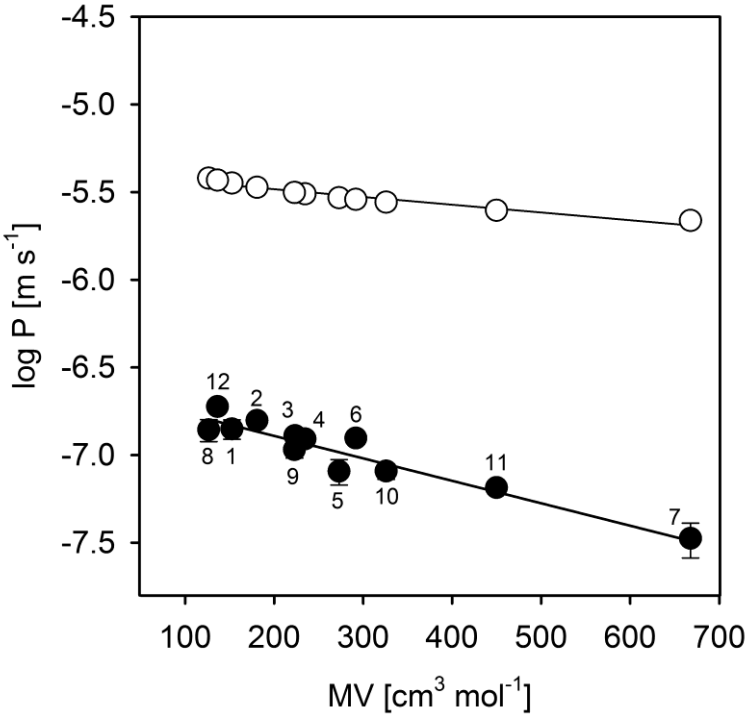

Figure 4.7: Logarithm of calculated permeances across a layer of free water of equal thickness to the pea seed coat (white symbols) in comparison to logarithm of the measured permeances across pea seed coats (black symbols) plotted versus molar volume (MV) of the model compounds, given as means with 95 % confidence intervals. The regression line for calculated permeances across a layer of free water is described by y = - 0.000443 x - 5.39 (R^2 = 0.93). Numbers refer to Table 2.1.

The resulting size selectivity for permeation across a layer of water of the same thickness as the testa is taken from the slope of the regression line in Figure 4.7 and amounts to -0.0004 mol cm^{-3}. This value is about threefold smaller than the size selectivity for permeation across seed coats. Figure 4.7 also shows that permeation across the pea seed coat is slower than permeation across a layer of free water, as indicated by the smaller permeances. This implies that permeation across the seed coat is hindered by structural constraints in narrow pores.

The mean pore radius of these pores can be calculated with an equation (equation 4.11) which was developed by Beck and Schultz (1972) and used by several authors in a modified form for the calculation of pore radii in plant cuticular permeation (Eichert and Goldbach 2008, Arand et al. 2010):

$$r_p = \frac{r_2 - r_1 \cdot \sqrt[4]{\frac{P_{C2}P_{W1}}{P_{C1}P_{W2}}}}{1 - \sqrt[4]{\frac{P_{C2}P_{W1}}{P_{C1}P_{W2}}}} \qquad (4.11)$$

The pore radius r_p can therefore be calculated from permeances across a barrier P_c and across a layer of free water P_w for two solutes 1 and 2 with different molecular radius r ($r_2 > r_1$). For permeation across isolated pea seed coats and calculated with permeances for abamectin and fludioxonil, the mean pore radius obtained from equation (4.11) is 1.57 nm. This pore radius is much larger than calculated pore radii for permeation via hydrophilic pathways across plant cuticles or extracted plant cuticles which lie in the range of 0.3 to 0.6 nm (Schönherr 1976, Popp et al. 2005, Arand et al. 2010). In polar leaf cuticular pathways the pathways for permeation are described to be formed by the sorption of water to free polar functional groups in the cutin matrix like hydroxyl, amino, and carboxyl groups (Schönherr 2006, Schreiber and Schönherr 2009). Since permeation across swollen pea seed coats can take place in the swollen cell wall material or even in the water-filled lumen of the dead cells or intercellular spaces between the hourglass cells (Figure 3.1) it is clear that the pore radius for aqueous pathways across seed coats has to be larger. It has to be kept in mind that the theoretical pore radius is a mean value and the distribution of pore sizes is not known, though.

From the plot of calculated permeances across a layer of free water of equal thickness to the pea seed coat in comparison to the measured permeances across pea seed coats (Figure 4.7), the theoretical permeance for a molecule of a molecular size of 0 $cm^3\ mol^{-1}$ is obtained from the y-intercept. In the case of permeation across pea seed coats this theoretical permeance P_{sc}^0 is 2.34 x 10^{-7} m s^{-1}. For permeation across a layer of free water of equal thickness the respective value P_w^0 is 4.07 x 10^{-6} m s^{-1} which is by a factor of 17 larger. Permeation across the seed coat is by a factor

of 17 slower than permeation across a layer of free water due to the tortuosity τ of the aqueous path across the seed coat and the porosity ε of the barrier (equation 4.12).

$$P_{sc}^{0} = \frac{\varepsilon}{\tau} \cdot P_{w}^{0} \qquad (4.12)$$

Inserting P_{sc}^{0} and P_{w}^{0} obtained from figure (4.7) in equation (4.12) gives a value of 0.057 for the term $\varepsilon\ \tau^{-1}$, but the exact value of ε and τ cannot be obtained from this equation. If one assumes the extreme case that the aqueous pores cross the seed coat in a straight line (τ = 1), ε becomes 0.057 and the seed coat porosity would be 5.7 %. With the porosity known, the number of pores per area can be calculated. For this calculation the mean pore area is calculated from the mean pore radius (obtained from equation (4.11), 1.57 nm) assuming circular shape, with a resulting mean pore area of 7.7 nm^2. Dividing the total pore area (0.057 $cm^2\ cm^{-2}$) by 7.7 nm^2 gives a number of pores of 7.4 x 10^{11} cm^{-2}. Since it can be assumed that the actual τ is smaller than 1, the actual pore number is smaller than this calculated value.

A second possible assumption which could be used for a calculation of τ would be the extreme assumption that during seed swelling the total increase in surface area would represent pores. During seed swelling, the seed coat area increases from 1.68 cm^2 to 2.70 cm^2 (chapter 3.1.1). The newly formed surface area therefore is 0.38 cm^2 cm^{-2}. If this area is taken to represent a porosity ε of 0.38, the resulting τ would be 6.7. Dividing ε = 0.38 $cm^2\ cm^{-2}$ by the pore area would result in a number of pores of 4.9 x 10^{12}. In this extreme assumption the resulting number of pores would be even larger than in the first assumption.

Both assumptions lead to pore densities on the seed coat surface which are higher than polar pore densities of 7.5 x 10^{10} cm^{-2} which were found in extracted plant leaf cuticles (Schönherr 1976).

4.4.4 Effect of temperature on permeation

Further insight into the nature of the permeation process can be gained from its temperature dependence. For permeation across a plant cuticle, temperature influences permeation both by a decrease of sorption and by an increase of mobility with increasing temperature (Schreiber and Schönherr 2009). The resulting temperature effect can be quantified by the activation energy (Baur and Schönherr

1995, Schönherr 2002, Popp et al. 2005). The activation energy for permeation can be calculated according to the Arrhenius formalism from permeances measured at different temperatures according to equation (4.13).

$$P = P_0 \cdot e^{\frac{-E_A}{R \cdot T}} \qquad (4.13)$$

P [m s^{-1}] is the permeance, P_0 the pre-exponential factor, E_A the activation energy [J mol^{-1}], R the universal gas constant [J mol^{-1} K^{-1}] and T the temperature [K]. This correlation is often shown in an Arrhenius plot, where the natural logarithm of the permeance is plotted versus the inverse of the absolute temperature [K^{-1}]. From an Arrhenius plot of the data of thiamethoxam seed coat permeation at different temperatures (Table 3.5 and Figure 4.8) the activation energy E_A [J mol^{-1}] is obtained by multiplying the slope of the regression line β with the universal gas constant R (8.314 J mol^{-1} K^{-1}) (equation (4.14)).

$$E_A = \beta \cdot R \qquad (4.14)$$

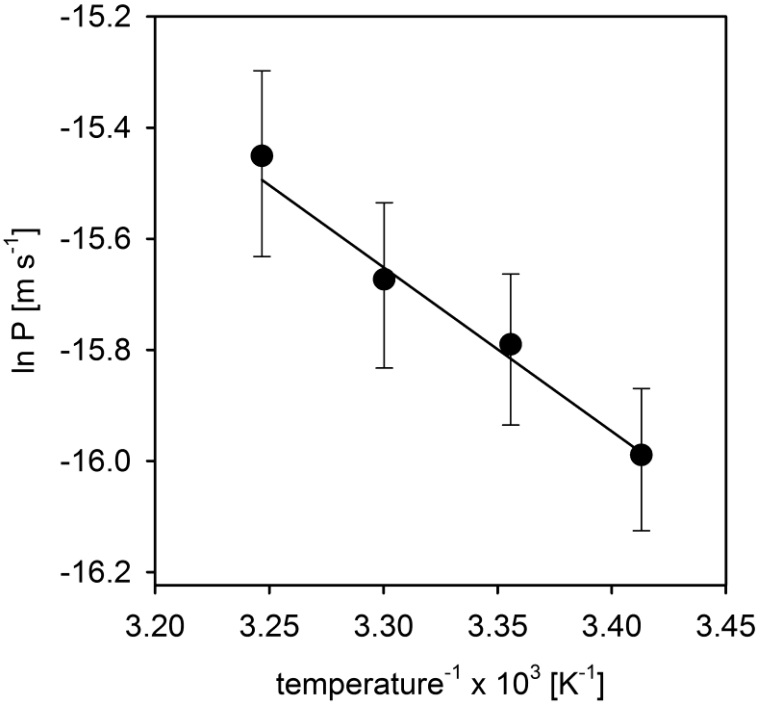

Figure 4.8: Effect of temperature on permeation of thiamethoxam across pea seed coats, shown in an Arrhenius plot. Results are given as means with 95 % confidence intervals. The regression line corresponds to the equation y = -2.95 x - 5.90 (R^2 = 0.99).

In lipophilic pathways high activation energies of 50 to 63 kJ mol^{-1} for cell membranes (Brahm 1983) or 75 to 189 kJ mol^{-1} for plant cuticles (Baur and Schönherr 1995, Baur et al. 1997a) were found. For polar solutes, however, the effect of temperature on permeation is rather low. Activation energies amount to values below 25 kJ mol^{-1} for permeation of polar solutes across plant cuticles (Schönherr 2002, Popp et al. 2005) or 5 to 54 kJ mol^{-1} for permeation of polar solutes across synthetic membranes (Ratner and Miller 1973, Sharma et al. 2003). The activation energy for permeation of thiamethoxam across pea seed coats was 24.5 kJ mol^{-1} (Figure 4.8). This small activation energy is typical for permeation via aqueous pathways.

4.4.5 Effect of a water potential gradient on solute flow

The application of a water potential gradient across a membrane induces a bulk flow of water only when a continuous aqueous pathway is present (Verkman 2000). This bulk flow of water can be driven by a hydrostatic pressure or by an osmotic water potential gradient (Meyer et al. 2007). PEGs of a molecular weight of ≥4000 g mol^{-1} were assumed to be practically unable to cross the pea seed coat (Manohar 1966). This can be confirmed by an extremely low permeance for the PEGs used in the present experiments in the order of 2.7×10^{-15} m s^{-1} which can be estimated from equation (4.8). Therefore, receiver solutions containing PEGs generated an osmotic water potential gradient across the seed coat. It was demonstrated with synthetic porous membranes that a bulk flow of water induced by a water potential gradient can drag along solutes ("*solvent drag*") and thereby increases the overall solute flow (Yasuda and Peterlin 1973, Van Bruggen et al. 1982). In the present study, this phenomenon has also been observed as the solute flow across the *Pisum sativum* seed coat increased when an osmotic water potential gradient was applied (Figures 3.9 and 3.10).

This shows that there are two possible mechanisms for passage of solutes across the seed coat: (1) diffusion and (2) movement via viscous bulk flow of water. Both fluxes take aqueous pathways across the testa. These pathways may be assumed to have a distribution of pore widths of unknown form ranging from the microscopic dimensions of cracks to narrow pathways at the molecular scale. Viscous flow of water can take place already in very small water-filled structures. (Ticknor 1958) demonstrated that for the bulk flow of water being higher than the diffusive flow, the pore radius in cellophane membranes has to be larger than twice the radius of a water molecule, which is about 0.20 nm. For plant cuticles, it was shown that pore sizes as small as 0.45 nm (Schönherr 1976) allow a bulk flow of water.

Under natural conditions this increase in solute transport across the seed coat mediated by a bulk flow of water can occur during seed swelling when the low water potential of the dry seed drives a bulk flow of water across the seed coat. In this transport situation both a solute concentration gradient and a water potential gradient act as driving forces for transport processes. After seed swelling is finished the bulk flow of water stops and the concentration gradient is the only driving force for solute

permeation across the seed coat. When seeds are fully swollen only diffusive permeation can take place.

4.4.5.1 Quantification of solute flow during solvent drag transport situation

The total solute flow F_{total}^{solute} in the presence of solvent drag across the seed coat is the sum of the solute flow caused by solvent drag $F_{solvent\ drag}^{solute}$ driven by a gradient of water potential and the diffusive solute flow $F_{diffusive}^{solute}$ driven by a concentration gradient of the solute (equation 4.15).

$$F_{total}^{solute} = F_{solvent\ drag}^{solute} + F_{diffusive}^{solute} \quad (4.15)$$

The solute flow $F_{solvent\ drag}^{solute}$ caused by the water potential gradient is described as the bulk flow of water F_{bulk}^{water} [g s^{-1}] multiplied with the concentration in this flowing water c_{solute} [g g^{-1}] (equation 4.16).

$$F_{solvent\ drag}^{solute} = F_{bulk}^{water} \cdot c_{solute} \quad (4.16)$$

The bulk flow of water can be calculated with equation (4.17) by multiplication of the seed coat hydraulic conductivity L_{hydr} [m s^{-1} MPa^{-1}], the area A [m^2] involved in the transport process, and the water potential gradient $\Delta\Psi$ [MPa] as driving force:

$$F_{bulk}^{water} = L_{hydr} \cdot A \cdot \Delta\Psi \quad (4.17)$$

Combining equations (4.16) and (4.17) leads to a calculation of the solute flow $F_{solvent\ drag}^{solute}$ caused by the solvent drag mechanism (equation 4.18).

$$F_{solvent\ drag}^{solute} = L_{hydr} \cdot A \cdot \Delta\Psi \cdot c_{solute} \quad (4.18)$$

To calculate the diffusive flow $F_{diffusive}^{solute}$ equation (4.19) is used with the permeance P [m s^{-1}], the area A [m^2] and the concentration difference Δc [g m^{-3}].

$$F_{diffusive}^{solute} = P \cdot A \cdot \Delta c \qquad (4.19)$$

Equations (4.18) and (4.19) predict an increase in solute flow by factors of 1.6 for glucose and 1.7 for sedaxane when a water potential gradient of −2.89 MPa is applied as in the present study and the value of 0.0305 g s^{-1} m^{-2} MPa^{-1} (Figure 3.6) is taken as mean seed coat hydraulic conductivity. These effects are not significantly different from the values measured in the experiments (1.69 for glucose and 2.16 for sedaxane). The effect is similar for both solutes irrespective of differences in their physico-chemical properties (glucose is a polar, sedaxane is a lipophilic solute) as the water potential difference applied causes the same flow of solvent irrespective of the properties of the solute and, thus, the effect on solute flow is caused exclusively by solvent drag.

4.5 Simulation of seed treatment AI distribution in moist soil

After establishment of the basic mechanisms and theory of seed coat permeation with the help of the steady-state permeation experiments, the following experiments were aimed at understanding the seed uptake situation of a treated seed in a moist soil environment. This situation is more complex than permeation in the steady-state experiments. In the moist soil environment, the AI in the seed treatment residue dissolves and thus becomes mobile. Then a distribution of the AI between the competing compartments of seed interior and the surrounding soil takes place. The uptake mechanism of dissolved AI can be via diffusion or via solvent drag during seed imbibition when water moving into the seed can drag along the dissolved AI across the seed coat (chapter 4.4.5). Concentration gradients and water potential gradients as driving forces are continuously changing during seed swelling and AI uptake in soil. To study these complex processes, experimental setups were established with whole treated seeds and as a simplified screening tool also with isolated treated seed coat halves (chapter 2.7.3).

4.5.1 Established methods

4.5.1.1 Seed treatment methods

In commercial seed treatment products complex formulations are used for the application of the AIs which are often highly lipophilic (Backman 1978). These seed treatment formulations contain combinations of additives like antidust agents, dispersing agents, surfactants and others (Backman 1978) besides the AI. In the present experiments which are designed to analyse the uptake process of a treated seed in the field, such mixtures of additives would interfere with the transport process. The seed treatment solution used in the present experiments therefore had to contain as few ingredients as possible. Consequently, only the AI and adjuvant to be examined were applied as solution in water. Sedaxane was dissolved in 50 % acetonitrile in water because of its low water solubility (Table 2.1). With a formulation of sedaxane in water, it would not have been possible to apply the AI amounts needed for the experiments. The disadvantage of a treatment solution with acetonitrile is that the solvent could have led to alterations on the seed coat surface prior to evaporation. This possible source of error was accepted to be able to apply sufficient amounts of sedaxane to the seeds.

4.5.1.2 Experimental setups for analysis of seed treatment AI distribution

Two different experimental setups were established for the examination of seed treatment AI distribution. The first experimental setup with whole treated seeds was used to analyse the complete situation of a treated seed in the soil including the natural seed swelling process. The contact between seed and sand was not disturbed and thus seed dressing zones could form around the seed which can also affect uptake processes (Simmen and Gisi 1998). In these experiments, AI distribution was closer to the real situation of a treated seed in the field but also very complex and thus difficult to interpret. Another disadvantage of these experiments was that no nested samples could be obtained. Thus, with this experimental setup many samples were needed and the method was time consuming.

In the second experimental setup established, isolated treated seed coat halves were used. This experimental setup was developed as a simplified screening tool. The use of isolated treated seed coat halves instead of whole seeds for the experiments has several advantages. The receiver solution inside of the isolated seed coat is easily accessible and the amount of AI that has crossed the seed coat can be measured without embryo extraction. This makes it possible to obtain nested samples from one single seed coat and thus this experimental setup is less time consuming than the experiments with whole seeds. Yet the process of seed treatment AI distribution in the experiments with isolated treated seed coat halves is different to the AI distribution from an intact treated seed in the field. One difference lies in the swelling process of the seed coat and of the whole seed. By the use of water as receiver solution, a rapid swelling of the isolated seed coat is caused (Figure 3.5) while in whole seeds in soil the complete imbibition process is slower (Figure 3.4). Since aqueous pathways for a bulk flow of water and for solute permeation develop during the seed swelling process (chapter 4.1.1), this different swelling process can be expected to cause differences in AI uptake. Another difference to the real situation in the field is the lack of the water flow into the seed during seed swelling. Due to this, the solvent drag mechanism is excluded from the experiments with isolated treated seed coat halves. Instead of the bulk flow of swelling water into the seed there could even be a slight bulk flow of water into the sand direction caused by the slightly lower water potential of the sand (-0.3 MPa, chapter 3.6.3) in comparison to the water potential of the receiver solution which is close to zero. With equation (4.17) this

hydraulic bulk flow of water into the sand can be calculated. Inserting the water potential difference of 0.3 MPa and the hydraulic conductivity of the seed coat of 0.031 g s^{-1} m^{-2} MPa^{-1} (Figure 3.6) gives a resulting bulk flow of water of only 0.075 µl in the 2 min measuring interval. This very small bulk water flow was neglected. Therefore, in the experiments with isolated treated seed coat halves the diffusive AI distribution alone was examined and thus the uptake process was simplified. This simplification might be of advantage to gain insight into the dissolution and diffusive uptake of seed treatment AI across the seed coat. Possible effects of solute properties and adjuvants on these processes could be estimated, but it has to be kept in mind that the model simplifies the seed treatment AI distribution process.

4.5.1.3 Extraction of AI from seed coats and embryos

In order to determine the AI amounts in the seed coat and embryo samples of whole treated seeds, an extraction of the samples was necessary. The extraction method used in the present experiments to determine AI amounts in seed coats and embryos is based on a very fast ultrasonic solvent extraction method (Schlatter and Beste 2005, Bourgin et al. 2009). As it is a fast method, many samples can be extracted in little time. As shown by very high recovery rates in the extraction of seed coats (Table 3.2) and extraction of sedaxane from embryos (Table 3.6) the method is suitable for AI extraction from *Pisum sativum* seed material. The only exception was extraction of metalaxyl-M from pea embryos incubated in moist sand which gave low recovery rates (data not shown). For metalaxyl-M extraction from plant material high recovery rates of > 80 % are reported in literature, but these are obtained by extraction directly after spiking of plant material with metalaxyl-M (Gupta et al. 1985, Mehta et al. 1997, Bourgin et al. 2009). When living tissue is in contact to metalaxyl-M for some time, as for example when seedlings are grown from treated seeds, the extraction of this AI is reduced (Singh 1989). This is due to a metabolisation into an acid derivative (Gupta et al. 1985, Owen and Donzel 1986, Zadra et al. 2002) and subsequent binding (Senesi 1992, Gevao et al. 2000). Since the embryo is living tissue and embryo metabolism starts only a couple of hours after start of imbibition (Bewley 1997, Weitbrecht et al. 2011) metalaxyl-M can undergo metabolic changes in the embryo during the experiments with whole treated seeds placed in moist sand. This explains why the extraction of metalaxyl-M from embryos in experiments with whole treated seeds was not efficient while the same extraction method used for extraction of

metalaxyl-M from seed coat material, which is composed of dead cells, gave a high recovery rate (Table 3.2).

4.5.2 Experiments with whole treated seeds

4.5.2.1 Mobilisation of the AI from the seed treatment residue

In the experiments with whole treated seeds, sedaxane was mobilised slower from the seed treatment residue than metalaxyl-M. After 20 h 13 % of the applied metalaxyl-M and 56 % of the applied sedaxane were still associated with the seed coat (Figures 3.11 A and 3.12 A). The reason for this much slower mobilisation of sedaxane lies in the different water solubility of the AIs. Calculation with the water solubility (Table 2.1) gives a necessary volume of water for dissolution of the mean applied metalaxyl-M amount of 0.15 µl. For dissolution of the applied amount of the more lipophilic AI sedaxane, 1992 µl of water would be necessary. As a result the applied sedaxane dissolves slower.

Sedaxane was not only mobilised slower from the seed treatment residue than metalaxyl-M but it was also retained in a higher percentage associated with the seed coat at the end of the experiment. The percentage of sedaxane remaining associated with the seed coat did not decrease further after 60 hours (Figure 3.12 A), indicating that about 30 % remained associated with the seed coat. This can be caused by a sorption of the more lipophilic sedaxane in lipophilic compartments of the seed coat. The higher sorption of sedaxane than metalaxyl-M into lipophilic compartments in the seed coat was shown in the seed coat/water partition coefficients (Figure 4.1). The fraction of applied seed treatment AI which was absorbed in the lipophilic sorption compartments of the seed coat remained associated with the seed coat and did not readily move into either direction.

4.5.2.2 AI movement into the sand

During the first hours of the experiments a rapid movement of AI from whole treated seeds into the sand could be observed (Figures 3.11 B and 3.12 B). Within 8 h, about 30 % of the applied metalaxyl-M amount and about 20 % of the applied amount of sedaxane were washed off into the sand. Two reasons could contribute to

this rapid AI movement into the sand. The first reason is that AI uptake across the seed coat takes aqueous pathways (chapter 4.4.3) which are not yet developed in the dry seed (chapter 4.1.1) and thus AI passage across the still dry seed coat is restricted at the beginning of the experiment. Consequently, AI movement into the moist sand is the favoured direction. The second reason for the rapid AI movement into the sand is the higher uptake capacity of the moist sand during the early stages of the experiment. The sand had a water content of 0.2 g water per g dry weight from the beginning on. In comparison to this, the seed was dryer during the first hours of the experiment. Seed swelling in sand is very slow, after 4 hours only 0.04 g water per g dry seed were taken up (Figure 3.4). Therefore, at the beginning of the experiment the sand had a higher water content and thereby a higher uptake capacity for the seed treatment AIs.

In the experiments it could be seen that after 20 h, the AI percentage in the sand did not increase any more. The following reasons could contribute to this stop of AI movement into the sand. The first reason is that during seed swelling pathways for solute uptake across the seed coat as well as uptake capacities in the seed develop and consequently the alternative of solute movement into the seed increased in importance. When completely swollen the pea seed has taken up 0.95 g water per g dry weight (chapter 3.1.1) which could facilitate a higher AI uptake capacity especially for the water-soluble AI metalaxyl-M than the surrounding sand. Therefore, the driving force for movement into the seed was higher. A second reason is a depletion of the seed treatment residue (Figures 3.11 A and 3.12 A) which led to a decrease in the concentration gradient as driving force and thus to a reduction in solute flow. A third reason for the stop of AI movement into sand could be a local drying in the sand close to the seed due to water uptake by the seed, so that AI diffusion in the sand was slowed down due to less extensive and more tortuous diffusion pathways (Hartley and Graham-Bryce 1980).

4.5.2.3 AI uptake across the seed coat

Uptake by metalaxyl-M and sedaxane showed different kinetics. Metalaxyl-M uptake by whole treated seeds was rapid at the beginning of the experiments, within 4 h about 32 % of the applied amount were taken up. Uptake slowed down after about 8 h and after about 40 h the final uptake was reached (Figure 3.11 C). Sedaxane on

the other hand showed a slower but steadier uptake curve which was nearly linear for about 40 h (Figure 3.12 C). The rate constant for uptake of metalaxyl-M was by a factor of 24.7 larger than the rate constant for uptake of sedaxane (Table 3.7). This different uptake behaviour of the two AIs is caused by differences in their physico-chemical properties. First, sedaxane has a slightly larger molar volume than metalaxyl-M (Table 2.1) and thus is taken up across the seed coat slower (chapter 4.4.3). Since the difference in molar volume is very small but the difference in rate constant very large, further physico-chemical properties must play a role. The lower water solubility of sedaxane caused a slower dissolution from the seed treatment residue (chapter 4.5.2.1) and thus less sedaxane was available for uptake. The difference in water solubility has further effects on uptake by the two uptake mechanisms simultaneously taking place during seed swelling which are uptake by solvent drag and diffusive uptake (chapter 4.4.5). The first uptake mechanism is uptake by solvent drag which is coupled with the inflow of swelling water. The water takes up dissolved AI on the outer side of the seed coat and drags it across the seed coat into the seed. *Pisum sativum* seeds take up on average 0.301 ml of water during swelling (chapter 3.1.1). Assuming maximum AI concentration with regard to water solubility (Table 2.1) in these 0.301 ml of inflowing water the maximum AI amount taken up by the solvent drag mechanism is only 4.21 µg of sedaxane or 7826 µg of metalaxyl-M. This calculation shows that only a fraction of the applied sedaxane amount could be taken up by the solvent drag mechanism while in the case of metalaxyl-M the solvent drag mechanism can have much higher importance. This difference was seen in the slower and steadier uptake curve by sedaxane (Figure 3.12 C) in contrast to the faster uptake of metalaxyl-M (Figure 3.11 C). In the real situation the actual amount of AI taken up by solvent drag is lower than the maximum calculated uptake amount for three reasons. The first reason is that the AI concentration in the inflowing water will not necessarily reach water solubility concentrations. Dissolution of solids can be slow and in some cases water solubility is only reached after extensive stirring. The second reason is that not all water uptake during seed swelling in moist sand is by a bulk flow of water but a fraction is also by diffusive uptake of water from air humidity (compare Figure 3.4). Diffusive water uptake will not facilitate solvent drag uptake of solutes. The third reason for a reduced AI uptake by the solvent drag mechanism is that over time the seed treatment residue is depleted (Figures 3.11 A and 3.12 A) and therefore the AI

availability for uptake is reduced. The resulting decrease over time in uptake by solvent drag before completion of seed swelling could be observed in the AI uptake curve of metalaxyl-M treated seeds, since here AI uptake slowed down (Figure 3.11 C) long before seed swelling in sand is completed (Figure 3.4).

The second uptake mechanism taking place in seed treatment AI uptake by treated seeds is diffusive uptake. Uptake by diffusion is driven by a concentration difference across the seed coat as driving force (equation 4.19) which depends on the water solubility of the seed treatment AI. For the situation in the experiments with whole treated seeds, the maximum possible diffusive uptake of metalaxyl-M and sedaxane can be calculated with equation (4.19). The seed coat permeance for sedaxane and metalaxyl-M can be obtained from Table (3.4), as seed surface area A the mean value between the surface area of a dry and a swollen seed is used (2.19 cm^2) and as concentration difference Δc the water solubility is taken from Table (2.1). With this calculation a maximum diffusive AI flow can be calculated which is for sedaxane 0.00038 µg s^{-1} and for metalaxyl-M 0.73 µg s^{-1} which would result in an maximum diffusive uptake amount of 109 µg of sedaxane and 211543 µg of metalaxyl-M within 80 h. The importance of water solubility for the driving force for diffusive uptake can be clearly seen in this difference. This agrees with the much slower uptake of sedaxane than metalaxyl-M observed in the results (Figures 3.11 C and 3.12 C). The measured AI amount actually taken up in the experiments was much smaller than these calculated maximum uptake amounts for three reasons. The first reason is that the permeance which was measured with swollen seed coats is lower during the early swelling stages (chapter 4.1.1). The second reason is that water dissolution of solids can be slow and often reaches maximum water solubility concentration after extensive stirring only. Additionally, the AI concentration on the inner side of the seed coat might be larger than zero, depending on translocation speed within the embryo. Therefore, the concentration difference Δc has to be assumed to be smaller than water solubility. The third reason is that the AI amount left on the seed surface decreases after some time (Figures 3.11 A and 3.12 A). This leads to a reduction of the driving force after some time. The resulting reduction of diffusive uptake could be seen in the present results where uptake of both AIs decreased over time (Figures 3.11 C and 3.12 C).

Thus, AI uptake by a treated seed in moist sand is a complex process. It is combined of two different uptake mechanisms both of which have changing driving forces. Additionally, the hydraulic conductivity of the seed coat changes during seed swelling (Figure 3.7) and it has to be assumed that the seed coat barrier properties to diffusive AI uptake also change with increasing seed moisture content. By modelling of the uptake rate with equation (2.8) this complex process is simplified, resulting in a rate constant and final uptake amount for the uptake curves which can be used to quantify and compare the uptake kinetics.

4.5.2.4 Adjuvant effects

The effect of adigor on uptake in the present experiments with whole treated seeds was not significant (Table 3.7). A small effect could be seen in the mobilisation from the seed treatment residue which was slightly faster when adigor was added to the seed treatment formulation (Figures 3.12 A and D). The enhanced dissolution of sedaxane from the seed treatment residue can be explained by the emulsifying mode of action of adigor. The slightly enhanced dissolution did not lead to significantly increased uptake, though. In contrast to this small effect of adigor in the present experiments with whole treated seeds, a pronounced effect of adigor in leaf cuticular AI uptake was observed (Muehlebach et al. 2007). A difference in the adigor effect between the leaf and seed coat uptake situation was expected since for seed coat uptake aqueous pathways instead of lipophilic pathways are used (chapter 4.4.3). The fact that adigor did not increase uptake across the seed coat while permeation via lipophilic pathways across leaf cuticles is increased by adigor (Muehlebach et al. 2007) can also be seen as additional confirmation of the finding that aqueous pathways are taken for permeation across seed coats (4.4.3).

The second additive examined was the polymer NeoCryl A-2099. In the present experiments the polymer caused a slowed down AI mobilisation (Figures 3.11 A and D, B and E) and a tendency to slow down AI uptake which was statistically not significant (Table 3.7). Film-forming polymers like NeoCryl A-2099 can act as crop safeners in leaf applications and thus prevent phytotoxicity (Angst et al. 2010). For seed treatment formulations a slow release effect of polymers like NeoCryl A-2099 was described (Ding and Arar 2010). This slow release effect was in the present study rather small but could be confirmed. A possible reason for the more pronounced slow release effect caused by NeoCryl A-2099 in commercial seed

treatment formulations could be the fact that in complex commercial formulations the AI is present in a dispersed form.

The differences between both AIs are more noticeable than the effects of the additives examined, indicating that in the situation of a treated seed in the field the AI physico-chemical properties have a higher influence on distribution than the two additives tested.

4.5.2.5 Evaluation of experimental setup with whole treated seeds

The experimental setup with whole treated seeds is closer to the real situation of a treated seed in the field. The imbibition process which can have an influence on AI uptake (chapter 4.4.5) is included in the experimental process. Additionally the formation of seed dressing zones which can also affect uptake processes (Simmen and Gisi 1998) was included in this experimental setup. But working with intact treated seeds has the disadvantage that no nested samples can be obtained. For each measuring time point a new set of treated seeds has to be used. Therefore, the experiments with whole treated seeds are very time consuming. As an alternative experimental setup, an experimental setup with isolated treated seed coat halves was developed as a fast and simplified screening tool.

4.5.3 Experiments with isolated treated seed coat halves

4.5.3.1 Mobilisation of the AI from the seed treatment residue

In the experiments with isolated treated seed coat halves it could be observed that sedaxane was mobilised much slower from the seed coat than both metalaxyl-M and thiamethoxam (Figures 3.14 A, 3.15 A and 3.16 A). After 10 min, 77.8 % of the applied sedaxane were still associated with the seed coat half while only 1.1 % of the applied metalaxyl-M and 1.7 % of the applied thiamethoxam were left associated with the seed coat. This extreme difference can be explained with the different water solubility of the AIs. Calculation with the water solubility (Table 2.1) gives a necessary volume of water for dissolution of the applied thiamethoxam amount of 6.1 µl and for dissolution of the applied metalaxyl-M amount of 1.2 µl which are very small volumes. For dissolution of the applied amount of the more lipophilic AI sedaxane, 1071 µl of

water would be necessary. This explains why the dissolution of sedaxane from the seed treatment residue on the isolated treated seed coat halves was much slower than dissolution of the other two AIs.

4.5.3.2 AI movement into the sand

In the experiments with isolated treated seed coats very small percentages of the AIs diffused into the sand (Figures 3.14 B, 3.15 B and 3.16 B). After 10 min, only 4.4 % of the applied metalaxyl-M and 2.7 % of the applied thiamethoxam have moved into the sand. In the case of sedaxane, a larger fraction of 18.5 % of the applied AI has moved into the sand which equals about 83 % of the dissolved fraction of sedaxane. Since in this experimental setup movement is by diffusion alone, the movement either into the sand or across the seed coat depends on the driving forces and on the diffusion coefficients in these two media. In that compartment where the diffusion coefficient is higher, the AI distributes faster and thus higher AI amounts could move into that compartment. Diffusion coefficients in soil are typically in the range of 10^{-10} m^2 s^{-1} to 10^{-12} m^2 s^{-1} (Hartley and Graham-Bryce 1980). Diffusion in soil material depends on moisture content, tortuosity of diffusion pathways and absorption on organic matter (Hartley and Graham-Bryce 1980). In the present study purified sand without organic matter and with a high moisture content was used as simplified soil material. Due to the high moisture content pathways for aqueous diffusion were comparably large and not very tortuous (Hartley and Graham-Bryce 1980). Consequently, AI diffusion in the sand was fast and diffusion coefficients can be assumed to lie in the higher part of the range of 10^{-10} m^2 s^{-1} to 10^{-12} m^2 s^{-1} described by Hartley and Graham-Bryce (1980). In order to compare this range with diffusion coefficients in the seed coats, diffusion coefficients in the seed coat were calculated from the seed coat thickness and measured permeances according to equation (4.20):

$$D_{sc} = P \cdot \Delta x \qquad (4.20)$$

In this equation D_{sc} is the diffusion coefficient for diffusion in seed coats [m^2 s^{-1}], P is the permeance [m s^{-1}] (Table 3.4) and Δx is the thickness of the seed coat which is 185.8 µm (chapter 3.1.2). The resulting calculated diffusion coefficients for diffusion

in the seed coat material D_{sc} are 2.4 x 10^{-11} m^2 s^{-1} for metalaxyl-M, 2.9 x 10^{-11} m^2 s^{-1} for thiamethoxam and 2.3 x 10^{-11} m^2 s^{-1} for sedaxane. These diffusion coefficients in pea seed coats can be slightly smaller than diffusion coefficients in the sand compartment and thus diffusive distribution of seed treatment AIs should theoretically tend to prefer the sand direction. Yet in the experiments with isolated treated seed coat halves the majority of the applied metalaxyl-M and thiamethoxam were taken up into the receiver solution instead. Therefore, the observed AI distribution must be caused by the driving forces in this situation. The sand had a very limited receiver capacity represented by 0.2 g water per g dry weight of sand. In contrast to this, inside of the seed coat half was a large volume of free water. Movement of the AI into the sand caused a rapid increase in AI concentration in the sand and thus a decrease of the driving force for further movement into the sand. Hydrophilic AIs crossing the seed coat reached a very large suitable receiver compartment and therefore the concentration gradient as driving force for metalaxyl-M and thiamethoxam uptake across the seed coat remained higher. Sedaxane on the other hand is hydrophobic and has very low water solubility. Water saturation was reached quickly in both sand and receiver solution and then driving forces into either direction were reduced. The larger fraction of sedaxane moving into the sand compartment could be caused by adhesion of sedaxane to sand particles. As silicon dioxide has a log *n*-octanol/water partition coefficient of 0.53 (estimated by EPI Suite software), adhesion to this surface might be energetically more favourable than movement into the volume of free water in the receiver. Another possible explanation might be that undissolved sedaxane seed treatment particles could have fallen of or been scraped off into the sand during handling of the seed coat halves at the measuring time points.

4.5.3.3 AI uptake across the seed coat

In the experiments with isolated treated seed coat halves, metalaxyl-M and thiamethoxam showed very rapid uptake across the seed coat. After 10 min, 94.5 % of the applied metalaxyl-M and 95.6 % of the applied thiamethoxam were taken up into the aqueous receiver solution. In contrast to this, only 3.7 % of the applied sedaxane were taken up across seed coat after 10 min (Figures 3.14 C, 3.15 C and 3.16 C). One reason for the uptake of sedaxane being slower than uptake of the other two AIs is that sedaxane has a larger molar volume (Table 2.1) and

consequently permeates the seed coat slower (chapter 4.4.3). But metalaxyl-M and thiamethoxam also have different molar volumes, yet the difference in uptake of these two AIs is much smaller (Table 3.8). Consequently, further physico-chemical properties must play a role. The low water solubility of sedaxane led to slow dissolution from the seed treatment residue (chapter 4.5.3.1). Therefore, little sedaxane was available for uptake. The lower water solubility of sedaxane also led to a lower concentration in solution and thereby to a smaller driving force for diffusive uptake. Metalaxyl-M and thiamethoxam, on the other hand, have higher water solubility (Table 2.1) and thus higher concentrations in solution are reached, resulting in higher concentration differences Δc across the seed coat as driving forces. The maximum possible diffusive uptake across the seed coat can be calculated with equation (4.19) with the permeance P taken from Table (3.4), the area A from chapter 2.6 and as Δc the water solubility taken from Table (2.1). According to this calculation a very rapid uptake across the seed coat is possible for the highly water soluble AIs. Maximum diffusive uptake across the seed coat is 135 µg in 10 min for metalaxyl-M and 25.9 µg in 10 min for thiamethoxam. In the case of sedaxane maximum permeation across the seed coat is only 0.0698 µg in 10 min which is lower than the measured permeation. Uptake across the seed coat in the experimental setup with isolated treated seed coats might be higher than uptake calculated with the permeance from the steady-state experiments because the treated seed coat area could have been larger than the contact area with the microtiter plate well or during seed coat treatment some AI might have already diffused into the seed coat material before drying of the seed treatment solution droplet.

The experiments with isolated treated seed coat halves show that the driving forces for uptake have a very high importance for uptake of seed treatment AIs across the seed coat. Especially in the experiments with isolated seed coat halves treated with metalaxyl-M and with thiamethoxam it could be seen that very high uptake rates across the swollen seed coat are possible, provided the concentration gradient as driving force is high.

4.5.3.4 Adjuvant effects

In the experiments with isolated seed coat halves treated with sedaxane and adigor it could be observed that the addition of adigor in the treatment led to an increased mobilisation of sedaxane from the seed coat halves (Figure 3.15 A and D) which shows the emulsifying action of adigor and the importance of stickers in commercial seed treatment formulations. The enhanced sedaxane mobilisation did not increase uptake across the seed coat, though. Instead, a higher percentage moved into the sand (Figure 3.15 E). This might be explained by the capture of sedaxane within adigor micelles outside of the seed coat. Shafer and Bukovac (1989) suggested that in solutions of a surfactant and an AI the AI can be dissolved within surfactant micelles in the case of the surfactant concentration being above critical micelle concentration. Adigor has a critical micelle concentration of 82.3 mg/l (chapter 3.6.2), which is in the lower range of critical micelle concentrations of surfactants (Adam et al. 2009). Therefore, a formation of micelles by adigor could occur at comparably low surfactant concentrations. Thus it can be assumed that the adigor solution outside of the seed coat in the sand formed a favourable partitioning compartment with micelles for sedaxane. These micelles then would have been very large since micelles are formed of typically 50 to 200 surfactant molecules (Adam et al. 2009) and consequently could not readily cross the seed coat.

NeoCryl A-2099 caused in the experiments with isolated treated seed coat halves a significant reduction of the mobilisation of metalaxyl-M and of uptake across the seed coat (Figure 3.14). For isolated treated seed coat halves with thiamethoxam the effect was less pronounced but present (Figure 3.16). The film-forming polymer additive NeoCryl A-2099 led to a slowed down release of metalaxyl-M and thiamethoxam from the seed treatment residue in the experiments with isolated treated seed coat halves. Such a slow-release action of polymers in seed treatment formulations was also suggested by Ding and Arar (2010).

4.5.3.5 Comparison with experiments with whole treated seeds

The AI distribution and additive effects observed in the experiments with isolated treated seed coat halves showed some differences to the results observed in the experiments with whole treated seeds. The first difference is that AI dissolution from

the seed treatment residue was much faster in the experiments with isolated treated seed coats than in the experiments with whole treated seeds. The reason for this is that in the experimental setup with isolated treated seed coat halves the water availability was higher. The water used as receiver solution led to a rapid swelling of the seed coat (compare Figure 3.5). Since no dry embryo was present inside of the isolated seed coat the high water content of the seed coat and of the sand adjacent to the seed coat were maintained. Consequently a faster dissolution of the seed treatment residue was possible. The second difference was that in the experiments with isolated treated seed coats only a small percentage of the applied water soluble AIs moved into the sand. The reason for this could be that the water saturated isolated seed coat and volume of water as receiver had higher uptake capacities than the sand. In contrast to this, in the experiments with whole seeds the dry seed at the beginning of the experiment had very little AI uptake capacity and the moist sand was favoured as receiver compartment. The third difference between the two experimental setups was that uptake across isolated treated seed coat halves was faster than uptake into whole treated seeds. The rate constant for uptake of metalaxyl-M across isolated treated seed coats was 46 times higher than the rate constant for uptake into whole treated seeds (Tables 3.7 and 3.8). The maximum uptake rate of sedaxane across isolated treated seed coats was 17 times higher than the maximum uptake rate into whole treated seeds (Figures 3.15 and 3.12). This difference can be due to two reasons. First, the aqueous pathways for uptake are formed in the isolated seed coat due to the rapid swelling (Figure 3.5) within minutes while the swelling process of whole seeds in moist sand takes much longer (Figure 3.4, chapter 4.1.1). The second reason is that the AI availability was higher in the experiments with isolated treated seed coats. Due to the rapid swelling of the seed coats the seed treatment residue could dissolve faster and AI availability was higher. In the experiments with whole treated seeds the water availability at the seed coat and consequently mobilisation of the AI were slower. The fourth difference between the two experimental setups was that the adjuvant effects both of NeoCryl A-2099 and of adigor were more pronounced in the experiments with isolated treated seed coats than in the experiments with whole treated seeds. Possible reasons for this can only be supposed. In the case of NeoCryl A-2099, the reduction of uptake which was observed in the experiments with isolated treated seed coats might have been less pronounced in the experiments with whole treated seeds because a high fraction of

uptake into whole seeds was by solvent drag and the physical forces by the bulk flow of water might have been too high for a retention of the AI by the polymer. In the case of adigor, the formation of micelles outside of whole treated seeds could have been reduced because the local moisture content at the seed coat surface was lower.

4.5.3.6 Evaluation of experimental setup with isolated treated seed coat halves

The experimental setup with isolated treated seed coat halves holds many advantages over experiments with whole seeds and therefore could prove to be a valuable screening tool if further optimisation was achieved. One point which could be optimised is the use of water as receiver solution. This is quite different from the natural situation where the embryo is at the inner side of the seed coat. Water, in contrast to the embryo, contains no uptake compartments for lipophilic solutes. As a consequence, lipophilic AIs are not readily taken up across isolated treated seed coats into the receiver solution whereas uptake of water soluble AIs is very high. In the situation with an intact seed, however, the driving force for uptake of lipophilic AIs is higher since lipophilic AIs can be taken up into the lipophilic embryonic cuticle. The driving force for uptake of hydrophilic AIs can be lower depending on translocation within the embryo. To provide both uptake capacities for lipophilic and hydrophilic AIs in the receiver solution in the experiments with isolated treated seed coats, the use of an aqueous soybean lecithin suspension (phospholipid suspension, PLS) as receiver solution could be tested (Baur et al. 1997b). Another approach to optimise this experimental setup could be to use a different vessel for the sand compartment than the microtiter plate. In a larger vessel the contact area between sand and treated seed coat surface could be larger. In addition to this, the isolation of seed coat halves from intact treated seeds should be considered, since then the seed treatment residue would be distributed evenly on the complete seed coat surface area. The use of isolated seed coat halves from intact treated seeds would also bring the advantage that during treatment of whole seeds the volume of liquid is smaller and the treatment solution dries faster, which is closer to the commercial seed treatment procedure.

4.5.4 Soil properties influencing AI distribution

Movement of the AI away from the treated seed into the soil can have a considerable effect on AI uptake. In the case of AIs with high mobility in the soil, the availability for uptake by the seed can be reduced. The mobility and the distribution of AI in soil depend both on the properties of the AI and of the soil (Simmen and Gisi 1996, Simmen and Gisi 1998). A soil property which has high importance for AI mobility is the organic matter content. Organic matter in the soil can cause absorption and thus reduce mobility especially of lipophilic AIs (Hartley and Graham-Bryce 1980, Nicholls 1988, Simmen and Gisi 1996, Haberhauer et al. 2000). Chemical reactive groups on pesticides also lead to increased binding to soil (Barriuso et al. 2008) and thus reduce availability of the AI. Normal soils have an organic matter content of 1 to 6 % (Troeh and Thompson 2005). In contrast to this, the purified sand used in the present experiments can be assumed to contain no organic matter at all. AI mobility was therefore not reduced by sorption effects in the present experiments. Another soil property which has an important influence on AI mobility and distribution in soil is soil moisture content or water potential (Simmen and Gisi 1998). With increasing moisture content of the soil, pathways for diffusion in soil become more extensive and less tortuous (Hartley and Graham-Bryce 1980). The high moisture content in the present experiments led to comparably high AI mobility. In a field situation the AI availability and mobility might be smaller than in the present experiments due to organic matter or less moisture in the soil.

4.5 Outlook

Many aspects of the uptake of solutes across seed coats and the distribution of seed treatment AIs in a moist soil environment have been examined by newly devised methods in the present work. *Pisum sativum* seeds were used as model seeds to establish methods and concepts since these seeds are easy to handle and have a simple seed anatomy. Further work should be performed with a grain crop like *Zea mays* in order to examine whether the developed concepts also apply to this group of plants and how solute permeation across the maize pericarp differs from permeation across the pea seed coat.

An aspect which requires further examination is the effect of different soil moisture contents on AI uptake by intact treated seeds. With a different soil water content, the two different uptake mechanisms of diffusion and solvent drag will have different importance for AI uptake by treated seeds. Since in the present experiments sand with 91 % field capacity was used and thus the availability of liquid water was comparably high, the solvent drag mechanism had a comparably high importance for AI uptake. In sand with a lower moisture content, the solvent drag uptake mechanism would play a smaller role. An experimental setup with a treated seed imbibing in water saturated air would provide the extreme case of uptake by diffusion alone since no bulk flow of water would take place. Such experiments with different availability of liquid water would provide further insight into seed treatment AI uptake by the two uptake mechanisms.

Furthermore, by the use of seeds treated with a complete commercial seed treatment formulation with the AI in suspension or dispersion the experiments with intact treated seeds would be a step closer towards the actual situation of a treated seed in the field.

5. References

Abraham, M. H. and Mcgowan, J. C. (1987). The use of characteristic volumes to measure cavity terms in reversed phase liquid-chromatography. *Chromatographia* **23**(4): 243–246.

Adam, G., Läuger, P. and Stark, G. (2009). Physikalische Chemie und Biophysik. Springer-Verlag, Berlin, Germany.

Aloni, R., Enstone, D. E. and Peterson, C. A. (1998). Indirect evidence for bulk water flow in root cortical cell walls of three dicotyledonous species. *Planta* **207**(1): 1–7.

Angst, M., Ayoub, S., Baum, S., Burri, P., Mulqueen, P. J., Stock, D. and Williams, J. M. (2010). Crop safeners. WO-patent WO/2010/020477.

Arand, K., Stock, D., Burghardt, M. and Riederer, M. (2010). pH-dependent permeation of amino acids through isolated ivy cuticles is affected by cuticular water sorption and hydration shell size of the solute. *Journal of Experimental Botany* **61**(14): 3865–3873.

Arechavaleta-Medina, F. and Snyder, H. E. (1981). Water imbibition by normal and hard soybeans. *Journal of the American Oil Chemists Society* **58**(11): 976–979.

Backman, P. A. (1978). Fungicide formulation: relationship to biological activity. *Annual Review of Phytopathology* **16**: 211–237.

Bardner, R. (1960). Effect of formulation on toxicity to plants and insects of some systemic insecticidal seed dressings. *Journal of the Science of Food and Agriculture* **11**(12): 736–744.

Barriuso, E., Benoit, P. and Dubus, I. G. (2008). Formation of pesticide nonextractable (bound) residues in soil: magnitude, controlling factors and reversibility. *Environmental Science & Technology* **42**(6): 1845–1854.

Baur, P., Buchholz, A. and Schönherr, J. (1997a). Diffusion in plant cuticles as affected by temperature and size of organic solutes: similarity and diversity among species. *Plant, Cell and Environment* **20**(8): 982–994.

Baur, P., Marzouk, H., Schönherr, J. and Bauer, H. (1996). Mobilities of organic compounds in plant cuticles as affected by structure and molar volumes of chemicals and plant species. *Planta* **199**(3): 404–412.

Baur, P., Marzouk, H., Schönherr, J. and Grayson, B. T. (1997b). Partition coefficients of active ingredients between plant cuticle and adjuvants as related to rates of foliar uptake. *Journal of Agricultural and Food Chemistry* **45**(9): 3659–3665.

Baur, P. and Schönherr, J. (1995). Temperature dependence of the diffusion of organic compounds across plant cuticles. *Chemosphere* **30**(7): 1331–1340.

Beck, R. E. and Schultz, J. S. (1972). Hindrance of solute diffusion within membranes as measured with microporous membranes of known pore geometry. *Biochimica Et Biophysica Acta* **255**(1): 273–303.

Becker, M., Kerstiens, G. and Schönherr, J. (1986). Water permeability of plant cuticles: permeance, diffusion and partition coefficients. *Trees-Structure and Function* **1**(1): 54–60.

Bewley, J. D. (1997). Seed germination and dormancy. *Plant Cell* **9**(7): 1055–1066.

Bewley, J. D., Bradford, K. J., Hilhorst, H. W. M. and Nonogaki, H. (2013). Seeds: physiology of development, germination and dormancy. Third edition. Springer-Verlag, Berlin, Germany.

Beyer, M., Lau, S. and Knoche, M. (2005). Studies on water transport through the sweet cherry fruit surface: IX. Comparing permeability in water uptake and transpiration. *Planta* **220**(3): 474–485.

Black, M., Bewley, J. D. and Halmer, P. (2006). The encyclopedia of seeds: science, technology and uses. CABI Publishing Wallingford, United Kingdom.

Börner, H. (1960). Liberation of organic substances from higher plants and their role in the soil sickness problem. *Botanical Review* **26**(3): 393–424.

Bourgin, M., Bize, M., Durand, S., Albet, J. and Violleau, F. (2009). Development of a rapid determination of pesticides in coated seeds using a high-performance liquid chromatography-UV detection system. *Journal of Agricultural and Food Chemistry* **57**(21): 10032–10037.

Bradford, K. J. and Nonogaki, H. (2007). Seed development, dormancy and germination. Blackwell Publishing, Oxford.

Brahm, J. (1983). Permeability of human red cells to a homologous series of aliphatic-alcohols: limitations of the continuous flow-tube method. *Journal of General Physiology* **81**(2): 283–304.

Buchholz, A. (2006). Characterization of the diffusion of non-electrolytes across plant cuticles: properties of the lipophilic pathway. *Journal of Experimental Botany* **57**(11): 2501–2513.

Buchholz, A. and Schönherr, J. (2000). Thermodynamic analysis of diffusion of non-electrolytes across plant cuticles in the presence and absence of the plasticiser tributyl phosphate. *Planta* **212**(1): 103–111.

Bukovac, M. J. and Petracek, P. D. (1993). Characterizing pesticide and surfactant penetration with isolated plant cuticles. *Pesticide Science* **37**(2): 179–194.

Burghardt, M., Friedmann, A., Schreiber, L. and Riederer, M. (2006). Modelling the effects of alcohol ethoxylates on diffusion of pesticides in the cuticular wax of *Chenopodium album* leaves. *Pest Management Science* **62**(2): 137–147.

Chamel, A. and Vitton, N. (1996). Sorption and diffusion of C-14 atrazine through isolated plant cuticles. *Chemosphere* **33**(6): 995–1003.

Cohen, M. H. and Turnbull, D. (1959). Molecular transport in liquids and glasses. *Journal of Chemical Physics* **31**(5): 1164–1169.

Collins, G., Stibbe, E. and Kroesbergen, B. (1984). Influence of soil moisture stress and soil bulk density on the imbibition of corn seeds in a sandy soil. *Soil & Tillage Research* **4**(4): 361–370.

Cussler, E. L. (1997). Diffusion: mass transfer in fluid systems. Cambridge University Press, Cambridge, UK.

Ding, Y. and Arar, J. (2010). Method of controlling the release of agricultural active ingredients from treated plant seeds. US-patent US 7,774,978.

Duke, S. H. and Kakefuda, G. (1981). Role of the testa in preventing cellular rupture during imbibition of legume seeds. *Plant Physiology* **67**(3): 449–456.

Eichert, T. and Goldbach, H. E. (2008). Equivalent pore radii of hydrophilic foliar uptake routes in stomatous and astomatous leaf surfaces – further evidence for a stomatal pathway. *Physiologia Plantarum* **132**(4): 491–502.

Espelie, K. E., Dean, B. B. and Kolattukudy, P. E. (1979). Composition of lipid-derived polymers from different anatomical regions of several plant species. *Plant Physiology* **64**(6): 1089–1093.

Evenari, M. (1949). Germination inhibitors. *Botanical Review* **15**(3): 153–194.

Fernández-Pineda, C. and Mengual, J. I. (1977). Permeation of water at low pressure in cellulose acetate membranes. 2. Nature of flow. *Journal of Colloid and Interface Science* **61**(1): 102–108.

Finch-Savage, W. E. and Leubner-Metzger, G. (2006). Seed dormancy and the control of germination. *New Phytologist* **171**(3): 501–523.

Fiscus, E. L. (1975). The interaction between osmotic- and pressure-induced water flow in plant roots. *Plant Physiology* **55**(5): 917–922.

Freundl, E., Steudle, E. and Hartung, W. (1998). Water uptake by roots of maize and sunflower affects the radial transport of abscisic acid and its concentration in the xylem. *Planta* **207**(1): 8–19.

Frey, W. and Lösch, R. (2010). Geobotanik. Pflanze und Vegetation in Raum und Zeit. 3. Auflage. Spektrum Akademischer Verlag, Heidelberg.

Friedman, J. and Waller, G. R. (1983a). Caffeine hazards and their prevention in germinating seeds of coffee (*Coffea Arabica* L.). *Journal of Chemical Ecology* **9**(8): 1099–1106.

Friedman, J. and Waller, G. R. (1983b). Seeds as allelopathic agents. *Journal of Chemical Ecology* **9**(8): 1107–1117.

Garcinuño, R. M., Fernández-Hernando, P. and Cámara, C. (2003). Evaluation of pesticide uptake by *Lupinus* seeds. *Water Research* **37**(14): 3481–3489.

Gevao, B., Semple, K. T. and Jones, K. C. (2000). Bound pesticide residues in soils: a review. *Environmental Pollution* **108**(1): 3–14.

Gniwotta, F., Vogg, G., Gartmann, V., Carver, T. L. W., Riederer, M. and Jetter, R. (2005). What do microbes encounter at the plant surface? Chemical composition of pea leaf cuticular waxes. *Plant Physiology* **139**(1): 519–530.

Graham-Bryce, I. J., Nicholls, P. H. and Williams, I. H. (1980). Performance and uptake of some carbendazim-producing fungicides applied as seed treatments to spring barley, in relation to their physicochemical properties. *Pesticide Science* **11**(1): 1-8.

Gupta, J. P., Erwin, D. C., Eckert, J. W. and Zaki, A. I. (1985). Translocation of metalaxyl in soybean plants and control of stem rot caused by *Phytophthora megasperma* f. sp. *glycinea*. *Phytopathology* **75**(7): 865–869.

Haberhauer, G., Pfeiffer, L. and Gerzabek, M. H. (2000). Influence of molecular structure on sorption of phenoxyalkanoic herbicides on soil and its particle size fractions. *Journal of Agricultural and Food Chemistry* **48**(8): 3722–3727.

Hartley, G. S. and Graham-Bryce, I. J. (1980). Physical principles of pesticide behaviour. Academic Press, London.

Hartmann, M. A. (1998). Plant sterols and the membrane environment. *Trends in Plant Science* **3**(5): 170–175.

Hazen, J. L. (2000). Adjuvants – terminology, classification, and chemistry. *Weed Technology* **14**(4): 773–784.

Holloway, P. J. (1982). The chemical constitution of plant cutins. The plant cuticle. Ed.: Cutler, D. F., Alvin, K. L. and Price, C. E. Academic Press, London.

Iqbal, A. and Fry, S. C. (2012). Potent endogenous allelopathic compounds in *Lepidium sativum* seed exudate: effects on epidermal cell growth in *Amaranthus caudatus* seedlings. *Journal of Experimental Botany* **63**(7): 2595–2604.

Kanampiu, F., Karaya, H., Burnet, M. and Gressel, J. (2009). Needs for and effectiveness of slow release herbicide seed treatment *Striga* control formulations for protection against early season crop phytotoxicity. *Crop Protection* **28**(10): 845–853.

Keeling, B. L. (1974). Soybean seed rot and relation of seed exudate to host susceptibility. *Phytopathology* **64**(11): 1445–1447.

Kerler, F., Riederer, M. and Schönherr, J. (1984). Non-electrolyte permeability of plant cuticles: a critical evaluation of experimental methods. *Physiologia Plantarum* **62**(4): 599–606.

Kerler, F. and Schönherr, J. (1988a). Accumulation of lipophilic chemicals in plant cuticles: prediction from octanol/water partition coefficients. *Archives of Environmental Contamination and Toxicology* **17**(1): 1–6.

Kerler, F. and Schönherr, J. (1988b). Permeation of lipophilic chemicals across plant cuticles: prediction from partition coefficients and molar volumes. *Archives of Environmental Contamination and Toxicology* **17**(1): 7–12.

Kirsch, T., Kaffarnik, F., Riederer, M. and Schreiber, L. (1997). Cuticular permeability of the three tree species *Prunus laurocerasus* L., *Ginkgo biloba* L. and *Juglans regia* L.: comparative investigation of the transport properties of intact leaves, isolated cuticles and reconstituted cuticular waxes. *Journal of Experimental Botany* **48**(310): 1035–1045.

Koizumi, M., Kikuchi, K., Isobe, S., Ishida, N., Naito, S. and Kano, H. (2008). Role of seed coat in imbibing soybean seeds observed by micro-magnetic resonance imaging. *Annals of Botany* **102**(3): 343–352.

Larson, L. A. (1968). The effect soaking pea seeds with or without seedcoats has on seedling growth. *Plant Physiology* **43**(2): 255–259.

Laurent, F. M. and Rathahao, E. (2003). Distribution of [C-14]imidacloprid in sunflowers (*Helianthus annuus* L.) following seed treatment. *Journal of Agricultural and Food Chemistry* **51**(27): 8005–8010.

Leo, A., Hansch, C. and Elkins, D. (1971). Partition coefficients and their uses. *Chemical reviews* **71**(6): 525–554.

Levitan, H. (1977). Food, drug, and cosmetic dyes: biological effects related to lipid solubility. *Proceedings of the National Academy of Sciences of the United States of America* **74**(7): 2914–2918.

Lieb, W. R. and Stein, W. D. (1971). Implications of two different types of diffusion for biological membranes. *Nature-New Biology* **234**(50): 220–222.

Linkies, A., Graeber, K., Knight, C. and Leubner-Metzger, G. (2010). The evolution of seeds. *New Phytologist* **186**(4): 817–831.

Ma, F. S., Cholewa, E., Mohamed, T., Peterson, C. A. and Gijzen, M. (2004). Cracks in the palisade cuticle of soybean seed coats correlate with their permeability to water. *Annals of Botany* **94**(2): 213–228.

Manohar, M. S. (1966). Effect of osmotic systems on germination of peas (*Pisum sativum* L). *Planta* **71**(1): 81–86.

Manz, B., Muller, K., Kucera, B., Volke, F. and Leubner-Metzger, G. (2005). Water uptake and distribution in germinating tobacco seeds investigated in vivo by nuclear magnetic resonance imaging. *Plant Physiology* **138**(3): 1538–1551.

Marga, F., Pesacreta, T. C. and Hasenstein, K. H. (2001). Biochemical analysis of elastic and rigid cuticles of *Cirsium horridulum*. *Planta* **213**(6): 841–848.

Mehta, N., Saharan, G. S. and Kathpal, T. S. (1997). Absorption and degradation of metalaxyl in mustard plant (*Brassica juncea*). *Ecotoxicology and Environmental Safety* **37**(2): 119–124.

Meyer, C. J., Steudle, E. and Peterson, C. A. (2007). Patterns and kinetics of water uptake by soybean seeds. *Journal of Experimental Botany* **58**(3): 717–732.

Michel, B. E. (1983). Evaluation of the water potentials of solutions of polyethylene glycol 8000 both in the absence and presence of other solutes. *Plant Physiology* **72**(1): 66–70.

Mitragotri, S. (2003). Modeling skin permeability to hydrophilic and hydrophobic solutes based on four permeation pathways. *Journal of Controlled Release* **86**(1): 69–92.

Montfort, F., Klepper, B. L. and Smiley, R. W. (1996). Effects of two triazole seed treatments, triticonazole and triadimenol, on growth and development of wheat. *Pesticide Science* **46**(4): 315–322.

Muehlebach, M., Brunner, H.-G., Cederbaum, F., Maetzke, T., Mutti, R., Schnyder, A., Stoller, A., Wendeborn, S., Wenger, J., Boutsalis, P., Cornes, D., Friedmann, A. A., Glock, J., Hofer, U., Hole, S., Niderman, T. and Quadranti, M. (2007). Discovery and SAR of pinoxaden: a new broad spectrum, postemergence cereal herbicide. Pesticide Chemistry. Ed.: Ohkawa, H., Miyagawa, H. and Lee, P. W. WILEY-VCH Verlag, Weinheim, Germany.

Mullin, W. J. and Xu, W. L. (2001). Study of soybean seed coat components and their relationship to water absorption. *Journal of Agricultural and Food Chemistry* **49**(11): 5331–5335.

Nicholls, P. H. (1988). Factors influencing entry of pesticides into soil water. *Pesticide Science* **22**(2): 123–137.

Nobel, P. S. (1991). Physicochemical and environmental plant physiology. Academic Press, San Diego.

Owen, W. J. and Donzel, B. (1986). Oxidative degradation of chlortoluron, propiconazole, and metalaxyl in suspension cultures of various crop plants. *Pesticide Biochemistry and Physiology* **26**(1): 75–89.

Parida, T., Nayak, M. and Sridhar, R. (1990). Fate of carbendazim in rice tissues after seed or foliage treatments. *Pesticide Science* **30**(3): 303–308.

Phillips, R. E., Thompson, L. and Egli, D. B. (1972). Absorption of herbicides by soybean seeds and their influence on emergence and seedling growth. *Weed Science* **20**(5): 506–510.

Popp, C., Burghardt, M., Friedmann, A. and Riederer, M. (2005). Characterization of hydrophilic and lipophilic pathways of *Hedera helix* L. cuticular membranes: permeation of water and uncharged organic compounds. *Journal of Experimental Botany* **56**(421): 2797–2806.

Potts, R. O. and Guy, R. H. (1992). Predicting skin permeability. *Pharmaceutical Research* **9**(5): 663–669.

Powell, A. A. and Matthews, S. (1978). The damaging effect of water on dry pea embryos during imbibition. *Journal of Experimental Botany* **29**(112): 1215–1229.

Powell, A. A. and Matthews, S. (1979). The influence of testa condition on the imbibition and vigor of pea seeds. *Journal of Experimental Botany* **30**(114): 193–197.

Querou, R., Euvrard, M. and Gauvrit, C. (1997). Uptake of triticonazole, during imbibition, by wheat caryopses after seed treatment. *Pesticide Science* **49**(3): 284–290.

Querou, R., Euvrard, M. and Gauvrit, C. (1998). Uptake and fate of triticonazole applied as seed treatment to spring wheat (*Triticum aestivum* L.). *Pesticide Science* **53**(4): 324–332.

Ranathunge, K., Shao, S. Q., Qutob, D., Gijzen, M., Peterson, C. A. and Bernards, M. A. (2010). Properties of the soybean seed coat cuticle change during development. *Planta* **231**(5): 1171–1188.

Ratner, B. D. and Miller, I. F. (1973). Transport through crosslinked poly(2-hydroxyethyl methacrylate) hydrogel membranes. *Journal of Biomedical Materials Research* **7**(4): 353–367.

Refojo, M. F. (1965). Permeation of water through some hydrogels. *Journal of Applied Polymer Science* **9**(10): 3417–3426.

Reigosa, M. J., Souto, X. C. and González, L. (1999). Effect of phenolic compounds on the germination of six weeds species. *Plant Growth Regulation* **28**(2): 83–88.

Rieder, G., Buchholtz, K. P. and Kust, C. A. (1970). Uptake of herbicides by soybean seed. *Weed Science* **18**(1): 101–105.

Riederer, M. and Friedmann, A. (2006). Transport of lipophilic non-electrolytes across the cuticle. Biology of the Plant Cuticle. Ed.: Riederer, M. and Müller, C. Blackwell Publishing, Oxford, UK.

Riederer, M. and Schönherr, J. (1984). Accumulation and transport of (2,4-dichlorophenoxy)acetic acid in plant cuticles: I. Sorption in the cuticular membrane and its components. *Ecotoxicology and Environmental Safety* **8**(3): 236–247.

Riederer, M. and Schönherr, J. (1986). Thermodynamic analysis of nonelectrolyte sorption in plant cuticles: the effects of concentration and temperature on sorption of 4-nitrophenol. *Planta* **169**(1): 69–80.

Rolston, M. P. (1978). Water impermeable seed dormancy. *Botanical Review* **44**(3): 365–396.

Salanenka, Y. A. and Taylor, A. G. (2008). Seed coat permeability and uptake of applied systemic compounds. *Acta Horticulturae* **782**: 4.

Schaetzl, R. J. and Anderson, S. (2005). Soils. Genesis and geomorphology. Cambridge University Press, New York, USA.

Schlatter, C. and Beste, C. L. (2005). Method and device for direct quantitative determination of pesticide seed loading on individual seeds. WO-patent WO/2005/048683.

Schlegel, T. K., Schönherr, J. and Schreiber, L. (2005). Size selectivity of aqueous pores in stomatous cuticles of *Vicia faba* leaves. *Planta* **221**(5): 648–655.

Schönherr, J. (1976). Water permeability of isolated cuticular membranes: the effect of pH and cations on diffusion, hydrodynamic permeability and size of polar pores in the cutin matrix. *Planta* **128**(2): 113–126.

Schönherr, J. (1993). Effects of alcohols, glycols and monodisperse ethoxylated alcohols on mobility of 2,4-D in isolated plant cuticles. *Pesticide Science* **39**(3): 213–223.

Schönherr, J. (2001). Cuticular penetration of calcium salts: effects of humidity, anions, and adjuvants. *Journal of Plant Nutrition and Soil Science* **164**(2): 225–231.

Schönherr, J. (2002). A mechanistic analysis of penetration of glyphosate salts across astomatous cuticular membranes. *Pest Management Science* **58**(4): 343–351.

Schönherr, J. (2006). Characterization of aqueous pores in plant cuticles and permeation of ionic solutes. *Journal of Experimental Botany* **57**(11): 2471–2491.

Schönherr, J. and Schreiber, L. (2004). Size selectivity of aqueous pores in astomatous cuticular membranes isolated from *Populus canescens* (Aiton) Sm. leaves. *Planta* **219**(3): 405–411.

Schreiber, L. (2005). Polar paths of diffusion across plant cuticles: new evidence for an old hypothesis. *Annals of Botany* **95**(7): 1069–1073.

Schreiber, L. and Schönherr, J. (1992). Analysis of foliar uptake of pesticides in barley leaves: role of epicuticular waxes and compartmentation. *Pesticide Science* **36**(3): 213–221.

Schreiber, L. and Schönherr, J. (1993). Mobilities of organic compounds in reconstituted cuticular wax of barley leaves: determination of diffusion coefficients. *Pesticide Science* **38**(4): 353–361.

Schreiber, L. and Schönherr, J. (2009). Water and solute permeability of plant cuticles. Measurement and data analysis. Springer-Verlag, Berlin, Germany.

Scott, H. D. and Phillips, R. E. (1971). Diffusion of herbicides to seed. *Weed Science* **19**(2): 128–132.

Senesi, N. (1992). Binding mechanisms of pesticides to soil humic substances. *Science of the Total Environment* **123**: 63–76.

Shafer, W. E. and Bukovac, M. J. (1989). Studies on octylphenoxy surfactants. 7. Effects of Triton X-100 on sorption of 2-(1-naphthyl)acetic acid by tomato fruit cuticles. *Journal of Agricultural and Food Chemistry* **37**: 486–492.

Shao, S. Q., Meyer, C. J., Ma, F. S., Peterson, C. A. and Bernards, M. A. (2007). The outermost cuticle of soybean seeds: chemical composition and function during imbibition. *Journal of Experimental Botany* **58**(5): 1071–1082.

Sharma, R. R., Agrawal, R. and Chellam, S. (2003). Temperature effects on sieving characteristics of thin-film composite nanofiltration membranes: pore size distributions and transport parameters. *Journal of Membrane Science* **223**(1–2): 69–87.

Shaykewich, C. F. and Williams, J. (1971). Resistance to water absorption in germinating rapeseed (*Brassica napus* L.). *Journal of Experimental Botany* **22**(70): 19–24.

Sigler, W. V., Reicher, Z., Throssell, C., Bischoff, M. and Turco, R. F. (2003). Sorption and degradation of selected fungicides in the turfgrass canopy. *Water Air and Soil Pollution* **142**(1-4): 311–326.

Simmen, U. and Gisi, U. (1995). Effects of seed treatment with SAN-789-F, a homopropargylamine fungicide, on germination and contents of squalene and sterols of wheat seedlings. *Pesticide Biochemistry and Physiology* **52**(1): 25–32.

Simmen, U. and Gisi, U. (1996). Uptake and distribution in germinating wheat of [C-14]SAN 789 F and [C-14]cyproconazole applied as seed treatment. *Crop Protection* **15**(3): 275–281.

Simmen, U. and Gisi, U. (1998). Uptake of C-14-SAN 789 F and C-14-cyproconazole into germinating wheat following seed treatment at different soil matric potentials. *Soil Biology & Biochemistry* **30**(4): 517–522.

Simon, E. W. (1974). Phospholipids and plant membrane permeability. *New Phytologist* **73**(3): 377–420.

Simon, E. W. (1978). Plant membranes under dry conditions. *Pesticide Science* **9**(2): 169–172.

Simon, E. W. and Harun, R. M. R. (1972). Leakage during seed imbibition. *Journal of Experimental Botany* **23**(77): 1076–1085.

Singh, U. S. (1989). Studies on the systemicity of [C-14]metalaxyl in cowpea (*Vigna unguiculata* (L.) Walp.). *Pesticide Science* **25**(2): 145–154.

Stein, W. D. (1986). Transport and diffusion across cell membranes. Academic Press, London, UK.

Steudle, E. and Boyer, J. S. (1985). Hydraulic resistance to radial water flow in growing hypocotyl of soybean measured by a new pressure-perfusion technique. *Planta* **164**(2): 189–200.

Steudle, E. and Frensch, J. (1996). Water transport in plants: role of the apoplast. *Plant and Soil* **187**(1): 67–79.

Steudle, E. and Peterson, C. A. (1998). How does water get through roots? *Journal of Experimental Botany* **49**(322): 775–788.

Stevens, M. M., Reinke, R. F., Coombes, N. E., Helliwell, S. and Mo, J. H. (2008). Influence of imidacloprid seed treatments on rice germination and early seedling growth. *Pest Management Science* **64**(3): 215–222.

Suman, A., Shahi, H. N., Singh, P. and Gaur, A. (2002). Allelopathic influence of *Vigna mungo* (black gram) seeds on germination and radical growth of some crop plants. *Plant Growth Regulation* **38**(1): 69–74.

Suzuki, M., Hamamura, H. and Iwamori, M. (1994). Relationship between formulations of triflumizole and their efficacy to Bakanae disease in rice seed treatment. *Journal of Pesticide Science* **19**(4): 251–256.

Takahashi, Y., Tsubaki, S., Sakamoto, M., Watanabe, S. and Azuma, J. I. (2012). Growth-dependent chemical and mechanical properties of cuticular

membranes from leaves of *Sonneratia alba*. *Plant Cell and Environment* **35**(7): 1201–1210.

Thielert, W., Steffens, W., Fuhr, F., Kuck, K. H. and Scheinpflug, H. (1988). Uptake of triadimenol through wheat caryopsis after application by seed treatment. *Pesticide Science* **22**(2): 93–105.

Ticknor, L. B. (1958). On the permeation of cellophane membranes by diffusion. *Journal of Physical Chemistry* **62**(12): 1483–1485.

Troeh, F. R. and Thompson, L. M. (2005). Soils and soil fertility. 6th edition. Blackwell Publishing, Oxford.

Tyree, M. T., Scherbatskoy, T. D. and Tabor, C. A. (1990). Leaf cuticles behave as asymmetric membranes. Evidence from the measurement of diffusion potentials. *Plant Physiology* **92**(1): 103-109.

Van Bruggen, J. T., Chalmers, B. and Muller, M. (1982). Effects of solvent and solute drag on transmembrane diffusion. *Journal of General Physiology* **79**(3): 507–528.

Verkman, A. S. (2000). Water permeability measurement in living cells and complex tissues. *Journal of Membrane Biology* **173**(2): 73–87.

Vieth, W. R. (1991). Diffusion in and through polymers. Carl Hanser Verlag, München, Germany.

Vleeshouwers, L. M., Bouwmeester, H. J. and Karssen, C. M. (1995). Redefining seed dormancy: An attempt to integrate physiology and ecology. *Journal of Ecology* **83**(6): 1031–1037.

Weitbrecht, K., Müller, K. and Leubner-Metzger, G. (2011). First off the mark: early seed germination. *Journal of Experimental Botany* **62**(10): 3289–3309.

Werker, E. (1997). Seed anatomy. Borntraeger, Berlin, Germany.

Werker, E., Marbach, I. and Mayer, A. M. (1979). Relation between the anatomy of the testa, water permeability and the presence of phenolics in the genus *Pisum*. *Annals of Botany* **43**(6): 765–771.

Westwood, F., Bean, K. M., Dewar, A. M., Bromilow, R. H. and Chamberlain, K. (1998). Movement and persistence of [C-14]imidacloprid in sugar-beet plants following application to pelleted sugar-beet seed. *Pesticide Science* **52**(2): 97–103.

Williams, W. A. and Elliott, J. R. (1960). Ecological significance of seed coat impermeability to moisture in crimson, subterreanean and rose clovers in a Mediterranean-type climate. *Ecology* **41**(4): 733–742.

Yasuda, H. and Peterlin, A. (1973). Diffusive and bulk flow transport in polymers. *Journal of Applied Polymer Science* **17**(2): 433–442.

Yue, B. S., Wilde, G. E. and Arthur, F. (2003). Evaluation of thiamethoxam and imidacloprid as seed treatments to control European corn borer and Indianmeal moth (Lepidoptera: Pyralidae) larvae. *Journal of Economic Entomology* **96**(2): 503–509.

Zadra, C., Marucchini, C. and Zazzerini, A. (2002). Behavior of metalaxyl and its pure R-enantiomer in sunflower plants (*Helianthus annus*). *Journal of Agricultural and Food Chemistry* **50**(19): 5373–5377.

Zeun, R., Scalliet, G. and Oostendorp, M. (2012). Biological activity of sedaxane – a novel broad-spectrum fungicide for seed treatment. *Pest Management Science*.

Zhang, S. T., Liu, J. P., Bao, X. H. and Niu, K. C. (2011). Seed-to-seed potential allelopathic effects between *Ligularia virgaurea* and native grass species of Tibetan alpine grasslands. *Ecological Research* **26**(1): 47–52.

Publications and presentations

Publications

Niemann, S., Burghardt, M., Popp, C. and Riederer, M. (2013). Aqueous pathways dominate permeation of solutes across *Pisum sativum* seed coats and mediate solute transport via diffusion and bulk flow of water. *Plant, Cell & Environment* **36**: 1027–1036.

Presentations

Congress "Botanikertagung": 18.–23.09.2011, Berlin, Germany. Poster "*Pisum sativum* seed coat permeability is dominated by hydrophilic pathways"

Symposium "Epos", 7th International Symposium organized by the students of the Graduate School of Life Sciences of the University of Würzburg:
16.–17.10.2012, Würzburg, Germany. Poster "*Pisum sativum* seed coat permeability"

Annual Progress Reports

09.11.2010, Syngenta Crop Protection Münchwilen AG, Münchwilen, Switzerland
17.11.2011, Syngenta Crop Protection Münchwilen AG, Münchwilen, Switzerland
26.03.2013, Syngenta Crop Protection Münchwilen AG, Stein, Switzerland

Curriculum vitae

Sylvia Niemann

Affidavit

I hereby confirm that my thesis entitled "Seed Coat Permeability of Active Ingredients" is the result of my own work. I did not receive any help or support from commercial consultants. All sources and / or materials applied are listed and specified in the thesis.

Furthermore, I confirm that this thesis has not yet been submitted as part of another examination process neither in identical nor in similar form.

Würzburg,
Place, Date Signature

Eidesstattliche Erklärung

Hiermit erkläre ich an Eides statt, die Dissertation „Permeabilität von Samenschalen für Aktivsubstanzen" eigenständig, d.h. insbesondere selbständig und ohne Hilfe eines kommerziellen Promotionsberaters, angefertigt und keine anderen als die von mir angegebenen Quellen und Hilfsmittel verwendet zu haben.

Ich erkläre außerdem, dass die Dissertation weder in gleicher noch in ähnlicher Form bereits in einem anderen Prüfungsverfahren vorgelegen hat.

Würzburg,
Ort, Datum Unterschrift